Master of Science Thesis

Conceptual design of a passenger aircraft for in-flight refueling operations

P.P.M. van der Linden B.Sc.

5 July 2013

Faculty of Aerospace Engineering · Delft University of Technology

TU Delft

Conceptual design of a passenger aircraft for in-flight refueling operations

Master of Science Thesis

For obtaining the degree of Master of Science in Aerospace Engineering
at Delft University of Technology

P.P.M. van der Linden B.Sc.

5 July 2013

Faculty of Aerospace Engineering · Delft University of Technology

Delft University of Technology

Delft University Of Technology
Department Of
Design, Integration and Operations of Aircraft and Rotorcraft

The undersigned hereby certify that they have read and recommend to the Faculty of Aerospace Engineering for acceptance a thesis entitled **"Conceptual design of a passenger aircraft for in-flight refueling operations"** by **P.P.M. van der Linden B.Sc.** in partial fulfillment of the requirements for the degree of **Master of Science**.

Dated: 5 July 2013

Head of department: _____
Prof.Dr.-Ing. G. Eitelberg

Supervisor: _____
Dr.ir. G. La Rocca

Reader: _____
Dipl.-Ing. S. Zajac

Reader: _____
Mo Li M.Sc.

Summary

Nowadays a big challenge in aviation is represented by the scarcity of fossil fuels. Hence, there is a need for a more fuel efficient air transport system. A possible innovation is a change in operating mode. Conceptual design studies showed staged flight operations to be up to 40% more fuel efficient than non-stop operations. Staged flight operation uses extra stops to split up long range missions. An even more novel concept is in-flight refueling operation (IFR). IFR incorporates a fuel transfer system in midair. This eliminates the increase in travel time, which is associated with the extra take-off and landings of staged flight operations, while maintaining similar fuel saving as staged flight operations.

This thesis focuses on the design of the cruiser, the passenger aircraft that will be refueled. The design of the tanker and of the whole operational concept are outside the scope of the thesis. The design of the cruiser is performed with the Initiator, an automated design tool. The modifications to the Initiator to enable it to produce an accurate design of the cruiser are described in the thesis.

The cruiser was found to have a higher payload range efficiency (PRE) as the non-stop aircraft. 10.4% better than the 5000nm non-stop aircraft and 29.4% better than the 7500nm non-stop aircraft. Top level requirements of existing aircraft were used to produce concepts with similar payload requirements (B767-300 payload=26500kg) and with similar range requirements (B737-800 range=2500nm). They were outperformed by 7.3% and 9.6% in PRE, when operated with similar passenger comfort levels as the cruiser. Since only the cruiser design is considered no exact conclusions on the fuel savings can be given. Only a fuel budget can be provided for tanker operations. Comparing tanker fuel consumptions from literature 9 of 12 tanker designs outperformed the staged flight operation, 12 of 12 the non-stop operations.

In-flight has to be further researched, however initial studies show IFR can be a possible solution for a more fuel efficient air transport. The cruiser outperformed existing aircraft for the given range of 2500nm.

Acknowledgements

This thesis is the last part of my Master program at the faculty of Aerospace Engineering of the Delft University of Technology. I would like to thank a number of people for their support during this last part of my Master.

First of all, I would like to thank my supervisor Gianfranco La Rocca. Who besides all the technical support made an effort in tutoring me the fine art of writing a thesis. Mo Li, who was always available for advice and discussion concerning the design. Furthermore, I would also like to thank the other members of the committee Georg Eitelberg and Stefan Zajac, who took the time to assess this thesis and share their expert opinions.

Then I would like to thank my fellow students in room NB2.40, who made for a good chat in the coffee corner. Besides their value in the coffee corner their expertise in many different parts of the thesis from writing to programming helped me out more than once.

Finally, I would like to thank all friends outside the faculty, who would lend an ear when thesis related ideas and solutions popped up after working hours. Understanding the content or not they were always ready to nod approvingly. In particular I would like to thank my parents Huub and Ineke, who watched all developments with great involvement. My brother Thijs and sister Stance. My girlfriend Annemiek and all friends who made the last year a good one.

Delft, The Netherlands
5 July 2013

P.P.M. van der Linden B.Sc.

Contents

List of Figures

List of Tables

Nomenclature

Symbols

A	Aspect ratio	–
C_{Di}	Induced drag coefficient	–
C_L	Three dimensional lift coefficient	–
e	Oswald factor	–
ff	fuel fraction	–
FM	Fuel mass	kg
L/D	Lift over Drag ratio	–
M	Mach number	–
MAC	Mean Aerodynamic Chord	m
$MTOW$	Maximum Take-Off Weight	kg
OEW	Operational Empty Weight	kg
PRE	Payload Range Efficiency	m
R	Range	m
b	Wing span	m
SFC	Specific Fuel Consumption	$1/s$
V	Aircraft velocity	m/s
W_4	Aircraft weight before cruise	kg
W_5	Aircraft weight after cruise	kg
WFB	Block Fuel Weight	kg
WFR	Reserve Fuel Weight	kg
WP	Payload Weight	kg

X	X-factor $\frac{V \cdot L/D}{SFC}$	m
Δy	Lateral distance between the centerlines of two aircraft flying in formation	m
Δz	Vertical distance between the centerlines of two aircraft flying in formation	m
η	Non-dimensional lateral spacing between the wings	$-$
σ_i	Influence factor for induced drag	$-$
ζ	Non-dimensional vertical spacing between the wings	$-$

Subscripts

$_{cr}$	cruise

Abbreviations

A point	Maximum Payload Operation point
CPACS	Common Parametric Aircraft Configuration Schema
D point	Design point
DEE	Design and Engineering Engine
GA	Genetic Algorithm
GUI	Graphical User Interface
HBPR	High By-Pass Ratio
IFR	In-Flight Refueling
LASR	Large Aircraft for Short Range
MMG	Multi-Model Generator
RCE	Remote Component Environment
RECREATE	REsearch on a CRuiser Enabled Air Transport Environment
TIXI	TIVA XML Interface

Chapter 1

Introduction

Since the first Wright brothers flight, airplanes experienced many improvements. Their airplane was constructed from wood and linen and propelled by a piston engine. Modern airplanes, feature aluminium and composite materials and are driven by turbo engines. These improvements were developed to achieve higher speeds and greater distances. Nowadays the biggest challenge is represented by the scarcity of fossil fuels. Hence, there is a need for a more fuel efficient air transport system.

In general, aircraft performance and technologies proceed in so called S curves of innovation (figure 1.1). New technologies require time and effort before they can be adopted in new aircraft development programs and provide a performance increase. Hereafter, a period of relative high performance increase will come and finally the concept will reach a phase, at which it is optimized to such an extent that an increase of performance will once again come at a high time and effort investment. Aircraft main architectures have been almost unchanged, since the introduction of the B47 in 1947 [15]. Now they are at the end of their S curve. Hence, innovations are required to further increase fuel efficiency.

A possible innovation is a change in operating mode. Conceptual design studies showed staged flight operations to be up to 40% more fuel efficient, than non-stop operations [16]. Staged flight operation uses extra stops in between long range missions. For example, a 8100nm mission can be divided into 3 shorter missions of 2700nm. In this staged operation mode the aircraft takes off with less fuel than it would need for the non-stop mission. This lower fuel mass decreases take-off mass, hence the fuel consumption per nm. Furthermore, a lower take-off mass will decrease the required wing and engine sizes, further decreasing take-off mass, and thus fuel mass.

An even more efficient operational concept than staged flight is represented by In-Flight Refueling (IFR). IFR uses a fuel transfer in midair to eliminate the increase in travel time, which is associated with the extra take-off and landings of staged flight operations, while maintaining similar fuel saving as staged flight operations. Although, IFR is new to civil aircraft operations, it is already a time proven concept in military operations.

The European research project REsearch on a CRuiser Enabled Air Transport Environment (RECREATE), is currently looking at IFR operation for passenger aircraft. This thesis work

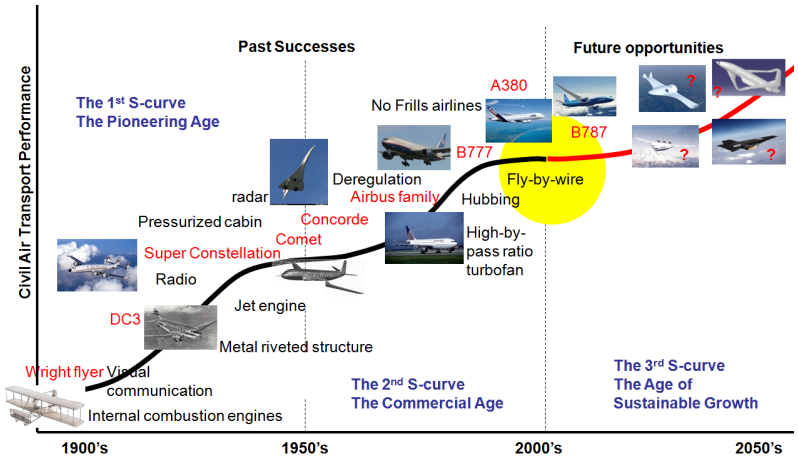

Figure 1.1: Illustration of the S curves of innovation, from La Rocca [1]

represents a significant contribution to the projects activities, related to the conceptual design of the passenger aircraft (the cruiser).

1.1 Objectives of this research

Although the Recreate project aims at investigating the whole IFR concept, including the design of the passenger cruiser, the tanker, the IFR systems and the overall operational concept this thesis will focus solely on the design of the cruiser. It will include a comparative study of aircraft designed for IFR, staged and non-stop flight operations.

Since only the cruiser design is considered, no conclusions on the fuel savings of IFR operation with respect to staged flight or non-stop operations can be given. However, the fuel consumed by the cruiser during IFR operation can be compared to the fuel consumed in staged flight and non-stop operation and fuel saved by IFR operations can be set as "budget" to operate the tanker. The main research goal is formulated as follows:

Develop the conceptual design of a passenger aircraft, the cruiser, for IFR operation and compare its fuel consumption to non-stop and staged flight operation.

The RECREATE consortium, provided this research with a set of requirements for the design of the cruiser. The requirements are as follows:

- Use a conventional configuration
- Single stage range of 2500nm
- Total range of 5000nm (With refueling, so passenger and crew comfort must be comparable to long range aircraft)
- Payload 250 passengers, in single class, twin aisle configuration

- LD-3 container storage capability
- Takeoff within 1500 m (BFL according to CS)
- Landing within 2600 m (BFL according to CS)
- Cruise mach number of 0.82
- Cruise altitude of 35000 ft
- Refueling capability at cruise speed and altitude
- Specific fuel consumption of 0.525 lb/(lbf·h)

The conceptual design for this research will be produced by a tool under development at the TUD, the so called Initiator. The Initiator is a Matlab based conceptual design tool. The use of the Initiator is chosen, because several conceptual designs and variants have to be generated and without an automated design tool this activity would require a too lengthy and repetitive work. Besides, the use of the one design tool to generate all the conceptual designs gives the possibility to generate consistent designs and obtain performance values for a fair comparison.

Being the Initiator in its early development phase, not all capabilities were in place to support the conceptual design study for this research. Therefore, a subgoal is formulated as follows:

Subgoal of the research :

Improve the Initiator in order to make it capable of producing the conceptual designs required to achieve the main research goal

Although the main interest here is in the comparison of the different aircraft designs, the accuracy of the conceptual designs must be guaranteed. For this reason the improved Initiator has been extensively verified and validated with existing aircraft.

1.2 Structure of this report

The contents of this report are organized as follows. Chapter 2 presents some results from literature, providing evidence on the fuel savings of staged flight compared to non-stop operations. Since both IFR and staged exploit fuel savings due to segmented operations compared to non-stop operations the conclusions found are relevant to this thesis. A major conclusion of this chapter is that segmented operations require a redesign of existing aircraft.

Chapter 3 discussed the cruiser-tanker configuration during the refueling manoeuvre. A trade-off between various IFR configurations is performed in order to find the most convenient one for civil applications, where different requirements apply than for military operations. The preferred configuration from the trade-off is the configuration where the cruiser flies in front and above the tanker and the approach manoeuvre is performed by the tanker. The benefit of this configuration in terms of cruiser design is that no special requirements apply than for the design of any conventional passenger aircraft.

Chapter 4 lists the designs required for the fuel efficiency comparisons. The components of the Initiator are described. The changes that enable a feasible design, in terms of range and fuselage size are performed. Finally, also the output modules for use during this thesis and for use by other tools for further analysis are created.

Chapter 5 with the design routine operating adequately, the Initiator is validated by generating designs with top level requirements of the reference aircraft and comparing them to the existing aircraft. Hereafter, the accuracy of the tool is proven by verifying individual modules Initiator, the class II weight estimation and the aerodynamic analysis module. Furthermore, incorrect dependencies of the design process are removed. The important changes are evaluated by a new validation, which again uses the top level requirements of the reference aircraft.

Chapter 6 presents the conceptual design of the cruiser. Furthermore, the designs required for the fuel efficiency comparisons are presented here. Also, the fuel consumption of the designed aircraft for IFR, staged and non-stop operations, as well as the fuel budget for the tanker operation, is computed in this chapter.

Finally, chapter 7 provides some conclusion & recommendation concerning both the design of the cruiser and the design tool.

Chapter 2

Operational concepts for fuel saving & transportation efficiency parameters

This section investigates the relation between range and fuel efficiency and introduces some performance parameters such as x and PRE quantify and compare the efficiency of the different aircraft and different operational concepts in terms of transportation efficiency. The success of staged flight concept revolves on the assumption, that an aircraft flying a mission divided in multiple smaller submission will use significantly less fuel as an aircraft flying the whole mission at once. The purpose of this chapter is to understand the effect of different operational concepts on the saving of fuel, with emphasis on staged flight. Furthermore, the potential benefit of these operational concepts is quantified in order to compare them with the more radical IFR concept.

2.1 Efficiency parameters

In order to quantify the fuel efficiency of aircraft, a parameter is needed to compare different aircraft and operation modes. To this purpose Nangia proposes the Payload Range Efficiency (PRE) parameter [3], which is defined by equation 2.1.

$$PRE[m] = \frac{WP[kg] \cdot R[m]}{WFB[kg]} \tag{2.1}$$

Where WP is the payload in kg, WFB the block fuel weight in kg and R the range in meters. The dimensions of PRE are meters.

The influence of range on fuel efficiency can be predicted by two simple calculation: Lets consider two different high-subsonic aircraft, each designed for a different mission length.

Both aircraft are non-existing conceptual aircraft, because using one existing aircraft, for both mission, would include the range preferences of the chosen aircraft, as explained in the next paragraph. Using two existing aircraft would include the performance differences between both aircraft aircraft, since these are never completely equal between different aircraft. Hence one of the two non-existing conceptual aircraft flies from Eindhoven to Pisa (970km) and the other from Eindhoven to Faro (1950km).

To describe the preference in range for an particular aircraft the payload range diagram is investigated (figure 2.1). Point A is the point where the aircraft operates with the maximum payload, that can be loaded into the aircraft. This point is often referred to as the maximum payload range. Point D is the design point. This operation corresponds with the payload that the aircraft can carry over its design range. The design point is mostly close to the maximum fuel range, point B. In point B all tanks are filled and payload is added to reach the $MTOW$. Finally there is the zero payload range, point C, where all tanks are filled and no payload is loaded in order to save weight and increase range. This latest mode of operation takes-off with less then the $MTOW$. Let us now assume that the existing aircraft has a D point at a range of 1950km (the distance to Faro) and an A point at 970km (the distance to Pisa). Operating at point A the flight to Pisa will carry maximum payload, this means a high density seating configuration and full cargo bay. A high density, hence low volume per payload weight will result on a low fuselage drag per payload weight for this flight. The flight at point D will feature a lower payload density, hence a high fuselage drag per payload weight and will thus be, apart from any range effects, in a disadvantage with respect to the flight to maximum payload.

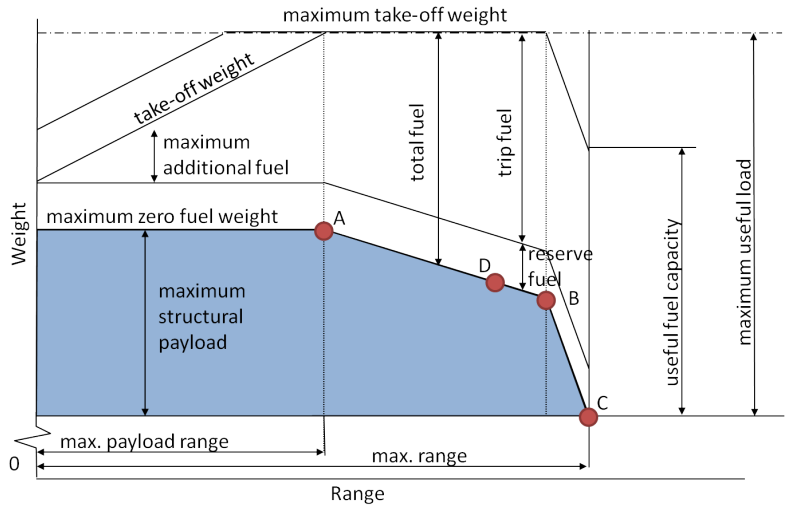

Figure 2.1: Example payload range diagram

Therefore, the two non-existing conceptual aircraft are designed at the same operating point, namely the design point. The difference between A and D point is discussed after these range efficiency calculations. The range efficiency calculations will start with the Breguet range equation 2.2:

$$R = \frac{V}{SFC} \cdot \frac{L}{D} \cdot ln\left(\frac{W_4}{W_5}\right) \tag{2.2}$$

Where V is the velocity of the aircraft, SFC the specific fuel consumption of the engines, L/D the lift over drag ratio of the aircraft and W_4 and W_5 the aircraft weight before and after the cruise phase. Equation 2.2 can be rewritten to calculate the fuel fraction (ff) for cruise (W_5/W_4):

$$ff_{cr} = e^{\frac{-R \cdot SFC_{cr}}{V_{cr} \cdot \left(\frac{L}{D}\right)_{cr}}} \tag{2.3}$$

Where the subscript cr denotes the value of the given parameter in the cruise phase. The other flight phases are calculated using fuel fractions. Table 2.1 lists the fuel fraction retrieved from literature [17]. Figure 2.2 depicts a simple representation of the mission definition. The diversion and loiter stages are included in the reserve fuel fraction.

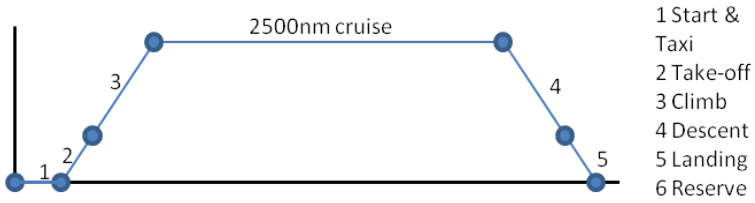

Figure 2.2: Mission definition with fuel fractions

Table 2.1: Fuel fractions off the various non-cruise phases

$ff_{\text{Take-off}}$	0.995	[-]
ff_{Climb}	0.98	[-]
ff_{Descent}	0.99	[-]
ff_{Landing}	0.992	[-]
ff_{Reserve}	0.955	[-]

The WFB is defined as all the fuel used by the aircraft during the mission. The fuel mass (FM) includes the reserve fuel as well as the WFB, which can be seen in equation 2.4:

$$\begin{aligned} ff_{WFB} &= ff_{\text{Take-off}} \cdot ff_{\text{Climb}} \cdot ff_{cr} \cdot ff_{\text{Descent}} \cdot ff_{\text{Landing}} \\ WFB &= (1 - ff_{WFB}) \cdot MTOW \\ ff_{FM} &= ff_{WFB} \cdot ff_{\text{Reserve}} \\ FM &= (1 - ff_{FM}) \cdot MTOW \end{aligned} \tag{2.4}$$

Where $MTOW$ is the maximum take-off weight of the aircraft. The performance parameters L/D, SFC and V are kept equal for both aircraft. They are chosen to be similar to a Boeing B737-800, a typical aircraft for both flights in the example.

The results of the fuel fraction calculations are given in 2.3.

Table 2.2: Performance parameters for both aircraft

SFC_{cr}	0.6	[1/h]
V_{cr}	860	[km/h]
L/D_{cr}	16	[-]

Table 2.3: Fuel fractions Eindhoven to Pisa and Faro

Destination	ff_{cr}	ff_{WFB}	ff_{FM}
Pisa	0.959	0.918	0.877
Faro	0.918	0.880	0.840

All aircraft from the database, appendix A, are used in the regression of figure 2.3. The relation between $MTOW$ and the Operational Empty Weight (OEW) is written in equation 2.5.

$$OEW = 0.4766 \cdot MTOW + 4674.2 \tag{2.5}$$

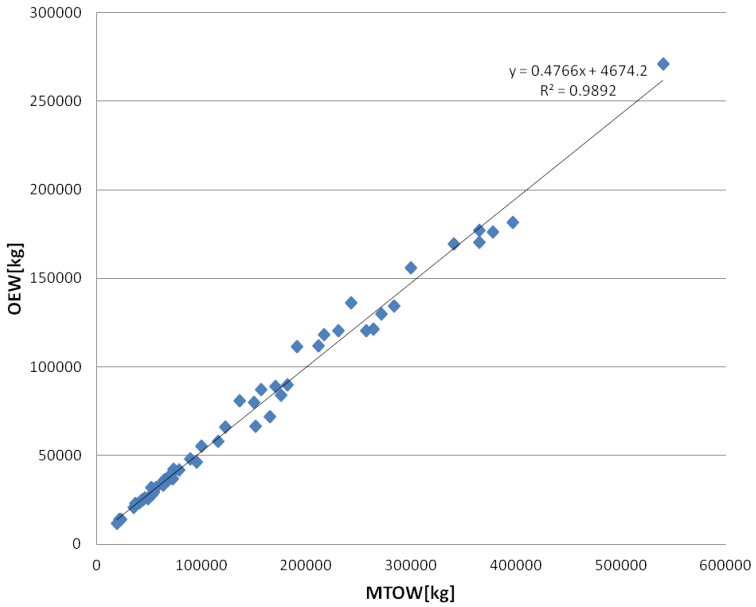

Figure 2.3: OEW versus $MTOW$

The payload is set to 189 passengers at 100kg/person, resulting in a WP of 18900kg. Assuming both aircraft take-off at their $MTOW$:

$$MTOW = WP + OEM + FM \tag{2.6}$$

Substituting, equations 2.3 and 2.4 into equation 2.6 together with the values from tables 2.1 and 2.2 the fuel weights and PRE values are obtained and reported in table 2.4.

Table 2.4: Fuel efficiency for Eindhoven to Pisa and Faro

Destination	R	WP	$MTOW$	WFB	PRE
Pisa	970[km]	18900[kg]	58927[kg]	4834[kg]	3793[km]/2048[nm]
Faro	1950[km]	18900[kg]	64874[kg]	7813[kg]	4717[km]/2547[nm]

This indicates that, for high-subsonic aircraft very short ranges are unfavorable for achieving high PRE values.

With similar calculations also the other side of the range domain, the very long range, is examined. The longest ranged flight to date is 15,345km from New York to Singapore, flown by an Airbus A340-500. It will be compared to a flight from New York to Tokyo 10,830km. The same routine is used as the previous comparison between Pisa and Faro, including the same fuel fractions indicated in table 2.1. To compute the cruise fuel fraction performance parameters similar to those of the Airbus A340-500 are used. The values are listed in table 2.5.

Table 2.5: Performance parameters similar to the Airbus A340-500

SFC_{cr}	0.545	[1/h]
V_{cr}	881	[km/h]
L/D_{cr}	20	[-]

Table 2.6 lists the fuel fraction of both flights.

Table 2.6: Fuel fractions New York to Tokyo and Singapore

Destination	ff_{cr}	ff_{WFB}	ff_{FM}
Tokyo	0.715	0.685	0.654
Singapore	0.622	0.596	0.569

The payload is set to 258 passengers at 100kg/passenger, resulting in a WP of 25800kg. The same class one weight estimation, as for the Pisa and Faro example, is used. Table 2.7 shows the resulting fuel weights and PRE values.

Table 2.7: Fuel efficiency for New York to Tokyo and Singapore

Destination	R	WP	$MTOW$	WFB	PRE
Tokyo	10,830[km]	25800[kg]	171576[kg]	54040[kg]	5171[km]/2792[nm]
Singapore	15,345[km]	25800[kg]	330009[kg]	133405[kg]	2968[km]/1602[nm]

This example shows that the highest PRE values are achieved at range shorter than this very long range of 15,345km and at a longer range than the very short mission from Eindhoven to Pisa (970km).

Figure 2.4 depicts the PRE values of existing aircraft. As already mentioned the A point PRE values of an aircraft are higher than its D point PRE values. Furthermore, the D point PRE values see a decline with very long ranges. The PRE decline for very short range is less pronounced because of the lack of D point at ranges shorter than 2500nm. For the A point values the trend is similar to that of the D points. Furthermore, the decline for very short ranges is for A points better visible.

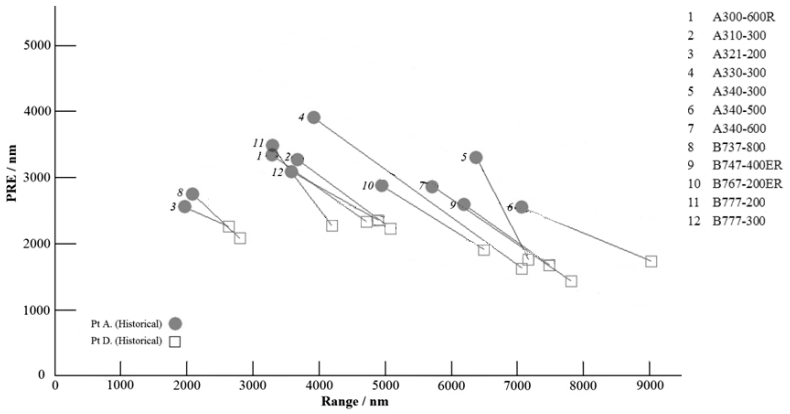

Figure 2.4: PRE vs Range relationships, from historical data [2]

In [3] Nangia describes, the effects of range on PRE. He plotted different weights as fractions of the $MTOW$ versus range for a number of existing Boeing and Airbus aircraft. The weight plotted were, OEW, WFB, WP, $(OEW + WP)$ and the reserve fuel weight (WFR). The plots were made for operation points A and D, respectively figures 2.5a and 2.5b. A difference between older engines and the newer High By-Pass Ratio (HBPR) engines can be observed. The newer engines have a lower fuel consumption, however they are bigger and heavier. This difference is visible by double trend lines for OEW, $(OEW + WP)$ and WFB. The top trend lines for OEW and $(OEW + WP)$ are for the HBPR engines due to their larger weights. For the WFB trend lines, the bottom one corresponds to the HBPR engines due to their lower fuel consumption and thus less required fuel.

The weight fraction plots have two functions. First off all, they are used to validated the weight division of the cruiser. Secondly, they can be used to computed PRE versus range plots using equation 2.7.

$$PRE[m] = \frac{WP/MTOW[-] \cdot R[m]}{WFB/MTOW[-]} \tag{2.7}$$

This new plot gives the opportunity to verify figure 2.4. The domain is almost the same as well as the average point A and D values, that respectively lie at PRE around 3500nm and 2000nm. Finally the higher PRE values lie in the middle of the domain for both figures. Concluding figure 2.6 is a good match to figure 2.4. Unfortunately no aircraft type names are attached to figure 2.6. It does however contain more point as figure 2.4 in proximity the cruiser design range (2500nm), make for better PRE comparisons to the cruiser.

Subsequently, it is of interest to find a trend in the PRE including the difference in performance parameters of the different aircraft. In order to do so Nangia uses the parameter X

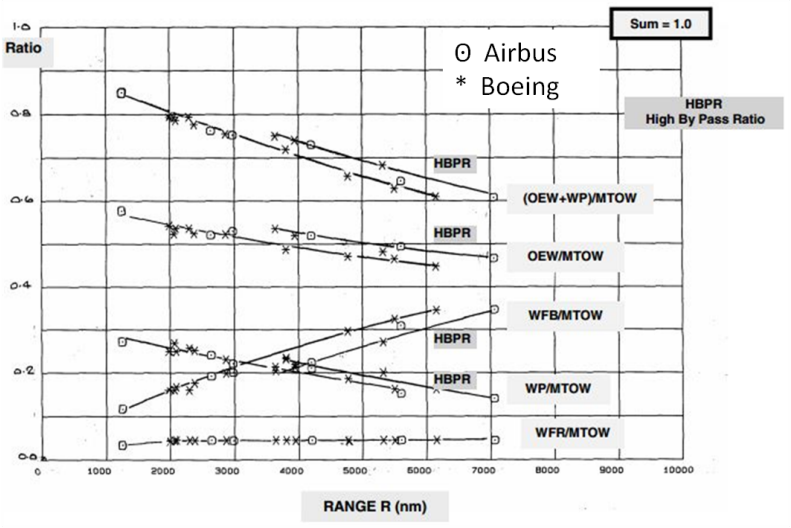

(a) Pt A, commercial aircraft

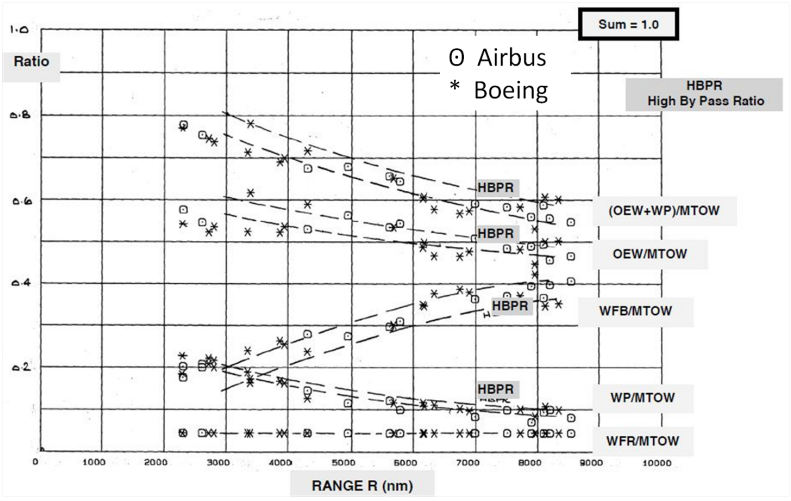

(b) Pt D, commercial aircraft

Figure 2.5: Derived fuel and payload ratio trends, from Nangia [3]

(2.8). Note that this parameter is derived from the Breguet range equation. Nangia uses this parameter to make a non-dimensional analysis. The parameter X includes the flight speed and the technology levels, lift-drag ratio and specific fuel consumption. The non-dimensional axis then become PRE/X and $Z = R/X$.

$$X[m] = \frac{V[m/s] \cdot L/D[-]}{SFC[1/s]} \tag{2.8}$$

Plotting the aircraft PRE values in a PRE/X and R/X frame of reference gives figures 2.7a and 2.7b. These plots clearly indicate the reduction of PRE/X with the increase in R/X.

Nangia creates trend lines (with constant X values) for the PRE/X versus Z, in the same article. Based on these trend lines, he concludes that: *An efficiency*[1] *improvement of 159%*

[1]With efficiency improvement all solutions that reduces fuel burn are meant. So with more efficient engines, better aerodynamic efficiency and lower structural weight a 9000nm aircraft can have the same fuel burn per kg payload per nm as a 3000nm aircraft. Would both aircraft have the same performance parameters the 9000nm aircraft would use 159% more fuel as the 3000nm per kg payload per nm.

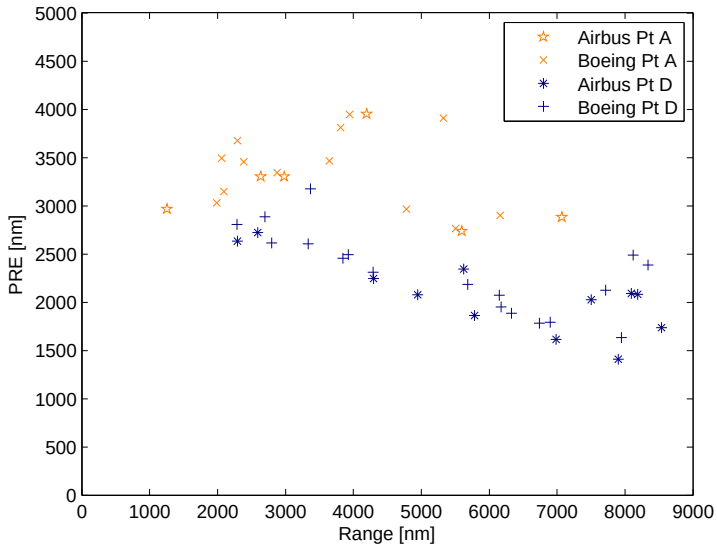

Figure 2.6: PRE and Range relationships based on weight fractions

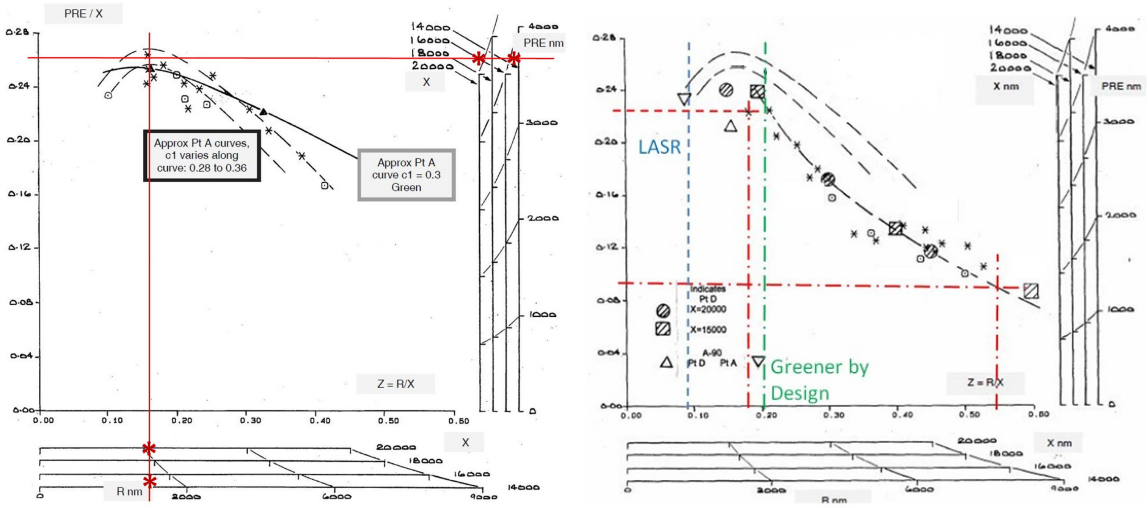

(a) Pt A, commercial aircraft

(b) Pt D, commercial aircraft

Figure 2.7: Derived fuel and payload ratio trends, from Nangia [3]

would be required for a 9,000nm range aircraft (at X = 15,000nm) *to achieve the same* PRE/X *level as a 3,000nm range aircraft*. This statement complies with the assumption needed for the IFR concept to be feasible, meaning that it is more efficient to fly 3 times 3000nm with one aircraft than once 9000nm with another (when both aircraft are designed for their assigned ranges).

Using data from literature the X values for a number of aircraft are calculated to get a better understanding of the magnitude of the numbers used in the different researches. The results are given in table 2.8.

The trend lines are X dependent, meaning that the optimum range, i.e. the range yielding

Table 2.8: Typical X values calculated with reference values, from [13]

Aircraft Type	X value	units
A380-800	$19 \cdot 10^3$	nm
B747-400	$15 \cdot 10^3$	nm
A320-200	$12 \cdot 10^3$	nm
B737-800	$12 \cdot 10^3$	nm
F100	$10 \cdot 10^3$	nm

maximum PRE, of an aircraft depends on its range parameter. Referring to figure 2.7a it can be observed that for X = 20,000nm maximum PRE (5200nm) can be obtained at a range of 3000nm. For X = 15,000nm, the maximum PRE (3900nm) would be achieved at a range of 2250nm.

For the D points, figure 2.7b, the trend line seems to increase with decreasing range. The trend line runs out of data points however before a maximum is reached. The reference values only go as low as $PRE/X = 0.18$. This would comply for X = 20,000nm to a PRE 4400nm at a range of 3600nm and for X = 15,000nm to a PRE 3300nm at a range of 2700nm.

Reflecting on the relation between fuel efficiency and range the following conclusions can be drawn:

- Aircraft operating at their A point show better PRE values, than when flying on their D point. This improvement in PRE is only useable when the requirements feature the transport of passengers and cargo. However, the requirements of the Recreate consortium do not include cargo for the 2500nm mission.
- The optimum range, for high PRE values depends on the X parameter. For X = 15,000nm the highest PRE value for a D point is found at a range of 2700nm. A long range aircraft with the same X value will have a significantly lower PRE value. A range of 8100nm yields a PRE value of 1350nm. Concluding, it seems promising to break flights of around 5400nm into two parts and longer flights of about 8100nm into three part of 2700nm.
- X values are important to the PRE value. In table 2.8 a tendency can be detected that bigger aircraft tend to have larger X values, suggesting that the cruiser with its high payload requirements can a higher PRE than aircraft of smaller size flying the same mission lengths.

2.2 Conceptual designs for staged flight

The previous section favored shorter (2700nm) ranges and big aircraft. Therefore, this section will analyze some large payload short range aircraft concepts, intended for normal or staged flight operations.

The Greener by Design report [16] finds a range for optimum PRE value to be 3240nm. The Green by Design group used a value of 16,512nm for X. Resulting in a PRE/X value of 0.196. This line is plotted in figure 2.7b. Furthermore two aircraft were designed: a short range version designed for 2700nm (5000km) and a long ranged version designed for 8099nm

(15000km). A 40% increase in fuel burn was found, when the large range aircraft flew a 8099nm mission, compared to the short range aircraft flying three 2700nm missions.

A report by Hahn [4] includes a redesign of the Boeing 777-200HG. The redesign is done for a 2700nm (5000km) range instead of the original 8099nm (15000km). Payload requirements are kept constant, hence the entire fuselage size is kept the same. The lifting surfaces are modified in order to comply with the lower WFB necessary due to the range reduction. The results of this redesign can be seen in figure 2.8. Hahn concludes that *Using three stages for a total of 15,000 km would likely yield a 17% improvement from operation alone, a further 12% improvement from redesign for the 5,000 km stage length, resulting in a total possible improvement of 29%.*

The research of Greener by Design and Hahn show some variance in the results. Nevertheless, they demonstrate the fuel can be saved using segmented flight instead of non-stop operations. This contributes to legitimacy of the RECREATE research on IFR operations. Furthermore, also the design of a new aircraft is justified, since the researches state that aircraft specially designed to the specific staged missions can further improve fuel consumption.

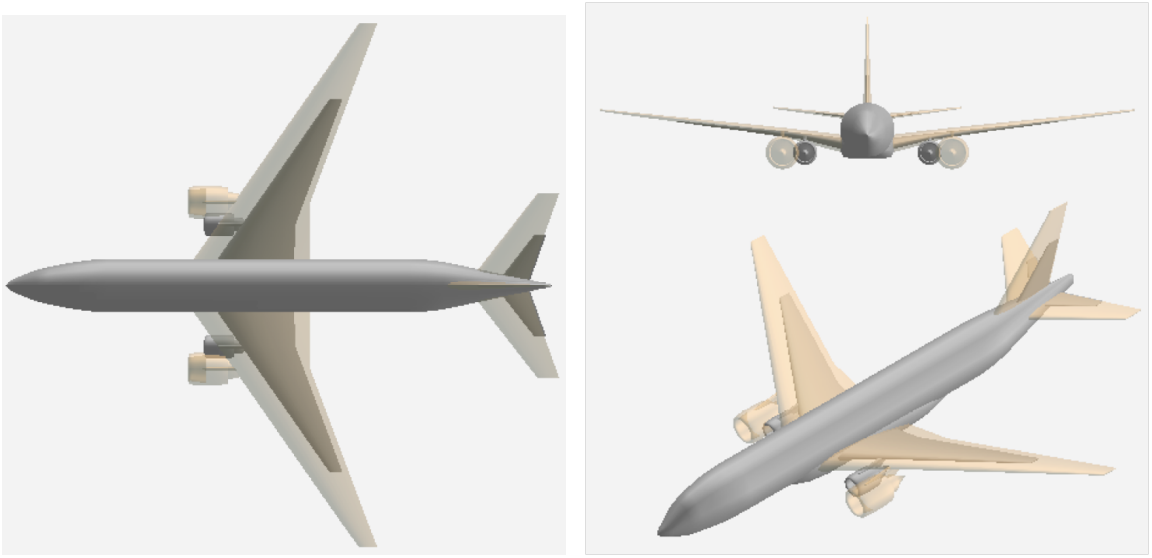

(a) Top view

(b) Front and isometric view

Figure 2.8: Top, front and isometric view of Hahn's redesign of the Boeing 777-2000HG, from Hahn [4]

These examples point out that there is a benefit on fuel efficiency when long flights are split up in segments of around 3000nm. Another interesting point in the range domain is the operation of an aircraft on a very short range. Kenway [18] introduces in his article a Large Aircraft for Short Range (LASR). This aircraft is designed to carry 279000kg on a 1500nm range (D point). It is more fuel efficient at a ranges equal to and smaller than 1500nm, than a small aircraft with a medium range (A320) and a large aircraft with a large range (A330-200).

Unfortunately the A point of LASR is not specified in the article. Anyway it is possible to compare the PRE of its D point to that of the reference aircraft. The PRE is 2595nm, which is higher than all other design point PRE values. The range parameters is about 16700nm,

which is also high for short ranged aircraft. Nevertheless, no sign of a PRE decrease is found for this short range. A decrease is expected when the range gets below a minimum range as explained by the example flights from Eindhoven to Pisa and Faro. Furthermore also the graphs from Nangia predict this decrease. Plotting the result in the Nangia figures, $Z = R/X = 1500/16700 = 0.9$, it can be seen that the aircraft is still near the top of the trend lines, see figure 2.7.

The conclusions of this section are listed below.

- Design studies for staged operation show improvements in fuel consumption when dividing long missions into multiple shorter missions.

- Although larger aircraft feature better X values, flying short missions with aircraft designed for larger missions is worse than using a redesigned aircraft for the specified short range. This is due to the extra unused capacity of the large aircraft. Operating aircraft below $MTOW$ implies that the structure is able to support more weight than it is actually used for, thus it is over dimensioned, resulting in an unnecessarily high OEW.

2.3 Discussion of in-flight refueling benefits with respect to staged flight

In-flight refueling could be better than staged flight for a various of reasons. First, of all the mission time for the cruiser would be less in IFR operation than in staged flight operation, since the aircraft would not have to land an take-off again, hereby increasing the passenger comfort and the turnaround time of the cruiser. The absence of extra take-off and landing has further benefits on the absence of extra take-off and landing fees, less fatigue loading on the fuselage due to the pressurization and less tyre wear. Furthermore, IFR has the fuel consumption benefit that it does not have to take-off and land. This action has however to be performed by the tanker. The tanker, specially designed for the transport of fuel might be able to outperform the cruiser in fuel efficiency in the process of obtaining the necessary fuel for the cruiser.

The following chapter try to compare the two approaches, by designing dedicated aircraft en estimating their fuel consumption. The fuel fuel consumption of the tanker does however have to come from literature since no tankers are designed.

Chapter 3

Cruiser-tanker close flight configurations for in-flight refueling

Before any cruiser design can be made the consequences on the cruiser of the IFR operation have to be considered. This chapter therefore, discusses upon the best cruiser-tanker configuration during the refueling maneuver and the consequences that the configuration has on the requirements of the cruiser.

The first section provides a historical overview of IFR, to investigate the evolution of in-flight refueling, from the first pioneering attempts until today where IFR operations are common in military aviation. The possibility to apply refueling configurations in commercial airliners airliners is then discussed.

Although current IFR operations with military aircraft always see the receiving aircraft approaching the tanker from behind and below in view of applying IFR to civil operation, the whole process is rediscussed and some alternatives are proposed. A systematic trade-off process is performed to select the most convenient procedure for a passenger aircraft to get refueled in the flight by a dedicated tanker aircraft.

3.1 Historical overview

Aerial refueling, also called air refueling, in-flight refueling (IFR), air-to-air refueling (AAR) or tanking, is the process of transferring fuel from one aircraft (the tanker) to another (the receiver) during flight [19]. The early pioneers of in-flight refueling used IFR to set records in distance and flight duration. Nowadays the military uses IFR to increase the range of combat aircraft such that they can achieve mission ranges, which would otherwise be impossible.

The first mid-air refueling between two planes occurred in 1923, between two Airco DH-4B biplanes of the United States Army Air Service. The aircraft were slow-flying and stable enough to perform the refueling with a hand-held hose. The connection was made by the pilot of the receiving aircraft. He manually catched and connected the hose for the refueling.

Gravity was used to transfer the fuel. In the same year an endurance record was set by three DH-4Bs, one receiver and two tankers. The receiving airplane remained aloft for more than 37 hours using nine mid-air refuelings. In 1929, a group of U.S. Army Air Corps fliers set an endurance record of over 150 hours. In 1930, the brothers John, Kenneth, Albert, and Walter Hunter set a new record of 553 hours 40 minutes using two Stinson SM-1 Detroiters as refueler and receiver.

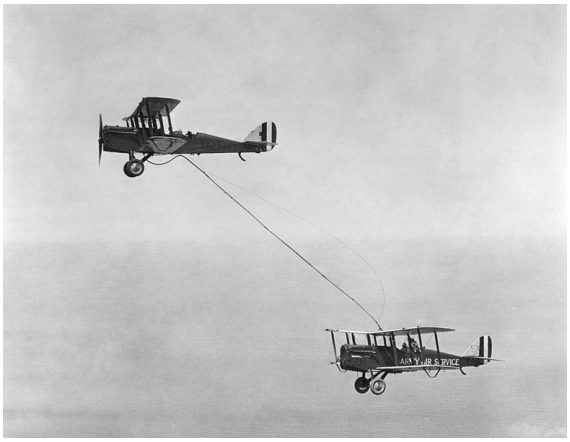

Figure 3.1: Capt. Lowell H. Smith and Lt. John P. Richter performing the first mid-air refueling in history (1923) [5]

Although the first successful IFR operations were performed by military aircraft for the sake of setting endurance records, the first serious use of IFR took actually place for civil applications. At the beginning of the 1930ties, people were considering trans-Atlantic flights for a faster postal service between Europe and America. In 1931, W. Irving Glover wrote an article concerning the challenges and the need for such a regular service and he mentioned the use of aerial refueling as a possible solution.

In 1934, A. Cobham founded Flight Refueling Ltd (FRL). One year later, the dangerous process of in flight refueling was tackled by a spill-free refueling nozzle designed by A. D. Hunter, not to be confused with one the four brothers from the endurance record. In 1938, FLR used their own IFR system to refuel aircraft as large as the Short Empire flying boat Cambria. Handley Page Harrows were used in the 1939 trials to aerial refuel the Empire flying boats for regular transatlantic crossings [20].

FRL was making use of the so called looped-hose system, which worked as follows: the receiving aircraft trailed a long horizontal line with a grapnel at the end. The tanker trailed a weighted line and approached the receiver from above, behind and to one side. It then crossed to the other side, causing the two lines to cross and touch. The receiver aircraft then hauled in the lines and the hose from the tanker. The RAF continued to refine this system, adding a drogue, which is a special type of parachute, to the hose. The drogue's purpose was to created drag to assist unrolling the hose and to ensure that the hose, when trailing behind the airplane, did not flap around, but remained at a steady position [21].

Later versions of the looped-hose system featured a tanker that approached from below and to the side. The tanker would launch a 300ft weighted line, the contact line, over the trailing line of the receiver. The fuel hose that was attached to the contact line was wheeled in by

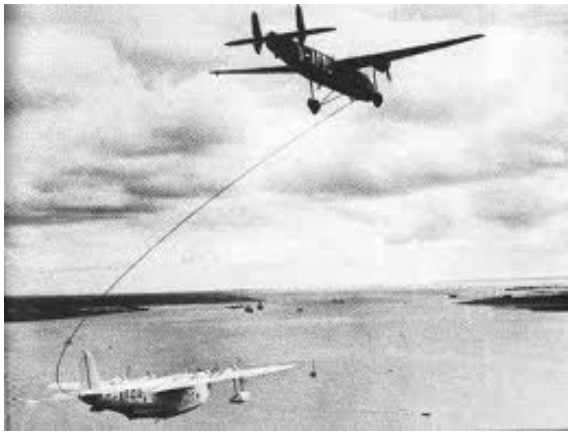

Figure 3.2: Flight Refuelling Ltd operated four Harrow tankers. One, shown here, 'tops up' an Imperial Airways 'C' Class flying-boat over Southampton's dock area prior to the non-stop transatlantic air mail service in 1939 [6]

the receiver. Hereafter, the tanker would ascent and use gravity transfer the fuel. However, this technique required low altitudes below 10,000ft and low airspeeds [22].

After the war, aircraft range had increased in such a manner that in-flight refueling was not necessary anymore for the trans-Atlantic crossings and refueling operations were limited to military operations. Since then, IFR remained limited to military operations.

Military refueling operations

At the end of World War II, plans were made to make use of the FRL looped-hose systems in operations against the Japanese homelands, however the war ended before the plans could be implemented.

The main disadvantage of the looped-hose system was the necessity of manual operation to make the connection between the two aircraft. To give crews a workable environment, the refueling procedure had to be done at low altitude where pressurization was not required. FLR began to work on an improved system, known as the probe-and-drogue system. The probe-and-drogue system was used by the Lucky Lady II to make the first non-stop flight around the world in 1949. Although this version still required the tanker to let out a cable which the receiver grabbed and wheeled aboard, the system was automated to such an extend that IFR could be carried out at high altitude [23].

Soon after the probe-and-drogue system was launched, the aft attachment point of the drogue and the wheeling in procedure, as inherited from the looped-hose system, changed to the use of a real probe on the receiver. The first use of aerial refueling in combat took place during the Korean War, involving F-84 fighter-bombers refueling from converted B-29s. This new probe-and-drogue system featured a probe located at one of the F-84's wing tips.

In the late 1940s, General Curtis LeMay, commander of the Strategic Air Command (SAC), asked Boeing to develop a refueling system that could transfer fuel at a higher rate than the probe-and-drogue system. The concept developed by Boeing was the flying boom system and the B-29 was the first aircraft to employ it. Between 1950 and 1951, 116 original B-29s,

Figure 3.3: In 1949, the Lucky Lady II was the first plane to circle the world nonstop–made possible with a fuel-delivery plane that refueled the bomber four times in the globe-circling flight [6]

Figure 3.4: 43rd Air Refueling Squadron KB-29M Superfortresses refueling 48th Fighter Wing F-84s over the Philippines, 1953 [7]

designated KB-29Ps, were converted by Boeing. In this concept a boom operator works from a station in the rear of the aircraft and control the boom using ruddervators. Ruddervators are control surfaces that combine the rudder and elevators functionalities. The ruddervators are visible on the boom as two small wings. The receiver aircraft has to take position 10ft behind and 25ft below the tanker. The boom operator then extends the boom into a socket in the receiver aircraft. The benefits of this system are higher reliability and capability to transfer fuel at a higher rate. Moreover, the method requires less skill from the receiver pilots, since the responsibility of making the connection lies mostly with the boom operator instead of the pilot of the receiving aircraft, who only needs to maintain a certain relative position to the tanker. An interesting detail in figure 3.5 is the extension on the rear of the B-29, which features a cable for the retraction of the boom.

Hereafter, Boeing developed the KC-97 Stratotanker. This tanker was based on the piston driven Boeing Stratocruiser, or B337. Extra kerosene tanks fed the boom, since the pistons worked on gasoline and the receiver aircraft were kerosene powered. Nonetheless 816 tankers were built. Furthermore, for the first time a transport aircraft frame was used as the base for a tanker aircraft. Something that remained the norm until today.

After the KC-97, Boeing began receiving contracts from the USAF to build jet tankers. The main advantages being that the same fuel could be used for the tanker and the receiver

Figure 3.5: United States' Boeing B-29 Superfortress bomber refueling a F-86 with the boom system [8]

aircraft. Furthermore, tanker aircraft would be able to reach similar speeds as the receiver aircraft, allowing high subsonic cruise formation. The high subsonic cruise formation is for instance used when fighter aircraft have to be moved from one airbase to another over long distances. Receiver and tanker take-off from the same base in this case and fly the same route. The formation removes the intercepting procedures, in which tanker and receiver have to meet up with each other, when departed separately. Furthermore, it can reduce fuel consumption due to the decrease of induced drag in formation flight. The design made by Boeing was based on the B367-80 airframe. The result was the Boeing KC-135 Stratotanker, which entered service in 1957. A total of 732 of these aircraft were built.

Figure 3.6: A B-52D, lower left, is refueled by a KC-135, upper right, Spain on 17 January 1966 [5]

Although the disadvantages of a lower fuel flow rate, lower reliability and a higher required receiver pilot skill, the probe-and-drogue system remained in use due its simplicity and size. It did not need a boom operator and could be installed on the tanker airframe as a pod. Meaning that a tanker could carry two or even three probe-and-drogue systems. Tankers with multipoint probe-and-drogue systems can allow two or three aircraft to refuel simultaneously. Tanking two aircraft simultaneously can reduce the time spent refueling by as much as 75% for a four aircraft strike package [24]. Furthermore, the probe-and-drogue system features a hose that approaches the receiver at a more horizontal angle. This makes the probe-and-drogue system more suitable for helicopter refueling, since the hose does not come in contact with the rotor, in contrast to the more diagonal approach of the refueling boom.

Today four boom carrying tankers are in service, five if one would include the B747s used by the Iranian Air Force. These four tankers are the Airbus A330 MRTT, the Boeing KC-135 Stratotanker, the McDonnell Douglas KC-10 Extender and the Boeing KC-767. Whereas the

Figure 3.7: Airbus A330 MRTT tanker refueling two F18s at once, from [5]

list of aircraft capable of carrying a probe-and-drogue system is significantly longer and ranges from fighters to tankers aircraft and many different air forces.

Evaluation of the historical overview

Two different IFR systems are in use today, the probe-and-drogue and the flying boom system. The advantages and disadvantages of flying boom with respect to the probe-and-drogue system are listed below:

Advantages:

- Higher fuel flow rate: 4600l/min versus 2650l/min for probe-and-drogue [25]
- Higher reliability
- Less susceptible to adverse weather conditions
- Does not require the fitting of refueling probes on receiving aircraft.
- Lower workload for the pilot of the receiving aircraft. (Most of the workload to connect the boom is for the boom operator.)

Disadvantages:

- Requires a dedicated boom operator. However, due to fly-by-wire technology the operator can be seated inside the cockpit.
- Heavier then probe-and-drogue.
- The size of the boom has limited use to larger tanker aircraft, while probe-and-drogue systems have been installed on smaller aircraft such as fighter aircraft.
- Can only refuel one aircraft at a time.

- The maximum separation distance in flight direction in shorter, due to the weight associated with the boom.

- The maximum separation in span wise direction is lower, although the boom can be steered left and right its attachment point lies always at the centerline in contrast to the probe-and-drogue systems. This prevents tanker and cruiser to fly in an V formation. Such a formation is flown by birds and combat aircraft for aerodynamic benefits.

3.2 In-flight refueling configurations trade-off

Although, IFR operations (and refueling systems) are time-proven in military operations civil applications of IFR will require considering some different and special aspects related to safety, passenger comfort and pilot workload. Hence, other formation flight configurations for IFR are considered, than the classical approach where the receiving aircraft flies behind and below the tanker and a systematic trade-off process has been performed to select the most convenient configuration for passenger transport application.

Since the relative positioning of the receiving aircraft with respect to the tanker is likely to have an impact on the architecture and internal layout of both aircraft, as well as on the design of the fuel transfer system and its operations, it was considered opportune to describe the performed trade-off in details, as reported here below and in the following sections.

The overall process of identifying, assessing and selecting various approach configurations for in-flight refueling is organized as follows:

- A preliminary design option tree is presented, where different fuel transfer systems are taken in consideration and logically organized. A first round of selection is performed where the least convenient or unfeasible solutions are eliminated. The rationale of each concept elimination is properly recorded.

- The survived nodes of the option tree are further expanded to consider all possible relative positioning of cruiser and tanker during aerial refueling operations. Again, the least convenient or unfeasible solutions are eliminated and decision rationale recorded.

- All possible approaching procedures are analyzed for the relative positioning solutions that survived the previous selection. Once again, the least convenient or unfeasible solutions are eliminated and decision rationale recorded.

- Formation aerodynamics are investigated to support an assessment of related score 'Formation aerodynamics'.

- An actual trade-off process is set up to compare the (four) remaining configurations. Twelve trade-off criteria are identified with relative weights. Criteria definition, assignment of weight, and scoring system are all documented.

- All concepts are graded and one winning concept identified.

3.2.1 Fuel transfer system

Before doing any configuration trade-off, it is important to (re)consider all the possibilities. The design option tree in figure 3.8 shows all possible fuel transfer systems.

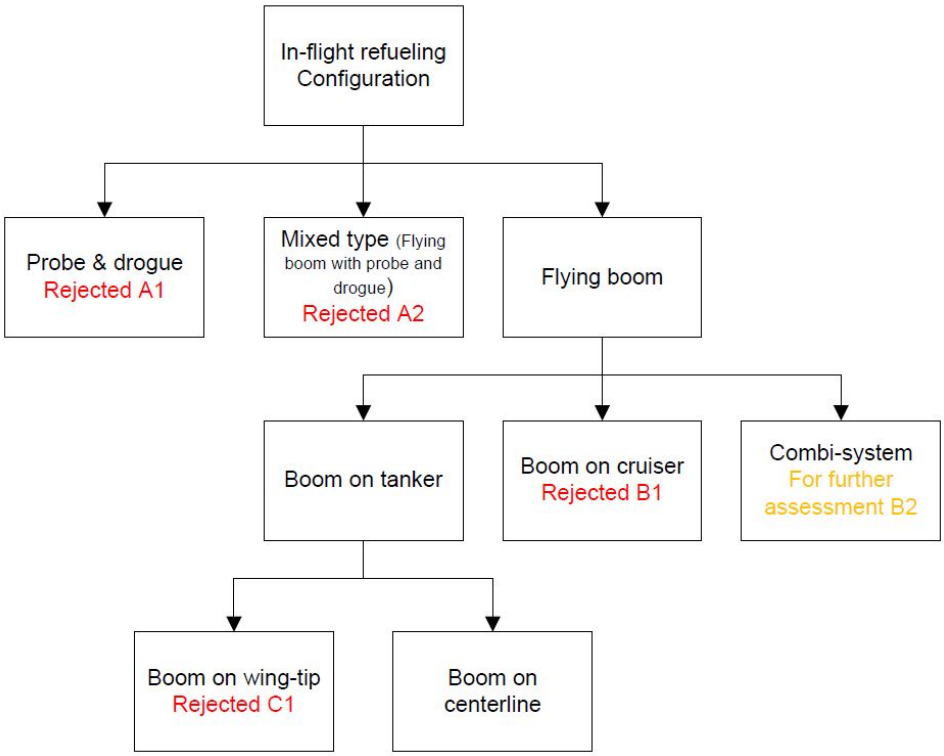

Figure 3.8: Design option tree fuel transfer system

Rejection motivation are stated below:
A1 Probe-and-drogue systems provides a too low fuel flow rate. The mass flow rate is a little over half of that of a flying boom system, 2650l/min versus 4600l/min [25], which means double refueling time. (The 2650l/min is for the fuselage mounted 805E Fuselage Refueling Unit, wing mounted 905E Wing Pods have even lower flow rates, 1703l/min. [26])
A2 Although this approach would enable more separation between both aircraft, a real mixed system will share fuel flow rates with the weakest link so those of the probe-and-drogue system and this is not enough. A flying boom system where the receptacle has some degrees of freedom is potentially possible, this is discussed at B2.
B1 Having a flying boom and boom operator on the cruiser will add to weight, performance and cost at a level that the benefit from the in-flight refueling will be severely compromised.
B2 (For Further Assessment) Having a short extending receptacle on the cruiser would allow a larger separation to the tanker and limit the length of the boom. However, this would increase the cruiser drag and increase the complexity of the overall system. Moreover, no such technology has yet been developed.
C1 Boom on wing-tip can provide wing-tip to wing-tip refueling. In this formation, the aerodynamic interference is beneficial. However, the wing-tip is flexible and vulnerable. Besides, extending a boom at wing-tip could cause great asymmetric moment.

Conclusion

As illustrated in figure 3.8, the most convenient refueling systems appears to be those where a flying boom is mounted on the tanker, aligned with its fuselage center line. The possibility of installing a short extending receptacle on the cruiser might also be investigated.

3.2.2 Relative tanker-cruiser positions during formation

With the fuel transfer system selected, all the possible relative tanker-cruiser positions for refueling are considered, see figure 3.9. The rejection motivations are listed below.

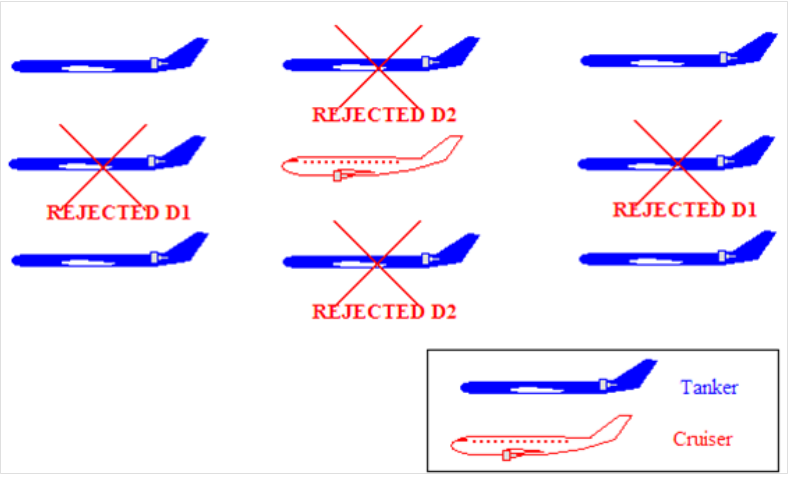

Figure 3.9: Relative tanker cruiser positions

D1 If the two aircraft fly in close formation at the same altitude, the wake from the front aircraft will strongly disturb the rear one. Besides, hot exhaust gas from the engines of the front aircraft can cause hot air ingestion to the engines of the rear aircraft. Moreover, without any vertical separation, any uncontrolled speed difference might create chances of collision.
D2 When two aircraft fly in close formation with one on top of the other, there are several problems:

- The collision potential becomes more severe because of the lose of the vertical degree of freedom for both aircraft, as shown in figure 3.10. If any aircraft experiences a gust (horizontal or vertical), there is a greater chance of collision.
- In overlapped close formation, the two planes look like a biplane, with strong negative aerodynamic interference between two pairs of wings, reducing total L/D and causing control difficulty. Figure 3.11 illustrates that in the conventional staggered refueling configuration, the two aircraft should always have a vertical degree of freedom. Therefore, a staggered configuration is required.
- Visibility is an isue since both pilots will lose visual contact if the aircraft are in overlapped formation.

Several possibilities exist for the location of the refueling receptacle on the airframe of cruiser. Wing mounted systems are not considered as the reason stated in figure 3.8. Figure 3.12

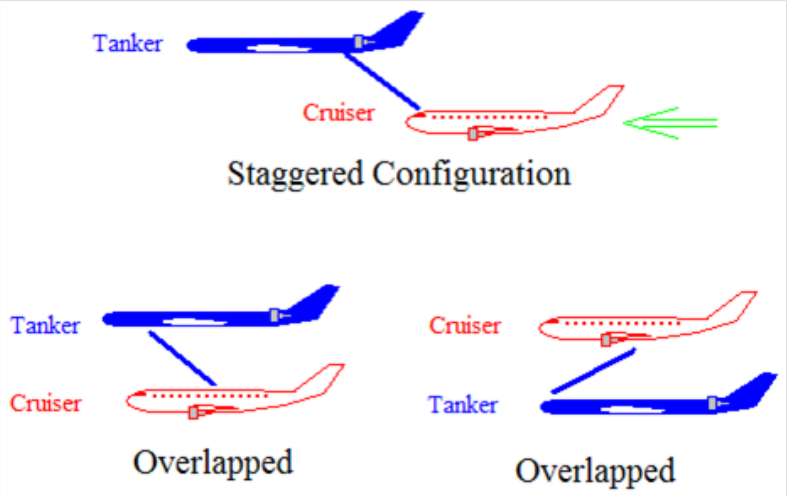

Figure 3.10: Overlapped configurations limit vertical degree of freedom for both aircraft compared to a staggered configuration

Figure 3.11: In current military in-flight refueling operations, tanker and receiver maintain vertical degree of freedom. Given the typical boom length, it should be noted how close the two airplanes should fly if not in a staggered configuration.

shows seven possible locations on the fuselage:
Point 1. on top of the fuselage nose,
Point 2. at the bottom of the fuselage nose,
Point 3. at top center of fuselage,
Point 4. at center bottom of fuselage,
Point 5. at rear bottom of fuselage, at bottom of fuselage,
Point 6. on top of the fuselage in case of a "U" or "H" tail-plane layout or on top of the vertical fin,
Point 7. at the end of the tail cone.

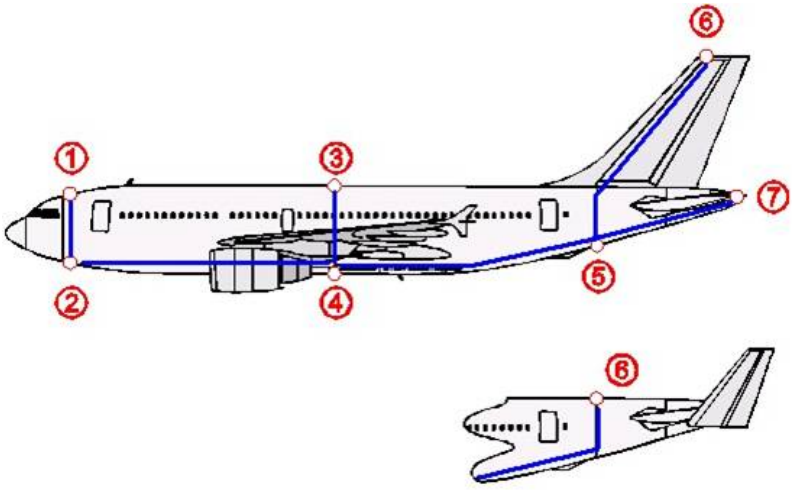

Figure 3.12: Possible fuselage mounted refueling points. The lower tail end shows alternative for point 6 in case of a "U"- or "H"-tail.

The characteristics of these receptacle points are listed as below:

- For staggered configuration as suggested above, point 3 and 4 are not favorable since these point make horizontal separation between both aircraft hard to achieve.
- Point 1 and 3: fuel is transferred though or around the cabin to the wing tanks of the cruiser, which is not favorable for safety considerations of fire issues. However, point 1 is the most convenient for conventional refueling configuration, which requires minimum modification on current aircraft.
- Point 2, 5, 6 and 7 have similar fuel transfer route: fuel pipe should pass under cabin floor. Such a schema has better safety character than point 1 and 3 in terms of fire hazard.
- Point 6 on top of the vertical fin and point 7 seem to be unrealistic from structural and systems considerations. The alternative point 6 on top of the rear fuselage however may be a realistic choice, but would require an unconventional tail configuration as illustrated in bottom of figure 3.12.

Conclusion

In order to maintain sufficient freedom of vertical movement, a staggered flight configuration is required. Receptacle points 2, 5, 6 and 7 are more convenient to maintain staggered refueling formation, while lowering fire hazard, because fuel pipes do not have to go through the cockpit or cabin.

3.2.3 Approaching procedure

Apart from the relative position during formation, also the possible approach methods to get in formation need to be evaluated. The identified possibilities are illustrated in figure 3.13.

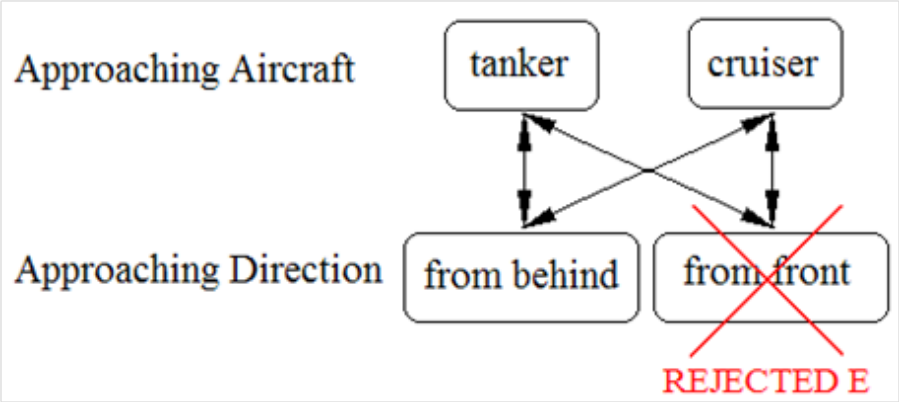

Figure 3.13: Approaching Possibilities

The approach from the front is discarded because of the following safety related motivations:
E1 When one of the two aircraft decelerates to join the following in a formation, there is no need for the following aircraft to use extra thrust (and fuel). However, when sufficient proximity is reached, the decelerating aircraft should again increase thrust to reduce the closing rate. If something goes wrong, there is less room left for the pilot to deal with, because more time is required to increase thrust and accelerate than vice versa.
E2 Aircraft usually have poor rear visibility. It is hard for approaching pilots to see the other plane behind. The increased risk of losing direct visual contact to the other can violate regulation of in-flight refuel based on military experience. One of the important criteria is the approaching aircraft should always have clear and stable contact to the other. "Operations are based on visual separation - losing visual contact is one of the hazards that may occur." and "any aircraft in close formation that loses visual contact will the tanker or the receiver upon which it is formatting is to take immediate action to achieve safe separation from the tanker, and if necessary, other receivers."

Conclusion

In order to guarantee safe refueling operations, the approaching aircraft should come from behind. This would facilitate a continuous and stable visual contact, as well as a high level of reactivity in case separation is required.

Figure 3.9 and figure 3.13 together leave only 4 possibilities, shown in figure 3.14. It should be noted, that the classical military configuration found in the historical overview is represented by option A. Configurations C and D require the use of a forward extending boom. Such a systems may have aeroelastic issues, which will increase the development difficulty for the boom system. Nevertheless, given that the design of a forward swept boom is possible the configurations C and D are promising.

3.2.4 Formation aerodynamics

During the in-flight refueling procedure formation aerodynamics are important to investigate. Negative aerodynamic effects can not only influence the selection of the configuration they

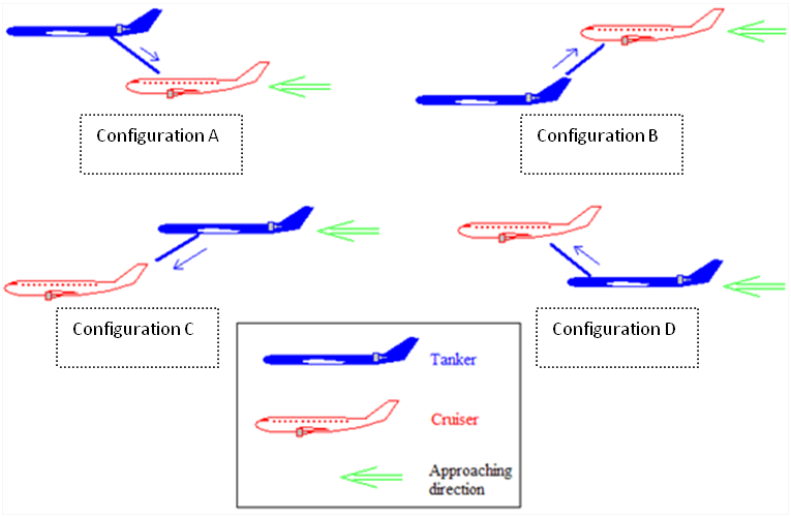

Figure 3.14: Four most promising configurations for In-flight Refueling

can also impose extra requirements on both aircraft. In this section the wake flow field is described. Then, a simple quantitative analysis is carried out.

Wake flows

The generation of lift is associated with the deflection of the free stream flow velocity. Amongst other effects the presence of an aircraft creates areas where the air is deflected up (upwash) and areas where the air is deflected down (downwash). This is visualized in figure 3.15.

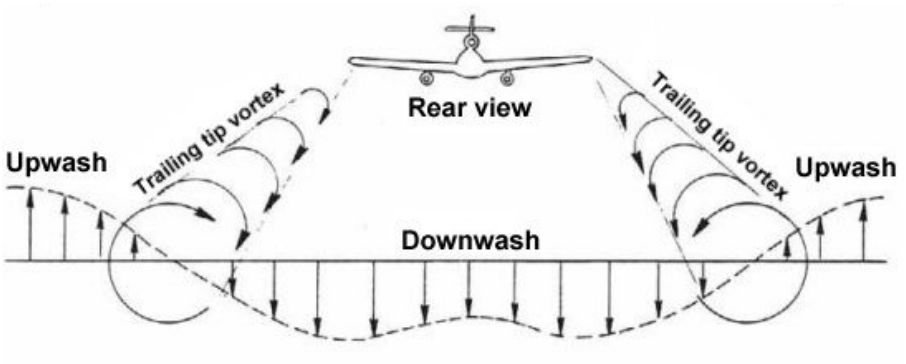

Figure 3.15: Visualization downwash behind an aircraft [9]

Since tanker and cruiser fly at close proximity during the refueling maneuver, they will be affected by each others presence. Flow information travels easier down than up stream at high mach numbers. Hence, the trailing aircraft is effected most. As shown in figure 3.16 the trailing aircraft will be effected negatively, if flying in-line with the leading aircraft, by the downwash. The leading aircraft is effected positively by the upwash of the trailing aircraft.

Flying in the downwash requires an increase in angle of attack and results in induced drag. A simple horse-shoe vortex model is used to predict the effects on the induced drag, as in an

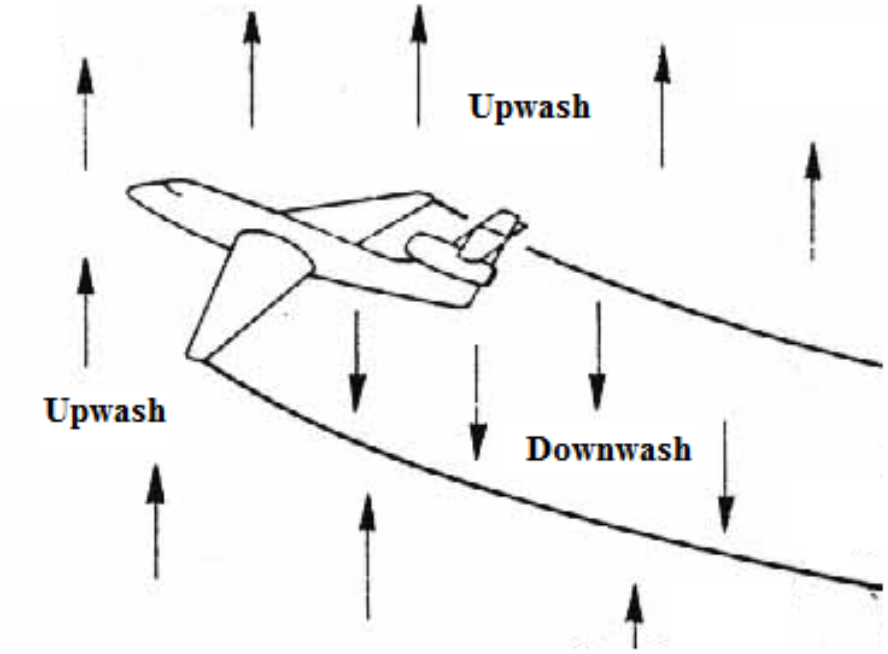

Figure 3.16: Visualization of up and downwash areas [10]

article by Blake and Multhopp [11]. Blake and Multhopp use Munk's theorem with infinitely spaced wings, (so that only the trailing vortices of the leading wing have to be considered), to come up with equation 3.1

$$C_{Di} = \frac{C_{L,1}^2}{\pi Ae} + \frac{C_{L,2}^2}{\pi Ae} + \frac{2C_{L,1}C_{L,2}\sigma_i}{\pi Ae} \tag{3.1}$$

Where, C_{Di} is the induced drag coefficient of the whole system including both aircraft. C_L is the three dimensional lift coefficient. Subscripts 1 and 2 denote the two different aircraft. The wing platforms of both aircraft are assumed to be equal. A is the aspect ratio of both wing platforms and e is the Oswald factor. The influence factor for induced drag σ_i is given in equation 3.2.

$$\sigma_i = \frac{1}{\pi^2} ln \left[\frac{\zeta^4 + 2\zeta^2(\eta^2 + (\frac{\pi}{4})^2) + (\eta^2 - (\frac{\pi}{4})^2)^2}{(\zeta^2 + \eta^2)^2} \right] \tag{3.2}$$

Where η is the lateral spacing between the wing centerlines Δy normalized with b (the wing span) and ζ is the vertical spacing between the wings Δz again normalized with b, see equation 3.3.

$$\begin{aligned} \eta &= \frac{\Delta y}{b} \\ \zeta &= \frac{\Delta z}{b} \end{aligned} \tag{3.3}$$

Figure 3.17 shows a plot of σ_i for varying η and ζ values.

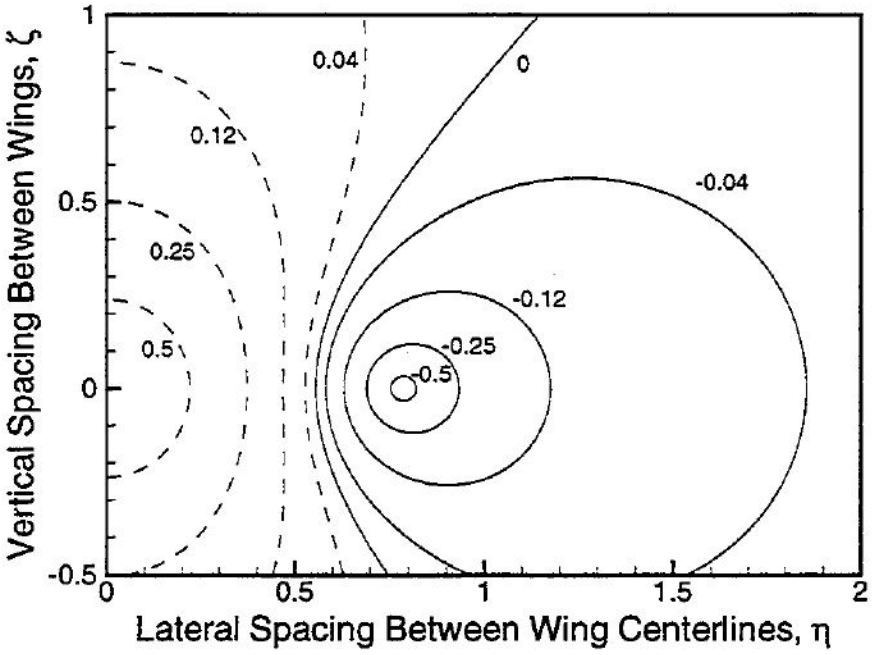

Figure 3.17: Induced drag increase due to relative position of both aircraft [11]

With the lateral separation not more than 0.2 wing spans (see figure 3.11), σ_i can go up to 0.5. Assuming that all effects of the wing interference fall to the trailing aircraft the last term of equation 3.1can be considered to be the extra drag experienced by the trailing aircraft. When using the same aircraft for leading and trailing aircraft:

$$C_{L,1} = C_{L,2} \tag{3.4}$$

The extra drag term becomes equal to the normal induced drag of the trailing aircraft. So the induced drag for the trailing aircraft will be double. Hence, the total drag, assuming a 50:50 distribution between lift depended and lift independent drag, will increase with a factor $3/2$, so 33.3%.

If the C_L of the leading aircraft is higher than that of the trailing aircraft or its aspect ratio lower (In other words if the C_{Di} of the leading aircraft is higher), the negative effects on the trailing aircraft will be even larger. This extra drag has to be compensated by extra thrust from the engines. However, the available thrust of a transport aircraft at cruise altitude is limited. The analysis of flight data sampled during typical transatlantic flights of an A340 reveals, that a typical step climb to adapt the cruise condition to the reduced mass is performed with a rather low climb rate of about 2 m/s (400 ft/min) at a flight speed of about 250 m/s (M=0.83) . Note that Airbus generally suggests for its larger airplanes to climb at 300 ft/min during cruise climb steps. This corresponds to a climb angle of only 1.3% and a required additional climb thrust of 20% of the cruise thrust. This implies that the engines of the trailing aircraft might have to be sized just to allow formation flight with extra drag.

Conclusions

The result of the brief investigation into the wake effects are summarized below.

- The aerodynamic efficiency may be reduced by more than 33% for the trailing aircraft in close formation.
  - The range of the tanker is shorter than that of the cruiser, which means it might be beneficial to put the burden of having extra thrust on the tanker, rather than the cruiser, in terms of total fuel consumption and operational empty weight. Furthermore, there are fewer tankers than cruisers. Hence installation costs of larger engines will be lower when the larger engines are installed on the tankers in stead of the cruisers.
- The trailing aircraft may experience similar downwash if located below or above the lead aircraft. Hence, the trailing aircraft will experience a similar loss of aerodynamic efficiency if it is above of below the leading aircraft.
- Size ratios between the trailing and leading aircraft have effect on the extra induced drag encountered by the trailing aircraft. It is beneficial to have smaller leading and a larger trailing aircraft. Also lower induced drag values for the leading aircraft compared to the trailing aircraft can help to reduce the extra induced drag encountered by the trailing aircraft.

3.2.5 Trade-off criteria

A trade-off process is set up to choose the most convenient of the four configurations left. The performance of the four proposed configurations will be evaluated with respect to a number of trade-off criteria. Each configuration is given a grade ranging from 1 to 9, where 9 is excellent performance and 1 is poor performance.

Each criterion is assigned a specific weight. The higher the weight, the more important the given criterion. The sum of the weights is 100. The score of a given configuration for a given criterion is computed, by multiplying the grade by the criterion weight. A total of 12 criteria have been identified. Their description and relative weight is given in table 3.1.

Table 3.1: Criteria of the trade-off

#	Criteria	Weight	Description
1	Pilot's visibility in the approaching aircraft	7	Pilots sitting in the approaching aircraft should easily achieve direct visual contact with the other aircraft. The visibility angle in the cockpit of the approaching aircraft can be used as measure for this criterion.
2	Component detachment hazard	10	It specifies the criticality in case a part or debris is detaching from the proceeding aircraft during close formation. When a fatal FOD accident happens to the tanker, the crew can bale out by ejection seats. But if the same happen to the cruiser, the consequence can be catastrophic.
3	Ride quality of cruiser	7	It accounts for passenger discomfort caused by the approaching maneuvers.

Continued on next page

Table 3.1 – *Continued from previous page*

#	Criteria	Weight	Description
4	Noise to the cruiser	4	It accounts for the increased noise level perceived by passengers during approaching and refueling.
5	Pump requirements	5	It accounts for the weight, power and reliability penalties caused by the installation of the refueling pump. Some configurations need more powerful pumps to contrast gravity.
6	Fuel pipe fire hazard	6	Failure of the fuel pipe can lead to fire. The location of the fuel pipe in the aircraft is of great influence to the severity of safety hazard resulting from this fire.
7	Boom structural weight	5	This accounts for the weight caused directly and indirectly by the boom. The first refers to the weight of the boom itself, the second to the modifications required, for example, to enlarge the tanker empennages to counteract the unbalancing effect of the reverse swept boom.
8	Boom stability	15	The forward swept boom will suffer from unstable aerodynamics and aeroelastic divergence problems. The solution can cause weight, complexity and cost penalties.
9	Maturity of Boom technology	14	Aft-up swept boom and forward swept boom require time and money to develop. This criteria concerns with the potential risk of development failure.
10	Formation aerodynamics	8	Formation flight can modify the overall aerodynamic efficiency of the two aircraft due to up/downwash and the interference of the tip-vortex on the following aircraft. This criteria is used to judge the aerodynamic efficiency of the system.
11	Training cost of approaching aircraft crew	9	Although autopilot can be used to reduce pilots workload, the pilot of the approaching aircraft must be able to operate manually as well. Maneuvering in the downwash of the proceeding aircraft can add to the level of difficulty, hence to skill and level of training of the pilot.
12	All weather refueling capability	10	"aircraft without radar or with only weather radar shall not proceed inside 1NM unless the tanker is in sight"[3] In order to perform all weather refueling operations, air-to-air radar is needed on the approaching aircraft. The larger feet of the approaching aircraft, the more cost to equip such kind of facility, the less grade a configure can get in this criteria.

3.2.6 Trade-off and selection

A grade (1-9) has been assigned to each of the four configurations, for each of the 12 criteria specified in table 3.1. The grades are based on analysis as much as possible.

#	Configuration	Grade	Description
1	**Pilot's visibility in the approaching aircraft**		
	approaching aircraft aft & below	9	current situation, most comfortable
	approaching aircraft aft & above	5	more downwards visual clearance is required
2	**Component detachment hazard**		
	cruiser front	9	passengers are at no risk
	cruiser behind above	3	
	cruiser behind below	1	cruiser most likely to be hit by any detached object in the formation
3	**Ride quality of cruiser**		
	tanker as approaching aircraft	9	no discomfort for passengers
	cruiser as approaching aircraft	1	passengers will feel the accelerations during the approaching maneuvers
4	**Noise to the cruiser**		
	cruiser front	9	cruiser receives least noise from tanker
	cruiser behind above	2	cruiser wings and cargo bay might provide some shield
	cruiser behind below	1	cruiser receives most noise from tanker
5	**Pump requirements**		
	cruiser below	9	same as current system. If pump fails, gravity will assist fuel transfer.
	cruiser above	8	pumping fuel against gravity costs 12kW (see Appendix for preliminary calculations), which is relatively low. However, backup pump(s) might be required adding weight and complexity.
6	**Fuel pipe fire hazard**		
	cruiser above	9	receptacle point 2 and 5 (as shown in Figure 6.5) can be used. The fuel pipes for refueling are of shorter route and do not have to go through and around pressurized cabin.
	cruiser front & below	7	receptacle point 6 or 7 can be used. The fuel pipe for refueling has to pass tail cone, where vital tail control systems are located.

	cruiser behind & below	5	only point 1could be served as receptacle, which leaves no other choice but fuel pipe goes through and around cabin.
7	**Boom related weight**		
	cruiser behind & below	9	short, aft swept boom can be achieved
	cruiser behind & above	8	in order to keep enough separation despite of fin(s) of tanker, the boom should be longer, yet still aft swept.
	cruiser front & above	2	short, forward swept boom should be developed
	cruiser front & below	1	long, forward swept boom should be developed
8	**Boom stability**		
	aft swept boom	9	naturally stable
	forward swept boom	1	use autopilot to maintain stability. Redundant control system for boom is needed to guarantee reliability. Tailored composite structure may be also required.
9	**Maturity of boom technology**		
	aft-down swept boom	9	current system
	aft-up swept boom	8	with current boom, but a new deploy system and control panel
	forward swept boom	1	completely new system
10	**Formation aerodynamics**		
	approaching aircraft @ above & below	5	approaching aircraft loss aerodynamic efficiency due to the downwash, regardless of being above or below the cruiser.
11	**Training cost of approaching aircraft crew**		
	tanker as approaching aircraft	9	only tanker pilots need be trained to perform the refueling approach. With frequent refueling actions (maybe 3 times per flight), it is easier for them to maintain proficiency.
	cruiser as approaching aircraft	1	all of the cruiser pilots should be trained to perform the refueling approach.
12	**All-weather refueling capability**		
	tanker as approaching aircraft	9	tanker should be equipped with air-to-air radar, along with other auxiliary sensors for close-in formation flight.
	cruiser as approaching aircraft	1	it is expensive to equip every cruiser with air-to-air radar

Conclusion

According to the weight and grading system described above, the final scores for the four short listed configurations can be computed. The trade-off results are shown in table 3.3.

The concept that scores the highest grade, hence the trade-off winner, is configuration D, which is again displayed in figure 3.18.

Table 3.3: Trade-off grading table

#	Criteria	Score				Weight	Score			
		A	B	C	D		A	B	C	D
1	Pilot's visibility of approaching aircraft crew	9	5	5	9	7	63	35	35	63
2	Component detachment hazard	1	3	9	9	10	10	30	90	90
3	Ride quality of cruiser	1	1	9	9	7	7	7	63	63
4	Noise to the cruiser	1	2	9	9	4	4	8	36	36
5	Pump requirement	9	8	9	8	5	45	40	45	40
6	Fuel pipe fire hazard	5	9	7	9	6	30	54	42	54
7	Boom related weight	9	8	1	2	5	45	40	5	10
8	Boom stability	9	9	1	1	15	135	135	15	15
9	Maturity of boom technology	9	8	1	1	14	126	112	14	14
10	Formation aerodynamics	5	5	5	5	8	40	40	40	40
11	Training cost of approaching aircraft	1	1	9	9	9	9	9	81	81
12	All weather refueling capability	1	1	9	9	10	10	10	90	90
	total					100	524	520	556	596

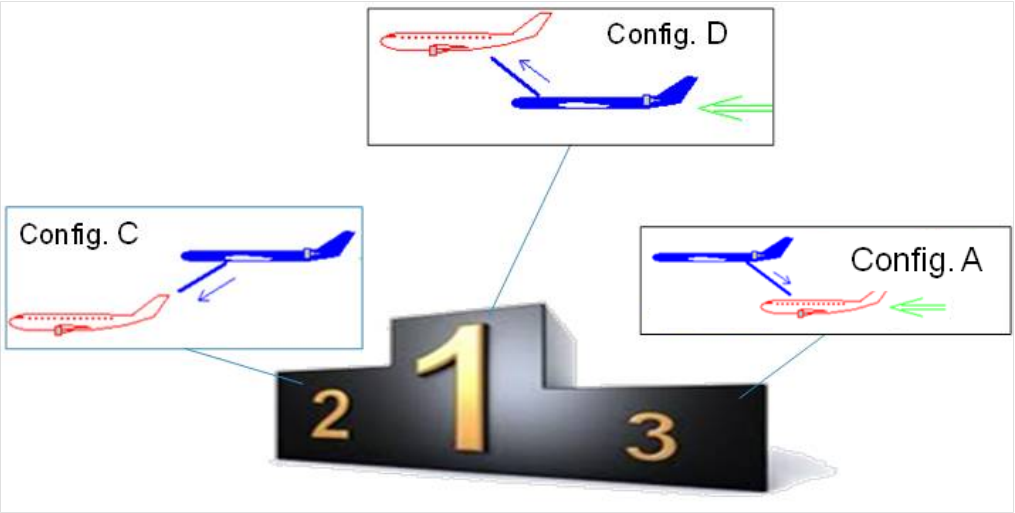

Figure 3.18: Configuration D, winner of the configuration trade-off

3.3 Discussion of the trade-off result

The winner configuration D has the advantages as below:

- Safety: no hazard of collision with parts and debris detaching from tanker
- Safety: in case of emergency, tanker can immediately separate by decelerating and reducing altitude, without any risk of collision

- Safety: no fuel pipe goes through or around the cabin (compared with configuration A); no fuel pipe crosses vital control equipment (compared with configuration C)
- Safety: tanker pilot has good visibility of passenger aircraft
- Safety/pilot training: cruiser pilot not required to perform approach maneuver, neither to fly in the wake of the tanker.
- Passengers comfort: passenger less exposed to flow perturbation and noise from tanker. Passengers not subjected to maneuvering acceleration
- Passenger aircraft architecture: passenger aircraft architecture minimally affected by the presence of the refueling system.
- Cost: Only tanker aircraft to be provided with air-to-air radar
- Performance: Cruiser engines not sized for formation flight

The challenges of configuration D are mainly concerned with forward extended boom

- A control system to fly the boom is required.
- A proper structural design to avoid divergence may be required if the boom has forward swept parts.
- A pump will be required to pump the fuel against gravity. Preliminary calculations show feasibility and low power and weight expenses [27].

The engineering difficulties are not expected to be technical show stoppers for the following reasons:

1. Technology already applied in the design of forward swept wings, such as tailored composite structures, can be used to develop the boom (or the wing like structure accommodating it)
2. The flying boom does not need to generate a lifting load in contrast to a forward swept wing.
3. Ruddervators at the fore-body of the boom can be used to balance and stabilize the boom.
4. A short drogue could be installed on the cruiser to shorten the boom length and consequently reduce the aerodynamic issues. (See option B2, figure 3.8)

An important consequence of the trade-off results is that, with the configuration selected, the cruiser design will encounter only minor modifications (with respect to a conventional aircraft configuration)to comply with this IFR configuration, apart from the expected downsizing of the wing and engines due to lower fuel weight to be carried. Therefore, the aircraft configuration can remain conventional and similar conceptual design tools as available for conventional aircraft can be used.

In case the forward boom would end up to be technically unfeasible, the most important change to the cruiser would be the required extra installed thrust to fly in the downwash of the tanker and a less convenient location of the fuel receptacle. Other aspects as crew work load and passenger comfort will effect the whole project, nevertheless the conceptual design (and required design tools) will not significantly change due to these consequences.

Chapter 4

Tool setup for conceptual design

As concluded in chapter 3 conceptual design tools, as available for conventional aircraft, can be used. The conceptual design tool used in the Initiator, The Initiator is described in the next section. The Initiator is not only used for the the generation of the cruiser design, but also for the other aircraft required for the fuel efficiency comparisons. The Initiator, as available at the beginning of this thesis has some limitations. These limitations are described in section 4.2. The current limitations have to be addressed before the Initiator can be used. The adjustments made to remove these limitations are also described in section 4.2.

4.1 The Initiator

The Initiator is used in this thesis for two main reasons. First of all, the fuel efficiency calculations require multiple conceptual designs. Therefore, it is beneficial to use an automated design process, such as the Initiator for the fast generation of conceptual designs. Secondly, the Initiator is an program under development at the TUD, allowing for full access to all files as well as all documentation of the program.

Langen [13] produced the first version of the Initiator during his thesis work at the Delft University of Technology. The Initiator is a Matlab based conceptual design tool. Its purpose is to automate the labor intensive part of the conceptual design. The Initiator is organized into three parts, the Initializer where a design is created, the analyzer where a design is analyzed and the optimizer that repeats the previous two parts in order to come to an optimum. All three parts will be discussed in a different section. The flowchart of the Initiator can be found in figure 4.1.

4.1.1 Initializer

The first module in the Initiator is called the Initializer. The Initializer generates an aircraft geometry for further analyses in the analyzer. The Initializer consists of five modules: Database

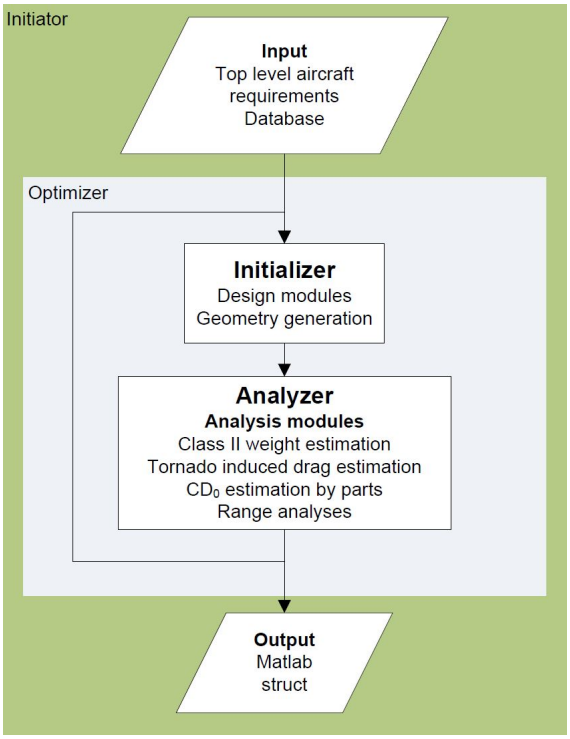

Figure 4.1: Flowchart of the Initiator

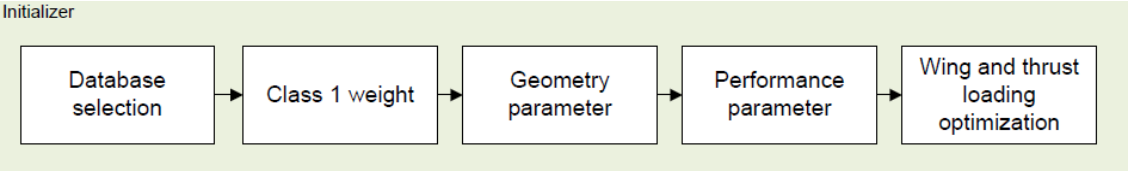

Figure 4.2: Main architecture Initializer

selection, class I weight, geometry parameter, performance parameter and wing&thrust loading optimization. The architecture is depicted in figure 4.2.

The first module, Database selection, loads a database containing 54 turbofan and 18 turboprop aircraft. Then, it selects the aircraft that will serve as reference aircraft to a new design. The aircraft are selected based on the similarities of payload and range in their top level requirements. A constraint on the selection procedure is the use of the initial service date of the aircraft. Furthermore, a minimum of 10 reference aircraft is required. When this minimum number of aircraft is not met, the Initiator will automatically relax the search margin on similar top level requirements.

The class I weight estimation method, determines OEW, WFB and $MTOW$ based on a curve fit of a OEW versus $MTOW$ plot and the Breguet range equation. The required performance parameters such as L/D are retrieved from the selected reference aircraft.

The geometry parameter module uses the information of the first two modules to come up with a geometry for the conceptual design. This is done with geometry parameters retrieved from curve fits combined with choices of the designer (such as high or low wing position).

Figure 4.3 shows two examples of the parameter determination by curve fits in the geometry parameter module.

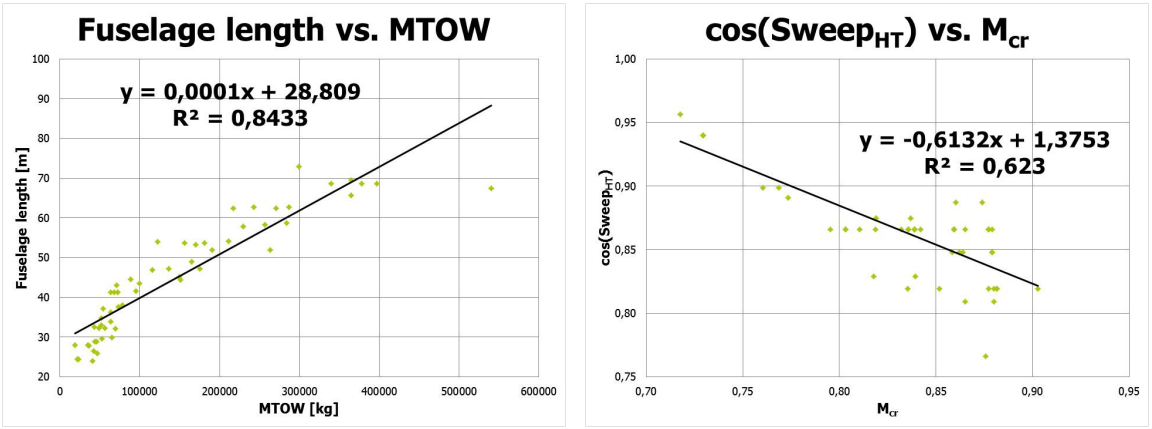

(a) Fuselage length vs. $MTOW$

(b) Quarter chord sweep of the horizontal tail vs cruise Mach number

Figure 4.3: Curve fittings to determine aircraft geometry

The performance parameter module then retrieves relevant performance parameters such as the Oswald factor to generate thrust vs wing loading diagram. This module retrieves parameters from curve fits such as figure 4.4, and uses simple analytical relations to calculated parameters for the thrust and wing loading diagram, such as the wing loading constrain for the landing stall speed.

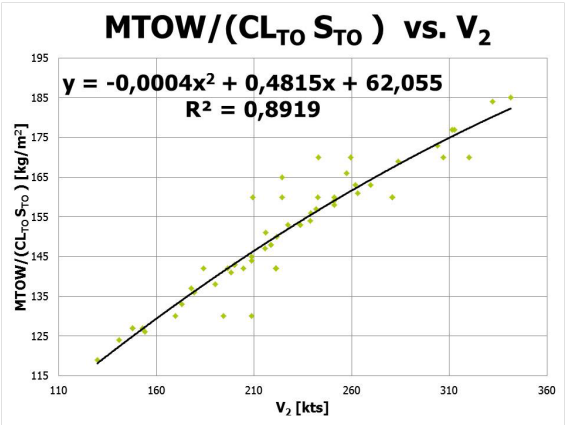

Figure 4.4: $MTOW/(CL_{TO} \cdot S_{TO})$ vs V_2

The the wing&thrust loading optimization module generates the thrust versus wing loading plot and thereby determines the wing size and engine thrust. An example of such a diagram is depicted in figure 4.5.

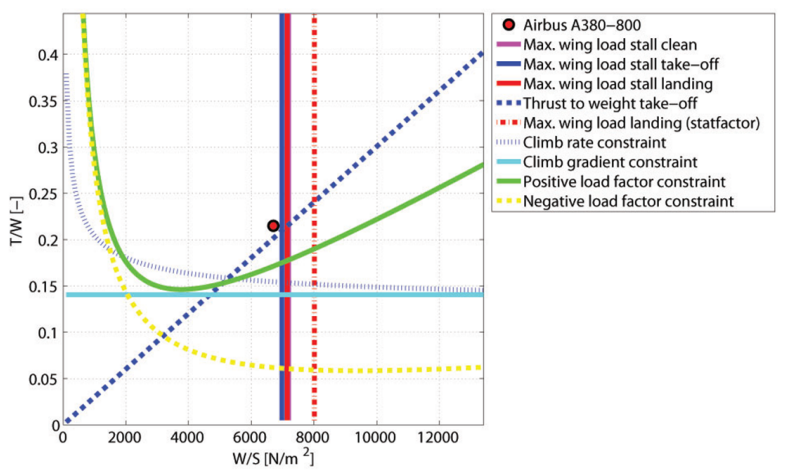

Figure 4.5: Thrust over weight vs wing loading plot of a Airbus A380-800

4.1.2 Analyzer

The analyzer consists of eight modules: the Multi model generator, Geometry analysis, Aerodynamic analysis, Weight estimation, Center of gravity analysis, Engine analysis, Range analysis and the Evaluation. For clarity the structure is depicted in figure 4.6.

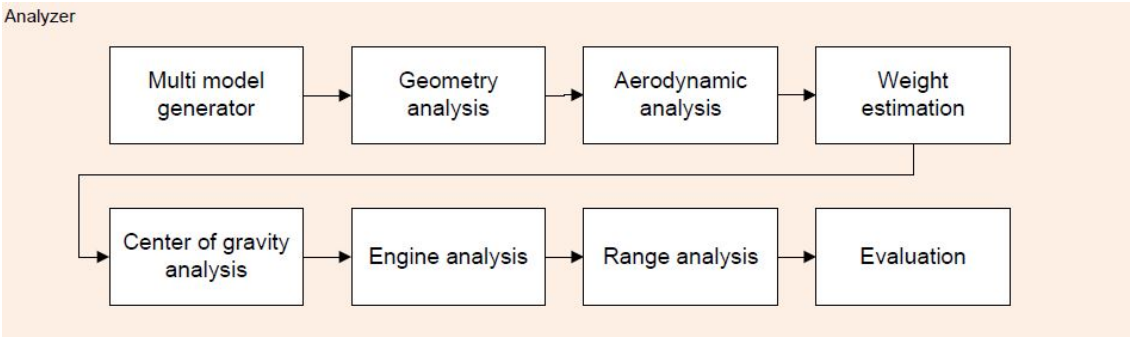

Figure 4.6: Main architecture analyzer

The Multi-model generator module uses the parameters from the Initializer to produces a simple surface model of the aircraft. An example can be seen in figure 4.7.

The Geometry Analysis module calculates the parameters that solely depend on the geometry of the aircraft, such as aspect ratio, mean aerodynamic chord (MAC), tank volume, etc.

The Aerodynamic Analysis uses Tornado [28] to calculate the induced drag. The lift independent drag is calculated using an empirical method, from Raymer [29].

Center of gravity Analysis determines the center of gravity position for a range of payload and fuel weights. The output is a 2D matrix of COG for different payload and fuel weights. This module calculates 3 different weights: OEW, WP and FW. The COG of all structural components, as well as the COG of system components is estimated using empirical relations by Roskam [30] and Raymer [29]. The payload part consists of loading cases for passengers and cargo. This results in a so called, loading diagram. Fuel is then added via a loading scheme, resulting in the total COG travel during all phases of the flight.

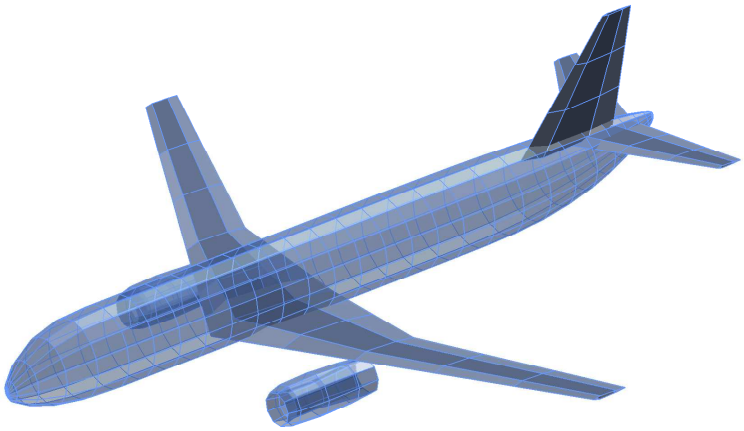

Figure 4.7: Geometry model generated by the multi-model generator

Engine analysis contains two options: the use of an engine model by Kok [31] or a fixed SFC method, which uses curve fits to derive length, height, width and weight of the engines based on thrust. Since the Recreate requirements state a fixed SFC, the fixed SFC is used together with the curve fits on weight and outer dimensions.

The range analysis module gives a more detailed prediction of the range. It divides the cruise phase in a number of sections (10 by default). Assuming constant altitude it trims the aircraft to maintain horizontal flight if the fuel mass and thereby the aircraft mass decreases. With the new found aerodynamic efficiencies it calculaties with breguet the range per cruise section.

Evaluation checks for controllability, stability, mach divergence, thrust and weight loading and stall recovery are performed as final step of the analyzer.

4.1.3 Optimizer

The optimizer is the final part of the Initiator. It will not be used during this thesis. However, it was an essential part in the original workings of the Initiator. The optimizer's purpose was twofold. In the first place it had to improve the design that came from the analyzer to better match the requirements. Secondly, it had to optimize a fitting design for better fuel efficiency, lower OEW or any other objectives specified by the user. The optimizer uses a genetic algorithm (GA).

4.2 Limitations of the Initiator

The Initiator, as available at the beginning of this thesis, presented some limitations, which needed to be addressed in order to make it usable to the purpose of this work. The proposed additions to the Initiator are listed below.

- The Initiator without the use of the optimizer produces designs which not necessarily comply with tol level range requirements. A weight loop is introduced to match the

range specified in the requirements to the design. This feature is important since the relation between range and fuel efficiency is one of the main variables of this thesis.

- The fuselage size is determined in the parameters geometry of the Initializer, based on $MTOW$ rather than on payload requirements. Since the fuselage of the cruiser is large compared to aircraft of similar $MTOW$, due to the fact that in general there is a correlation between payload capacity and range and the cruiser features a short range (2500nm) and a relative high payload requirements (250 passenger 1 class, long flight comfortability). Therefor a conceptual fuselage design tool is integrated into the Initiator

- Forcing of geometry & performance parameters. If for a given design parameter are known or desirable they have to be able to remain fixed.

- To test the accuracy of the Initiator the various modules should be tested with literature values of reference aircraft. To perform the analysis on a large number (n=54) of reference aircraft analysis should be able to be performed. There for an hands-off design routine is introduced. This hands-off routine is referred to as the batch mode.

The output requirements are listed below:

- In order to perform the fuel efficiency calculations the most important information needed is the fuel and the payload weights together with the weights such as $MTOW$ and OEW. These are visualized in a so called payload range diagram.
  In case a given aircraft does not operate at $MTOW$, for instance an existing aircraft with a larger range than 2500nm which flies the 2500nm cruiser mission, weights will have to be computed with information on aerodynamic and engine efficiency. These value should therefore also be provided by the Initiator.

- Performance and geometrical information is needed to assess and compare designs. Together with this data, drawings should be provided. This should include cabin layout information to justify the size of the fuselage.

- The designs produced by the Initiator should be suitable to feed external analysis and design tools. To enable communications between different programs, a compatible exchange data format has to be produced. The proposed format is CPACS, an XML data schema developed by DLR to store and exchange aircraft data between heterogeneous set of tools (details in section 4.2.6).

4.2.1 Batch mode operation

The first modification, is the addition of a batch mode functionality. Operating the design process in batch mode makes it faster since the program does not have to wait for input from the user. In addition, the absence of required user input makes loading the graphical user interface (GUI) unnecessary. Not loading the GUI decreases the required run-time even more. Finally, a tool able to operate in batch mode can be converted into an executable, making its integration with other tools easier.

The modifications to the Initiator to provide batch mode operation capabilities are quite simple. First the input that is obtained via the GUI input menus has to be provided by an

Table 4.1: Interactive vs batch mode

A300-600R	Reference	Interactive mode	Batch mode	units
Computational time[a]	-	113	19.4	s
Payload Pt A	41100	41100	41100	kg
Range Pt A	3283	4188	4188	nm
$MTOW$	170500	186560	186560	kg

[a]Core i3 2GH ram 32 bit processor, Matlab 2009b

input file. Second the design routine should be activated without any GUI interaction. Finally, the output should be stored for further analyses, again without any use of the GUI. The change in structure are schematically represented in figure 4.8.

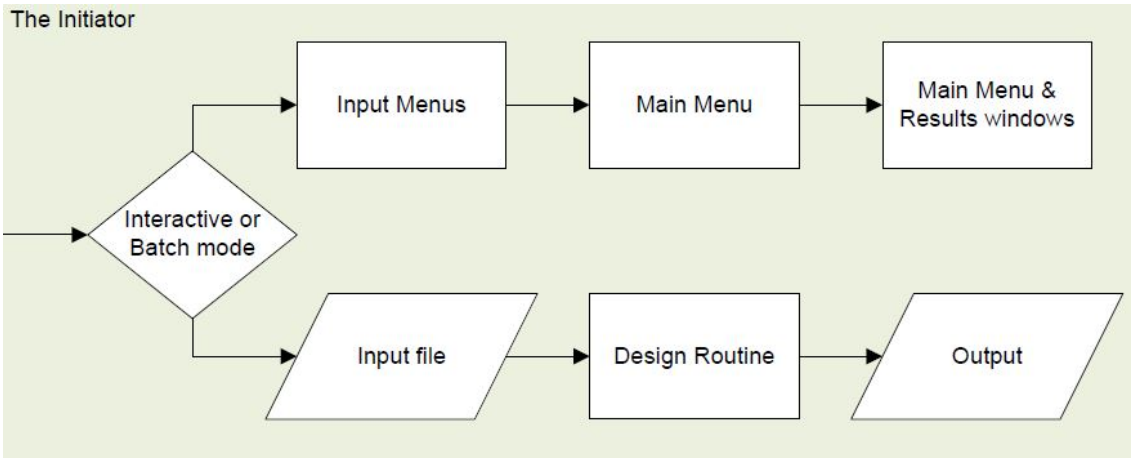

Figure 4.8: Workflow of the different operation modes of the Initiator

To show the effect of the modification, the top level requirements of the Airbus A300-600R are used to design an aircraft. The results of the design runs are given in table 4.1. The table contains the interactive and batch mode functionalities.

As expected there is no difference between the batch mode and the interactive mode in the conceptual design. The only impact is a reduction in required time. This time includes any user input that is required. The reduction of run time is almost sixfold, between batch and interactive mode.

Although, from the decrease in computational time it appears that batch mode is better than the interactive mode, there is one major shortcoming of the batch mode. With the batch mode functionality it is only possible to start with a list of top level requirements and follow the predefined design routine. This is in contrast to interactive mode where geometry parameters can be forced on the design. The only possibility to have forced parameter in batch mode is to specify this upfront in the design routine.

4.2.2 Design routine to match required range

The range calculated by Initiator did generally not match the range specified in the top level requirements (table 4.1). This was due to the results of the analyzer modules. These modules recompute L/D and OEW values. These recomputed performance values are used in the range prediction, since the performance values have changed the calculated range changes as well.

To solve this problem without having to make use of the lengthy optimizer routine an iteration loop is introduced. The structure of this loop can be found in figure 4.9.

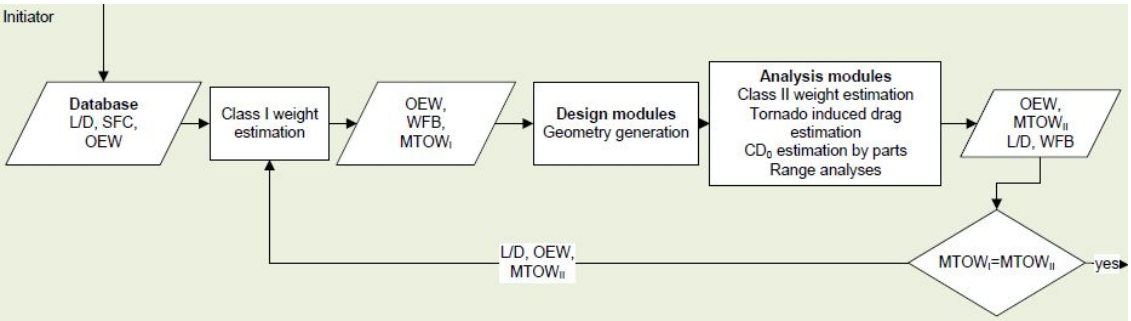

Figure 4.9: Integration loop in the Initiator

The converging variable of the iteration loop is $MTOW$. The Initializer produces a guess of $MTOW$ based on the class one weight estimation as described in section 4.1.1. The OEW and the L/D change due to the calculations of the analysis modules (Class II weight estimation and Tornado, respectively), which give a more accurate prediction. The difference in OEW results in a difference in $MTOW$. When it is not converged the Initializer uses the new OEW and L/D to recomputed the WFB to reach the given range. Furthermore, the geometry parameter module resizes the aircraft with curve fits to the new $MTOW$. Hereafter, the analyses modules are rerun until the design does not change anymore and $MTOW_I$ equals $MTOW_{II}$. Results of this weight loop can be found in table 4.2. An increase in computational time is a negative consequence of the introduction of the weight loop. Convergence on both OEW and L/D are not checked separately, the assumption is made that if $MTOW$ converges ($MTOW_II - MTOW_I <= 100kg$) the other parameters such as OEW and L/D have converged as well. If they would still fluctuate fuel weight or OEW would effect the $MTOW$ so much that convergence is not obtained.

Table 4.2: Introduction of the weight loop

A300-600R	Reference	Single design routine	Looped design routine	units
Computational time	-	19.4	120	s
Payload Pt A	41100	41100	41100	kg
Range Pt A	3283	4188	3283	nm
$MTOW$	170500	18656	178840	kg

4.2.3 Fuselage design

In the Initiator, the fuselage part holds only 3 variables to modify the fuselage shape namely, length, height and width. Furthermore, 10 other constant parameters hold information on the fuselage shape. The low number of variables makes all generated fuselages look alike, whatever the ype and size of the aircraft. Figure 4.10 depicts the biggest fuselage and the smallest, respectively that of and Airbus A380-800 and that of a CADair Reg.Jet 100.

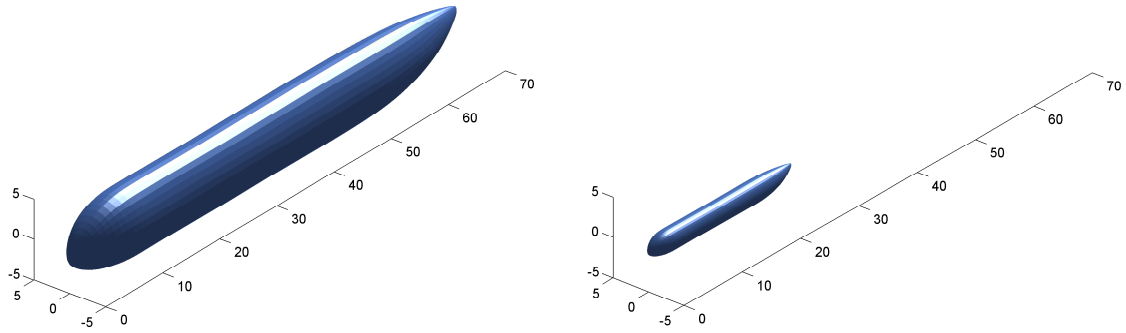

(a) Fuselage of an Airbus A380-800 (b) Fuselage of a CADair Reg.Jet 100

Figure 4.10: Fuselages produced by the Initiator

The Initializer sizes the fuselages according to $MTOW$ (see figure 4.3a). Another option is to set the three variables to manual values, which are based on existing fuselages. Nevertheless, a better solution is available. Within the DUT a fuselage design tool is available. This tool is part of the Multi-Model Generator (MMG) of the DUT Design and Engineering Engine(DEE). The DEE is an advanced design system to support and accelerate the design process of complex products, through the automation of non-creative and repetitive activities. This system consists out of a multidisciplinary collection of design and and analysis tools, where the MGG is one of these tools.
The fuselage design tool was developed by Brouwers [12] in 2010. It is a combination of GDL and Matlab code developed in order to generated fuselage geometries automatically, based the inside-out approach, the size of the fuselage is the result of the given payload and its accommodation.

In the new Initiator the fuselage design tool is integrated into the Initiator, as shown in figure 4.11. It has to be supplied with a number of extra input parameters as depicted in table 4.3.

The versatility of the fuselage design tool can be seen in the figures made of a A350-900 XWB and a the F106 Delta Dart, figure 4.12a and 4.12b. However, the results of the fuselage design tool that will be used by the Initiator are still only the length, height and width of the fuselage. This is because these three parameters have the largest impact on both the aerodynamic and weight estimations of the analyses modules.

For passenger aircraft the KBE fuselage design tool first builds the interior. Then this interior is used to construct the bounds for the cross-sections and thus the entire body. An example of its output can be seen in figure 4.13. Figure 4.13 shows the interior of an Airbus A300-600.

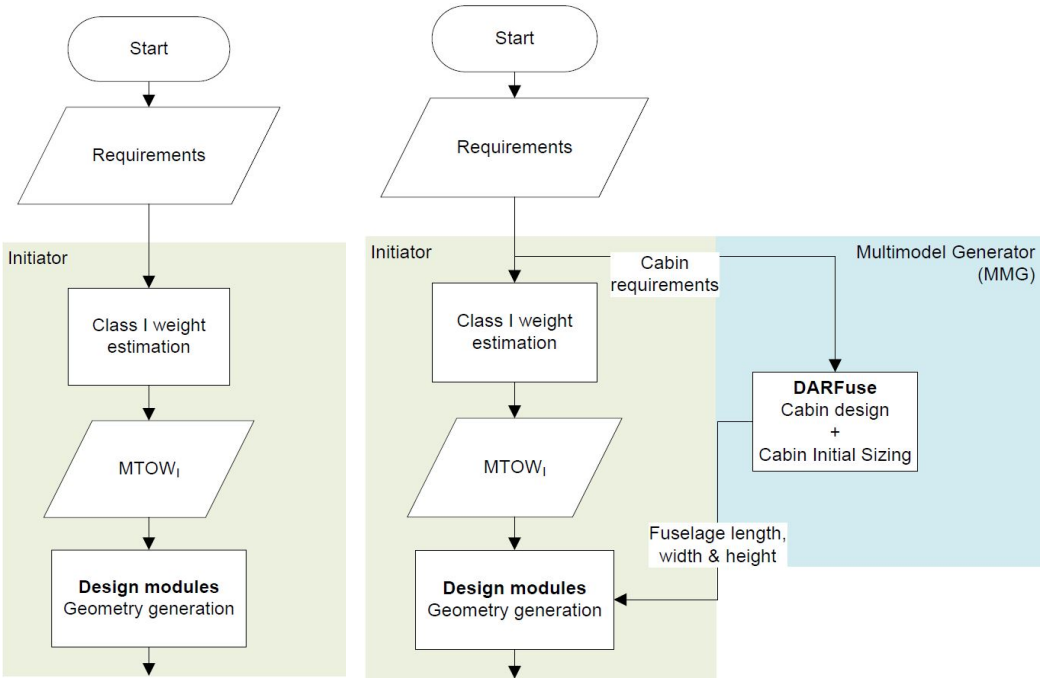

(a) Geometry generation without fuselage design tool

(b) Geometry generation with fuselage design tool

Figure 4.11: Workflow geometry generation with and without fuselage design tool

Table 4.3: Input fuselage design tool

Passengers	250	-
Economy class	1.0	-
Business class	0.0	-
First class	0.0	-
Seats abreast	8	-
Cargo type	container	-
Container type	LD-3	-
Double container	true	-

Brouwers kept the fuselage dimensions similar, by adjusting the number of seats slightly. The KBE tool resulted in a fuselage with 2 business seats less and 15 extra economy seats. So 13 seats extra on a plane of 265 seats, which is about 5% more seats for the same dimensions. This deviation is reasonable enough to use the KBE fuselage design tool for the dimensioning of the fuselage of the cruiser, which has to carry about the same passenger number, 250 passengers to be exact.

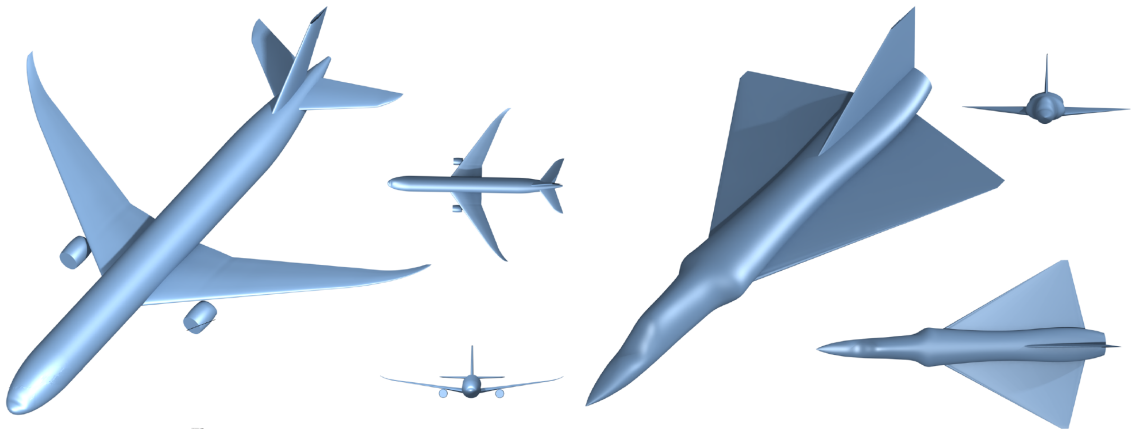

(a) A350-900 XWB (b) F106 Delta Dart

Figure 4.12: Two very different fuselages generated by the KBE fuselage design tool, from Brouwers [12]

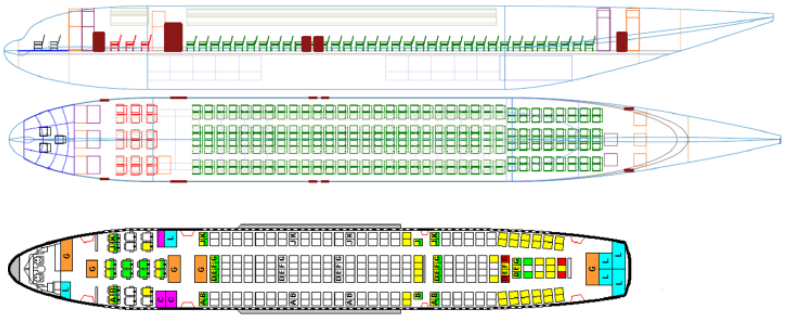

Figure 4.13: Comparison of he KBE fuselage design tool generated fuselage with the fuselage of an A300-600, from Brouwers [12]

4.2.4 Automatic report generation

For reporting, figures and renderings of the designs were obtained with the GUI an could be saved for later us in a report. Furthermore all performance parameters were written to Excel. However, these functionalities needed improvement. To start, the picture should be produced and saved automatically without the use of the GUI, (especially) when the Initiator is run in batch mode.

The aircraft designs produced during this project should be quickly comparable to each other and to reference aircraft. To do so a representation is needed with clear top, side, front and isometric views. Furthermore wing, tail, fuselage and engine dimensions should be clearly listed. Finally weight and performance parameters have to be included as well as payload range diagrams. Inspiration was taken from Roux's [32] book. See figure 4.14 for the representation of Airbus 330-200.

The figures come from the plot function of the Initiator and are automatically saved, the geometry and performance values are written from the project structure to a Latex code. WinEdt is used to compile the Latex code and produce a pdf file. These pdf file can be found

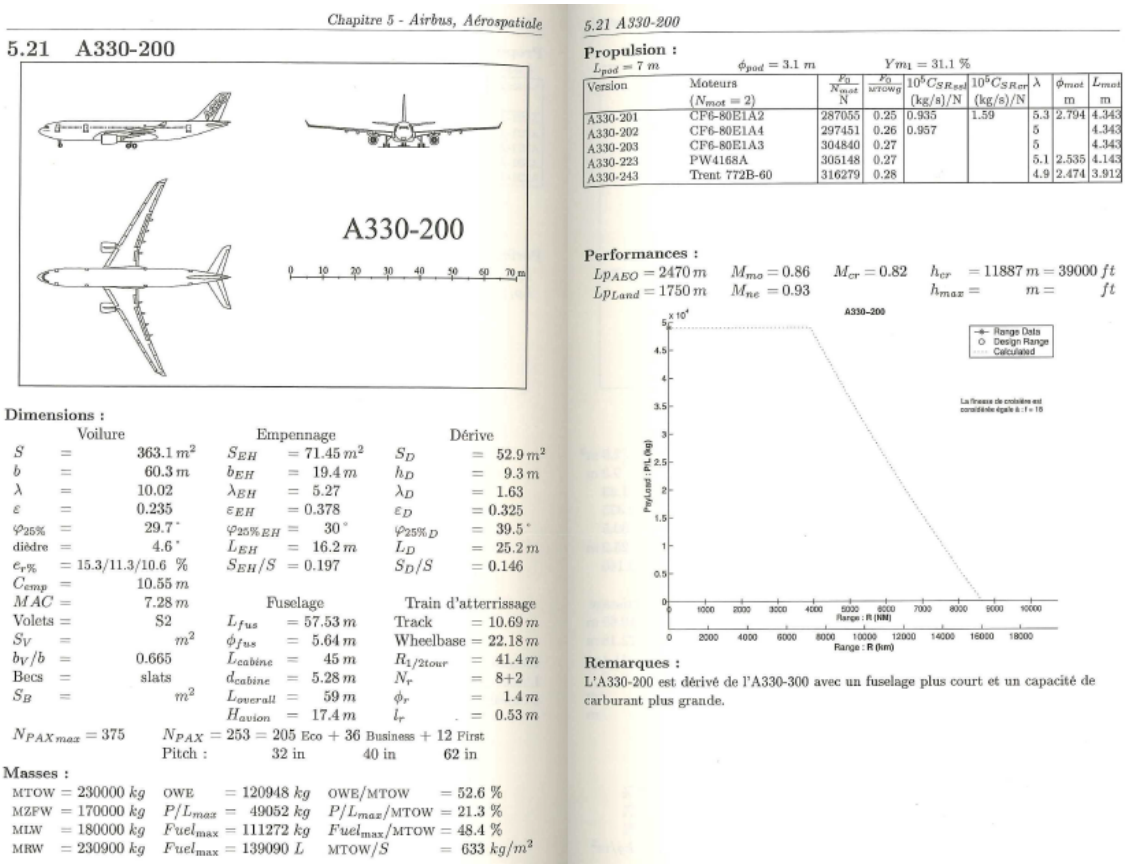

Figure 4.14: Roux's representation of an Airbus A330-200

in appendix D.

4.2.5 Forcing of geometry & performance parameters

During the design routine it can be desirable to force certain geometry and performance parameters on the design. Examples of these parameters are the SFC in cruise and loiter, the aspect ratio of the main wing, fuselage dimensions and maximum lift coefficients. The SFC of the cruiser for instance was set by the requirements to be $0.525/hr$. This value is forced by the use of a switch function in the appropriate submodule, `Para_EN.m`. This submodule belongs to the Geometry module, and this in turn to the Initializer (figure 4.15).

The switching function is activated by a variable that can be specified in an input file, along with the value that needs to be forced. Appendix **??** shows an example on in input file. The parameters `project.ToolSpecs.fixed.sfc` is set to 1 turn the switch forcing SFC on. The parameters `project.Fixed.sfc_cr` and `project.Fixed.sfc_lr` contain the SFC values for cruise and loiter that will be forced upon the design. Appendix F shows a relative simple input file. Not specified switches will remain off by default. Nevertheless, L/D, aspect ratio, OEW and $MTOW$ can be forced. For the interactive mode this functionality was already present by changing a value in the GUI.

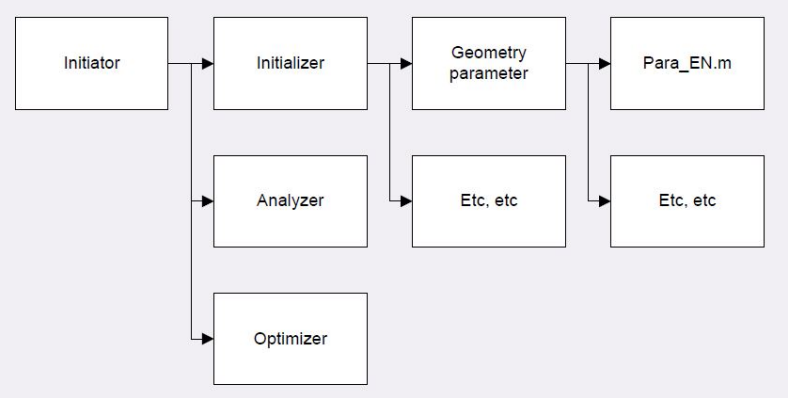

Figure 4.15: Structure tree of the Para EN function

4.2.6 Integration of the Initiator with other tools

The format for dat exchange between universities was already present in the original Initiator. Common Parametric Aircraft Configuration Schema (CPACS) is a XML schema developed by DLR. A CPACS file is basically a single hierarchic XML-file, containing the information required to describe an aircraft (or air transportation system). The advantages of this XML-structure are its well-known syntax and its clear and easy structure also the fact that it is a defacto data exchanging format, hence many xml reader/parser are available and several tools (also commercial tools) support input and output of XML files.

As test case, an open source framework took called Remote Component Environment (RCE) [33] was used to integrate the Initiator with the MMG module of the DEE. The workflow used for this integration can be found in figure 4.16. The Chameleon environment was chosen, because knowhow on this program was present at the DUT. The links between the different programs are based on the CPACS format.

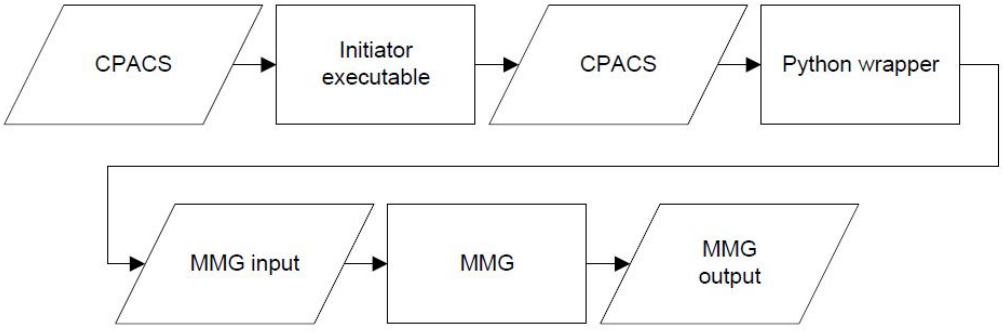

Figure 4.16: Workflow of Initiator MMG integration

Initiator executable

To make the Initiator work within the workflow of figure 4.16 it needed to be converted into an executable. Furthermore, this executable had to be able to read input, such as top level requirements, from a CPACS file and produce its output in the same format.

These read and write functionalities were added to the Initiator which now features three modes of operation (see figure 4.17):

1. The original interactive mode
2. One batch mode which uses a Matlab file as input and produces a number of output formats.
3. A second batch mode which uses CPACS input and output files

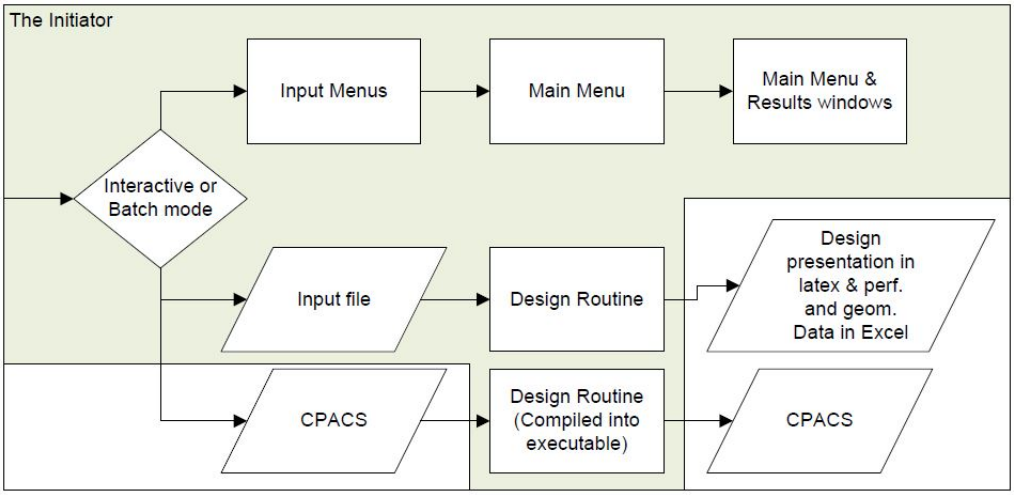

Figure 4.17: New workflow of the operation modes of the Initiator, including the CPACS batch mode

The Initiator executable is produced using the Matlab deployment functionality, which con compile the Matlab code. Since the Matlab code is not accessible after compilation, the default operating mode was set to the CPACS input/output batch mode. The other batch mode can be selected in the non compiled version, which has been used for the tool validation and verification. To run the Matlab executable a Matlab compiler is required. This compiler can be downloaded from the Matlab website.

TIXI wrapper

Within the Matlab environment the CPACS file can be loaded into Matlab structures. After these structures are modified, they can be written back to CPACS files. Within the RCE environment a different way of manipulating CPACS files is used. DLR developed the library *TIXI* to perform these manipulations. TIXI is a simplified XML processing library, written in C, wrappers are available for C++, Fortran, Python, Java and Matlab. Within the RCE environment it was customary to use a Python code. Therefore, the TIXI library in combination with the Python TIXI wrapper is used to modify the CPACS files within the RCE environment, in order to produce the MMG input.

The Multi-Model Generator of the DEE

The DEE has a Multi-Model Generator to visualize the design and connect to different programs for CFD and FEM analyses. Figure 4.18 shows examples of products of the MMG.

The input for the MMG is given in XML format. The Initiator will have to produce this XML format to enable the MMG to run automatically.

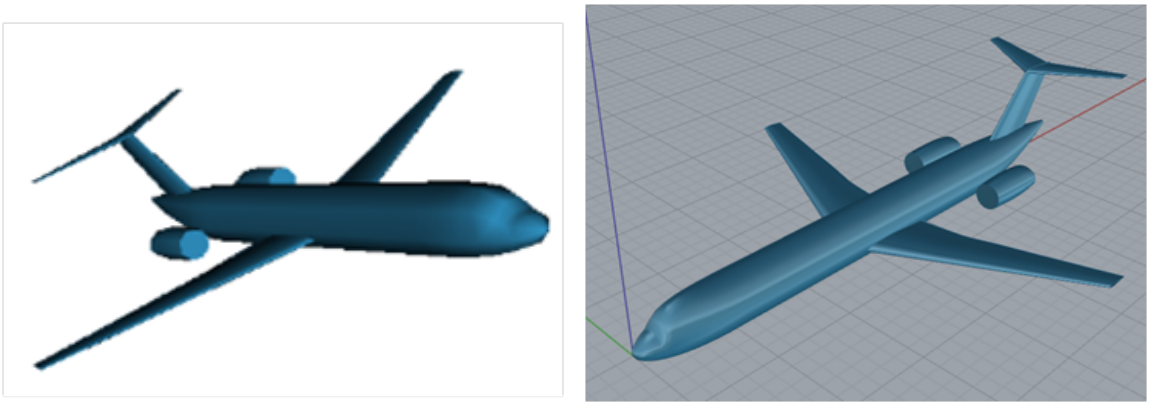

(a) A .vrml representation of the F100

(b) A .stp representation of the F100

Figure 4.18: A .vrml and a .stp representation of the F100

The MMG produces three types of presentable output for this research. A stp and vrml files gives a visual representation (see respectively figure 4.18b and figure 4.18a). Furthermore, different views of the interior are printed to a pdf format. These pdf files include top, front and cross-section views of the cabin (figure 4.19).

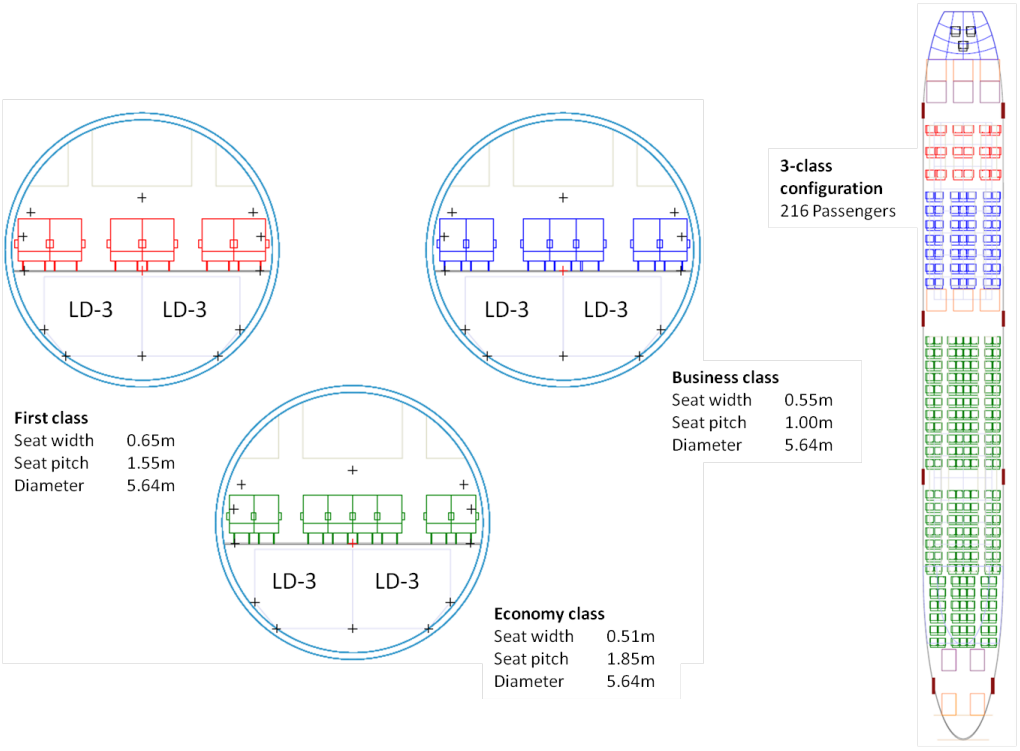

Figure 4.19: Interior renderings of the cabin

TIGL viewer

In order to verify the correctness of the CPACS files produced by the Initiator, it was made use of the 'TIGL viewer'. The TIGL viewer is also developed by DLR. The TIGL viewer is part of the TIGL library. It was developed to process geometric data. As an example, a CPACS description of a Fokker 100 is visualized by the TIGL viewer in figure 4.20.

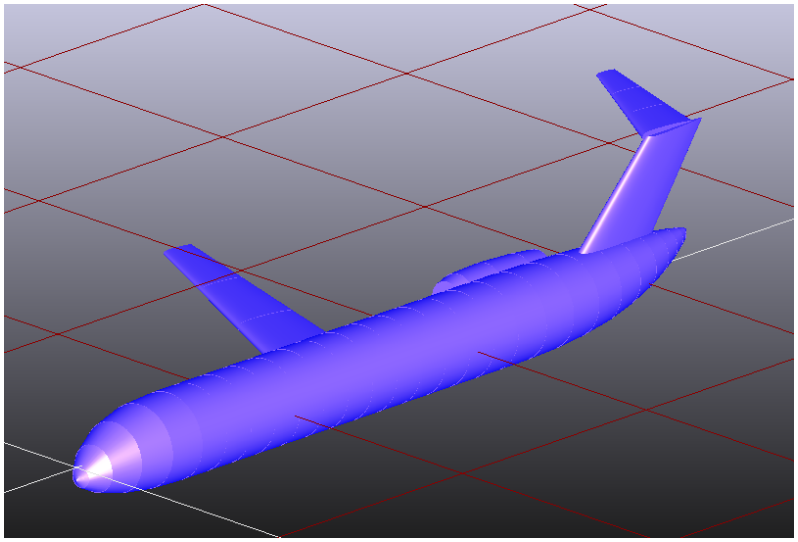

Figure 4.20: Fokker 100 in the TIGL viewer

The TIGL viewer uses the TIXI library to load, store and modify CPACS data in order to visualize a 3D-model of the aircraft described in the CPACS file. It calculates the Cartesian coordinates of all the surfaces points, and is able to output the model as an IGES-file.

Concluding on the workflow

Figure 4.21 gives an overview of final workflow of the Initiator. The presents of extra output functionalities visible in the to parallelograms in the bottom of the figure. The introduction of the weight loop can be found on the left side of the Initiator box. The introduction of the MMG is represented by a whole new box which receives information and produces out put back to the initiator for the fuselage dimensions. Furthermore, it is responsible for the output in the right parallelogram.

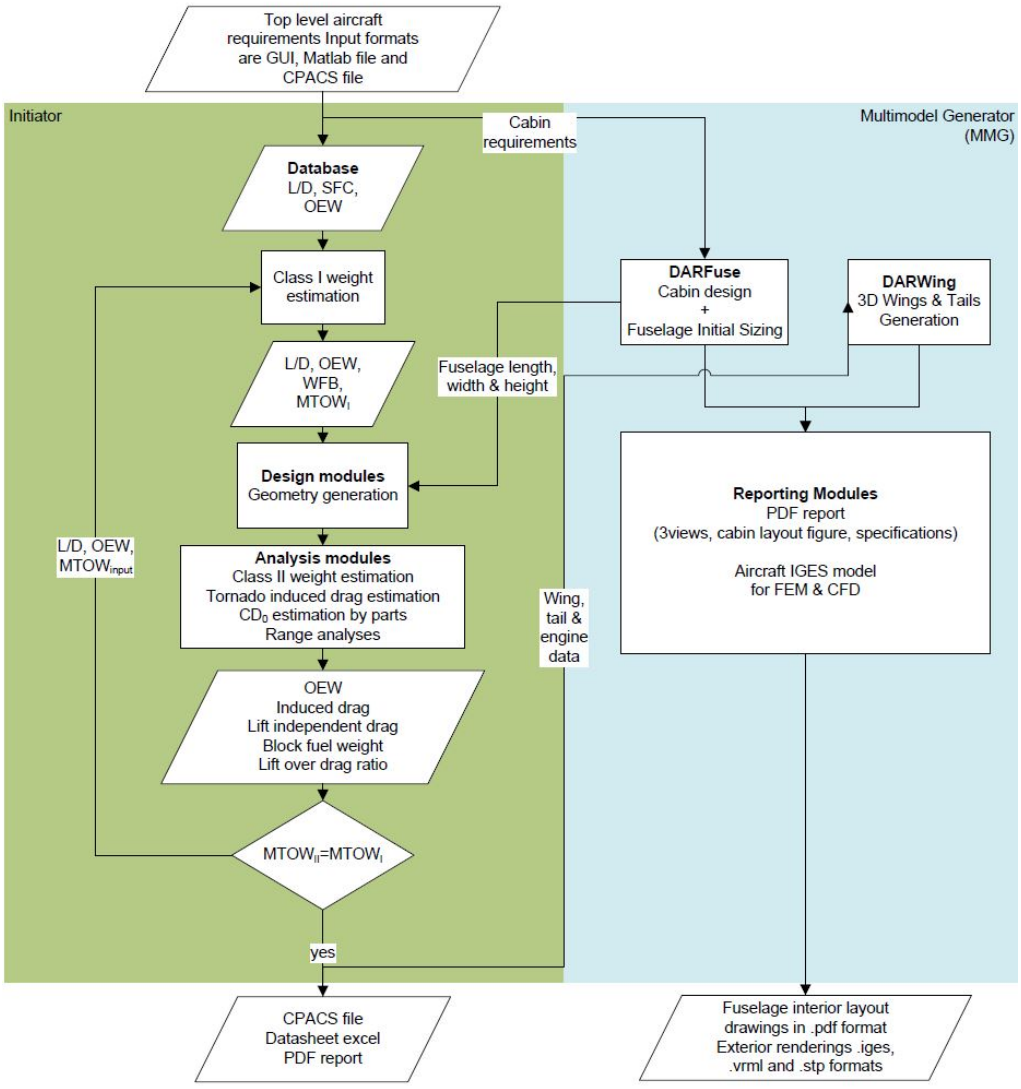

Figure 4.21: Final Initiator workflow

Chapter 5

Detailed Initiator modifications and validation

The previous chapter performed modifications on a interoperativity level. This chapter describes modifications on a lower level, it described the changes made to the design and analysis modules of Initiator. These modifications do not change the general design routine. The modifications are more focussed on to the accuracy and correctness of the conceptual design that are produced. The performed modifications are listed below accompanied by a brief explanation on the motivation of the given changes.

- **Multiple aircraft configurations**. The design modules are modified to enable multiple aircraft configurations, such that all configuration of the reference aircraft can be produced.

- **Database performance parameters**. The performance parameter of the database were faulty, resulting in wrong values used as reference and input for the design modules. This is corrected with new performance data from literature.

- **New curve implementation**. The fit of several curve fits used in the design modules is increased, with the introduction of a least square method.

- **Point of operation**. The ability to design aircraft based on design point requirements is added to ability to design aircraft based on their maximum payload point.

- **Landing stall speed**. Landing stall speed calculations were found to be runway independent, therefore a new method to estimate landing stall speeds is introduced.

- **Wing loading**. The wing and trust loading plots featured a constrain on take-off stall speed which was not found in literature and is therefore removed. Furthermore, old aircraft without supercritical airfoil featured lower wing loadings, because the could not handle high lift coefficients in cruise. An extra constrain in introduced to limit their wing

loading, which is necessary when a design is made based on the top level requirements to checked the design routine.

The results obtained by the modified version of the Initiator will be compared with reference values from the present database. This database can be seen in appendix B. Furthermore, the whole design tool is checked by using the top level requirements of all reference aircraft to produce conceptual designs. The obtained designs are then compared to the database values (Appendix B). Chapter 4 describes the introduction of the batch mode, the weight loop, the new excel output formats and the plot functionality that works GUI independently. These functionalities are used in the validation cases. The incorporation of the fuselage design tool will not be used for validation, since detailed interior variables were not found for all reference aircraft. The original, simpler $MTOW$ versus fuselage dimensions plots will be used.

Before any of the previously mentioned modifications is preformed on the Initiator a validation run is performed with the Initiator as available after the changes of chapter 4. The results of this validation are shown in appendix C. For comparison the database values used in appendix B are used.

5.1 Multiple aircraft configurations

Originally the Initiator only enabled designing aircraft with only 3 engine installation configurations. The selection of the configuration was based on the number of engines of the aircraft: Two engines resulted in a conventional wing mounted engine design, three engines included an extra tail mounted engine and an aircraft with four engines featured four wing mounted engines.

To enable the conceptual designs generated by the Initiator to match the configuration of the reference aircraft, it was necessary to modify the `para_geom.m`, a submodule of the Geometry Parameter module of the Initializer. The file location of `para_geom.m` is depicted in figure 5.1.

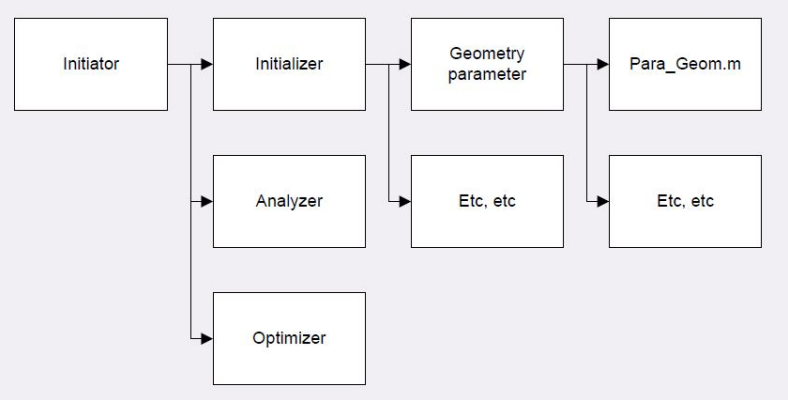

Figure 5.1: File location of the Para Geom function

Operating the Initiator in batch mode for the top level requirements of three different aircraft, a Fokker F100, a British Aerospace BAE 100 and an Ilyushin 62M IL62M, results in the

configurations of figure 5.2. Since the batch mode does not allow changes to the designs manually, the number of engines selected for a design was equal to the mean number of engines of the reference aircraft. The reference aircraft select for the design of the Fokker F100 featured a lot of three engine aircraft. Hence, it was designed with a three engine configuration. In similar fashion the British Aerospace BAE 100 was designed with three engines and the with Ilyushin 62M IL62M two. Furthermore, all these three aircraft feature a T-tail which was not implemented. Also fuselage mounted engines and high-wing configuration could not be designed.

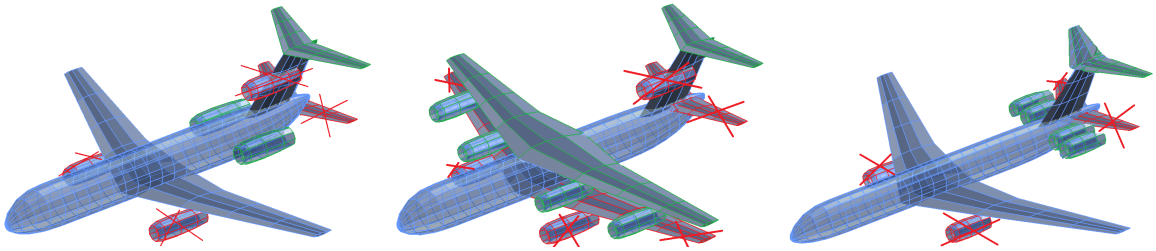

(a) Fokker F100 (b) British Aerospace 100 BAE100 (c) Ilyushin 62M IL62M

Figure 5.2: The configurations of three aircraft before any modifications to the Initiator. Their incorrect configuration aspect are highlighted in red (and crossed). The desired configuration aspect are highlighted green.

To enable the multiple configurations an extra number of switches is introduced in `para_geom.m` (figure 5.3). The control to these switches is done by a number of parameters. These can be specified in the input file of the batch mode or a new menu of the interactive mode. The parameters that control these switches can be found under the name `project.Configuration`.

It is important to note that due to the structure of the Initiator symmetrically placed engines were considered on engine group. Hence, a four engine aircraft has two engine groups, both containing two engines. Three engine aircraft feature one engine group with only one engine this engine is automatically placed in the centreline of the aircraft.

The different configurations have an impact on the wing planform. For instance the dihedral angle of high wing aircraft is mostly negative, whereas low wing configuration mostly feature a positive dihedral. Furthermore, taper and aspect ratios of the vertical tail depend on the tail type selected. Figure 5.4a depicts a convectional tail aircraft, which has a number of T-tail aircraft among its reference aircraft: The resulting tail features a high taper ratio and a low aspect ratio. Figure 5.5 lists the tail taper and aspect ratio for the different configurations.

To handle this discrepancy the geometry parameters influenced by the configurations choice were given a special selection filter for the reference aircraft, to select only aircraft of the required type. If none of the selected reference aircraft was of a similar tail type a default value for this tail type was used. The result of this modification can be seen in figure 5.4b.

Furthermore, figure 5.6 depicts the new conceptual designs after the above mentioned modification were implemented. It can be immediately clear that these configuration resemble the configuration of the aircraft of their top level requirements.

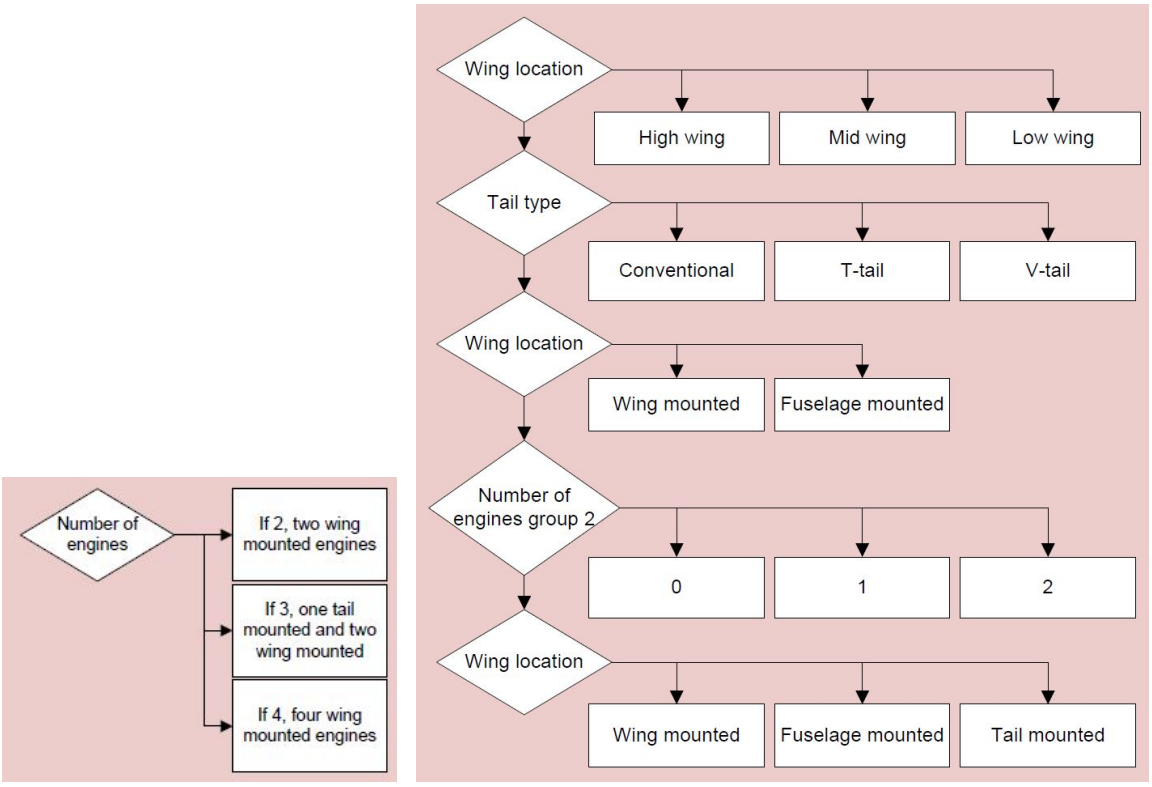

(a) Original (b) New

Figure 5.3: Switch structure of the original (left) and new (right) configuration selection

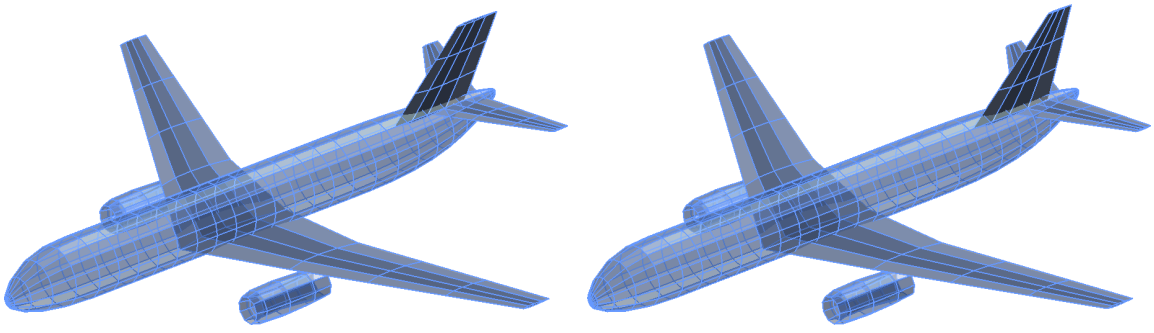

(a) Original (b) New

Figure 5.4: Conceptual designs by the Initiator based on the Boeing B737-600 top level requirements

5.2 Database performance parameters

The original database (appendix A) contained inaccurate values of L/D and SFC. The L/D values contained in the database weren actually computed with the Initiator aerodynamic analysis modules, using geometry data from available literature. Indeed they were not values from reliable sources (e.g. from manufacturers). The SFC values were obtained using the

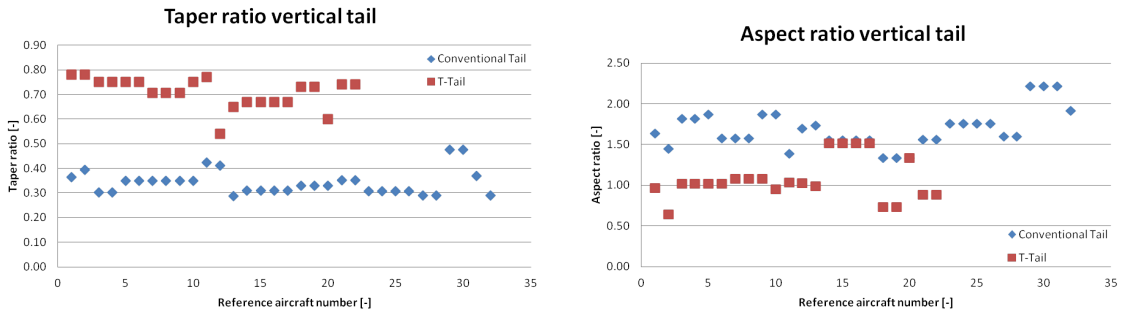

(a) Taper ratio of the vertical tail

(b) Aspect ratio of the vertical tail

Figure 5.5: Taper and aspect ratio of the vertical tail

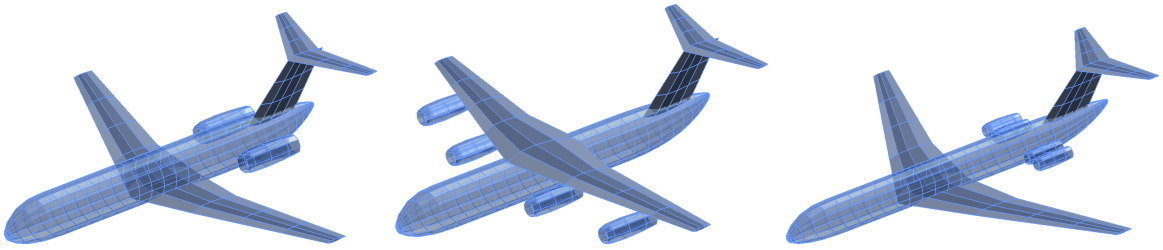

(a) Fokker F100

(b) British Aerospace 100 BAE100

(c) Ilumhs 62M IL62M

Figure 5.6: Varying configuration of the reference aircraft

Breguet range equation (equation 5.2).

$$R = \frac{V}{SFC} \cdot \frac{L}{D} \cdot ln\left(\frac{W_4}{W_5}\right) \tag{5.1}$$

Hence,

$$SFC = \frac{V}{R} \cdot \frac{L}{D} \cdot ln\left(\frac{W_4}{W_5}\right) \tag{5.2}$$

R, the range was obtained from the top level requirement of the selected aircraft. V was the product of the required Mach number and the speed of sound at the given cruise altitude. W_4, the aircraft weight at the beginning of the cruise phase, was obtained by multiplying the $MTOW$ with the fuel fractions of take-off and climb (equation 5.3). W_5, the aircraft weight at the end of the cruise phase, was obtained by adding the fuel fraction of descent, landing and reserve to the sum of the OEW and WP (equation 5.4).

$$W_4 = MTOW \cdot (ff_{\text{Take-off}} \cdot ff_{\text{Climb}}) \tag{5.3}$$

$$W_5 = OEW + WP - MTOW \cdot (1 - ff_{\text{Descent}} \cdot ff_{\text{Landing}} \cdot ff_{\text{Reserve}}) \tag{5.4}$$

Of course, inaccurate values of L/D and of other parameters would have accumulated to deliver an inaccurate SFC value. The false values were when possible by more reliable values from literature. The new L/D value were retrieved from Bolsunovsky [34], Lee [35], Linke [36] and Babikian [37]. The values for SFC were retrieved from literature [38] by Mo Li. The results of the new SFC values can be found in figure 5.7b the L/D values are listed in figure 5.7a.

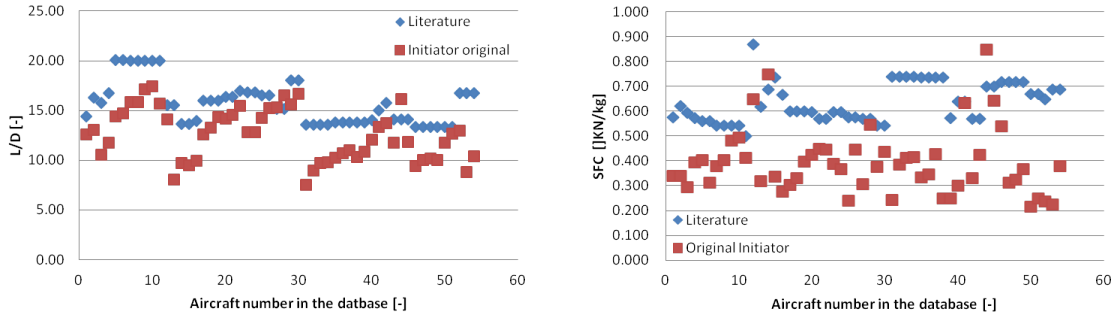

(a) Lift over drag per aircraft from the database

(b) SFC over drag per aircraft from the database

Figure 5.7: SFC and L/D reference values

The modifications done to the database resulted in better estimates of L/D and SFC. This resulted in faster convergence of a design to reach a specified range. This because the difference in estimated L/D and analyzed L/D were smaller. (SFC values were given as an input so the change in these values was not tested.)

5.3 New curve fit implementation

For the fuselage design, during the validation run, simple $MTOW$ versus fuselage height, width curve fits were used. The Initiator uses curve fittings throughout the design routine to determine geometry and performance parameters. For these curve fittings the Matlab function polyfit is used. This function fits a polynomial through a set of data points. The function polyfit is used 64 times throughout the Initiator.

The main short coming of the polyfit function was the inability to incorporate cubic and square root relations. Furthermore, there was no way to exclude certain terms from the polynomial. For example, all fit always included a constant value in the solution, so $y = Ax + b$ instead of $y = Ax$, which was impossible.

Matlab features a least square method where the desired terms of the solution can be given as an input. For example, the original fit through data points of figure 5.8 was linear. hence in the format $y = Ax + b$. Using the new least square method a solution in the format $y = Ax^{1/3} + Bx^{1/2}$ was found. This new curve increased R^2 from 0.725 to 0.867.

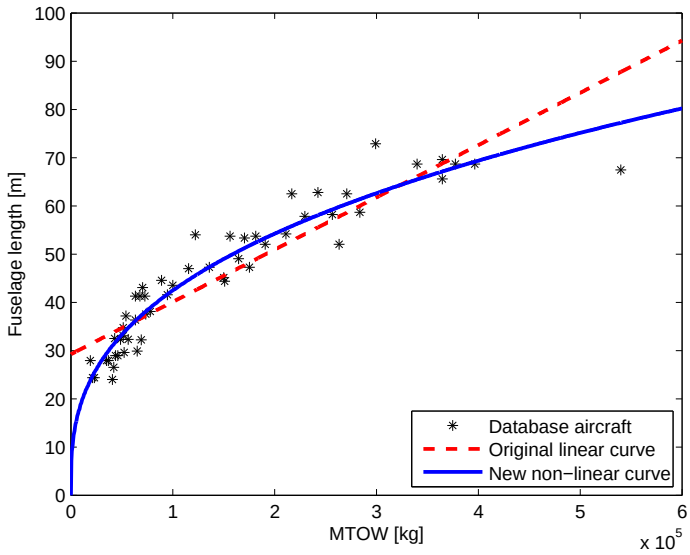

Figure 5.8: Fuselage length versus $MTOW$

This least square method was introduced for the fuselage width and height as well. Furthermore, all new features were provided with the new method, instead of the polyfit function. Existing m.files containing polyfit functions that were found to work adequately were left unchanged. The effort of changing them was expected to have little change on the conceptual designs, since as can be seen in the report of Langen [13] the R^2 of other fits was already quite high.

5.4 Point of operation

Originally, the requirements given in the database were all maximum payload range requirements. Hence, range achievable at maximum payload (Point A in the payload range diagram). In the present database also design point (D point) requirements are included. These values can be found in appendix B.

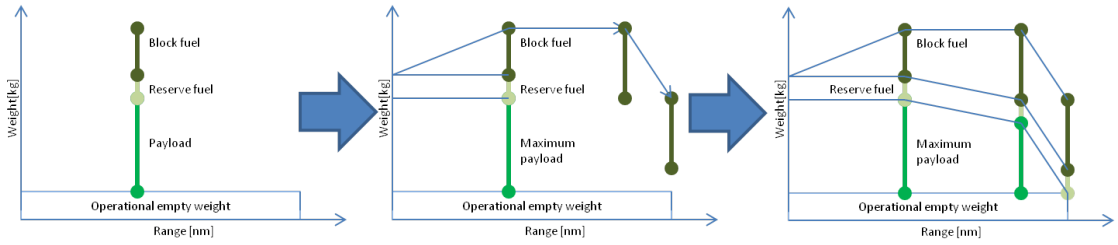

Figure 5.9: Payload range diagram construction based on the maximum payload point

Furthermore, the design routine expects a maximum payload point. After the weights for the maximum payload point are known, it constructs the payload range diagrams by calculating the performance of the design for a point B (Maximum fuel volume) and point C (Maximum

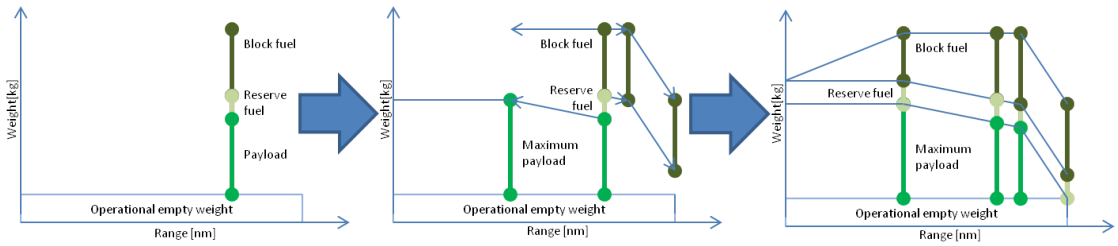

Figure 5.10: Payload range diagram construction based on the design point

fuel zero payload) operations (see figure 5.9).

The new approach starts the design from the design point. The payload range diagram is then constructed by calculating the designs performance the A,B and C point of operation as shown in figure 5.10. The new approach produces a correct payload range diagram when (and this is mostly the case in aircraft design) a design point instead of a maximum payload point is provided in the top level requirements. Furthermore, the selection of reference aircraft a design is improved since now the reference aircraft can be selected based on their similarities on the top level requirements of the same operation point. This is especially convenient for the non-stop aircraft used to compare cruiser fuel efficiency to that of direct flight in chapter 6.

5.5 Landing stall speed

Originally the Initiator determined the stall speed on the base of reference aircraft via the relation between the landing weight, the wing surface and the lift coefficient. An excellent Pearson-correlation coefficient (r^2) was found of 0.9659. This high level of correlation between these parameters is easy to explain, since they are coupled via the lift equals weight constraint, that has to be met during all 1g manoeuvrers and therefore also applies for landing (equation 5.5).

$$L = W = \frac{1}{2} C_L \rho V^2 S \tag{5.5}$$

Reexamining figure 5.11 with this knowledge, yielded some suspicion. When the above constrain holds all aircraft should lie exactly on one line, (when ρ is constant). All aircraft aligned perfectly, apart from 7 which were slightly of. This discrepancy is properly caused by small errors in the database.

The main problem with the use of the correlation of figure 5.11 is the absence off a dependency of the approach speed on the runway length. Furthermore, the variables MLW, C_L and S are taken from reference aircraft, resulting in an unnecessary database dependency. To create a dependency between approach speed and landing distance a method from Torenbeek was used. Inside in the landing maneuver itself was obtained by the book of Ruighrok. Plot 5.12 shows the original correlation of the reference aircraft stall speeds and landing distances.

The landing maneuver is depicted in figure 5.13, where the approach speed equals 1.3 times the stall speed, and the screen height (h_s) is 15m. The landing can be divided into three

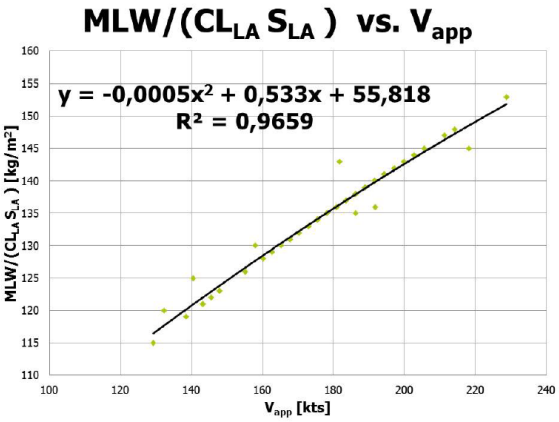

Figure 5.11: Original approach speed correlation

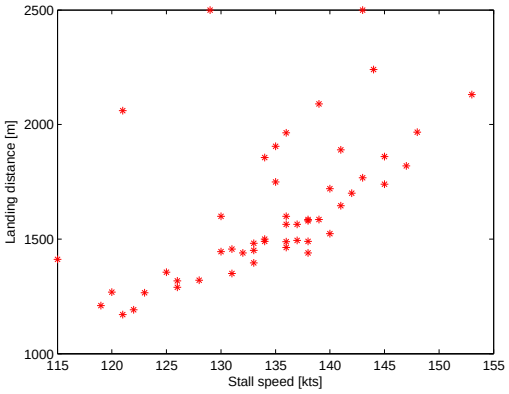

Figure 5.12: Stall speed versus landing distance

parts: The final approach, the transition part and the ground run. The first part is equal for all aircraft that fall under the 3 degree glide slope regulation. Then the transition part is a combination of aircraft flying characteristics and pilot skill. The final phase, the ground run, is most influenced by the braking power of the aircraft.

All the difference in landing distance is considered to be in the ground run, the braking power to be exact. Using this approach a fit is made with the new corrected database values. Figure 5.14 shows the results, all values lie within an a/g braking value of 0.275 and 0.51.

The problem is however that a 10% difference in approach speed can result in 21% difference in wing loading since the speed is quadratic. The first correlations seems to be that aircraft with shorter landing distances tend to have better braking coefficients. A good fit was found using the least square method of section 5.3. The produced trend line is in the format $Ax^2 + b$. In figure 5.14 the trend line is given in black.

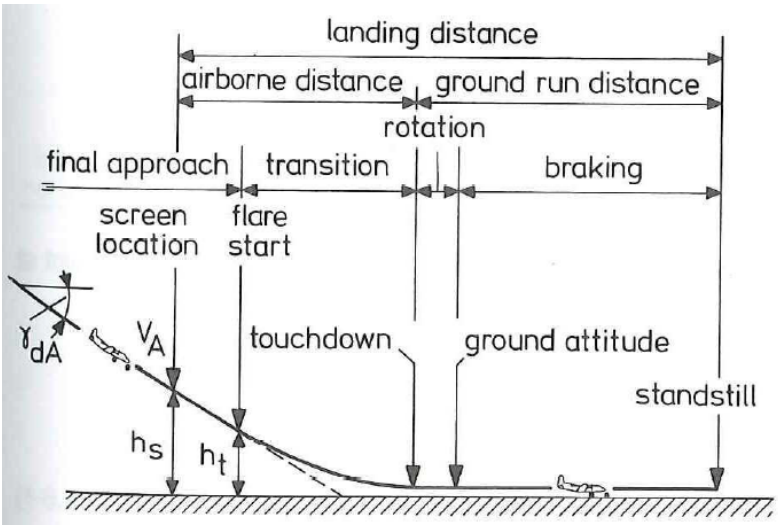

Figure 5.13: Landing maneuver

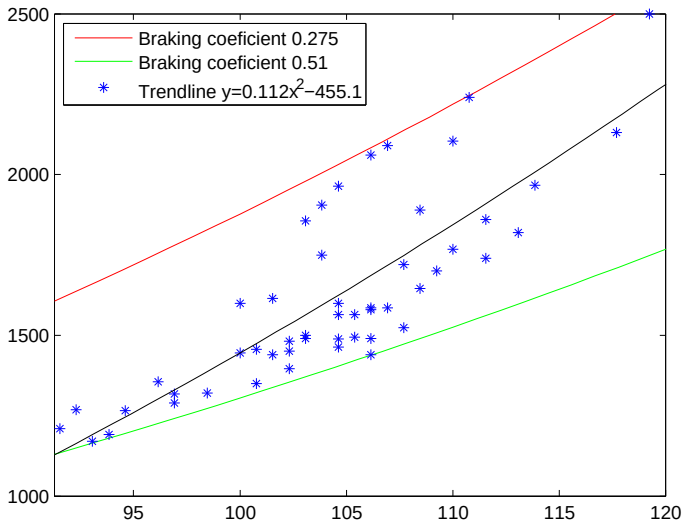

Figure 5.14: Landing maneuver

5.6 Wing loading

The wing loading of the conceptual designs was found to differ significantly from the reference values. One reason was the use of a constraint on the take-off stall speed. However, take-off constrains were incorporated in the TOP. No literature support was found for the stall speed constrain for take-off. Therefore, the stall speed take-off constrain was removed. This resulted in higher wing loadings of aircraft designed with the Initiator.

However, testing of the design routine (by design aircraft based on the top level requirements of existing aircraft and comparing these results to literature) a number of aircraft were found to have far to high wing loadings, when compared to literature. All these aircraft were old

aircraft. It was found that their wing loading was limited by the C_L values in cruise due to the absence of supercritical airfoil technologies. Therefore a extra Mach divergence constrain was introduced, based on a book by Torenbeek [39]. This resulted in a better match between the aircraft designs and the literature values.

5.7 Operational empty weight module

The Initiator uses a class II weight estimation method, from Raymer [29], to computed the OEW. This class II weight estimation requires $MTOW$. However, the $MTOW$ is a summation of OEW, WP and FM. To converge the original Initiator featured a small loop (figure 5.15).

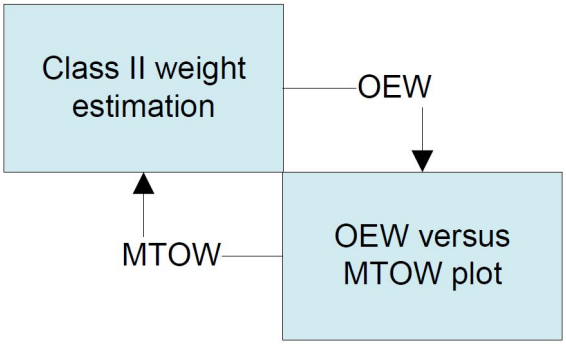

Figure 5.15: Original weight loop for the class II weight estimation

The computation of $MTOW$ in this loop was done width a curve fit between $MTOW$ and OEW reference values. Similar to the class I weight estimation of the Initializer. However, this time the $MTOW$ was the result and OEW the input.

The loop of figure 5.15 is not correct and it has been removed with the introduction of the weight loop of section 4.2.2. To verify the accuracy of the individual OEW module a verification analysis was conducted. In the new verification, the $MTOW$ values required by the OEW analyses module were derived directly from literature values included in the database. The entire list with results is shown in appendix C.

It should be noted that the four lightest aircraft of the database all have an over prediction of their OEW while the heaviest aircraft along with all aircraft with a tail mounted engine have an under prediction of OEW. On average the OEW is under predicted by 3.0%. The average absolute difference between literature and the analysis module is 6.0%. The worst results are -19.22 (EMB-145) and $+$12.86(DC-10-10).

5.8 Aerodynamic efficiency module

The aerodynamic module was revised as well. This alteration consisted of an alteration of cruise speeds in the database, debugging of the lift independent module and an elaborate alteration of the lift dependent drag module. First of all it was noticed by Vaessen during

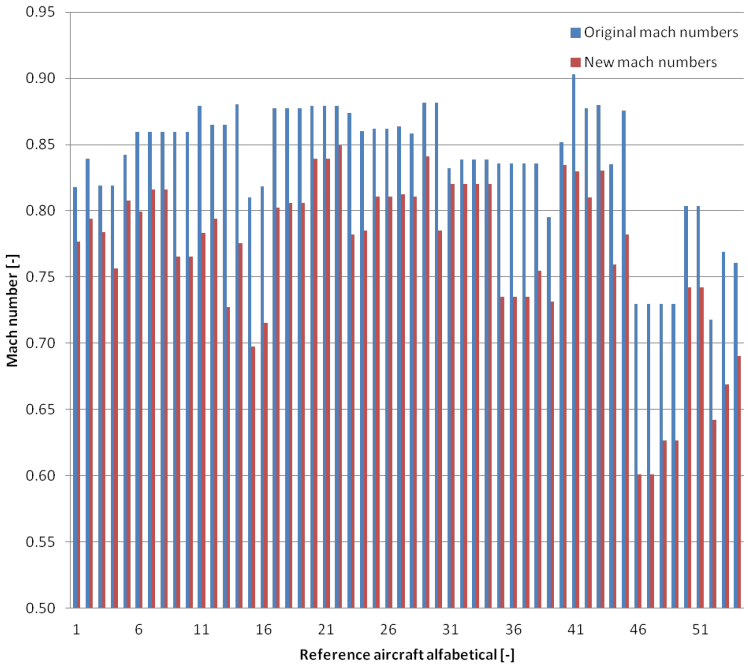

Figure 5.16: Original versus new mach numbers

his thesis [40] that the cruise Mach numbers specified in the top level requirements were too high. Figure 5.16 depicts the change in the database to the Mach numbers.

The lift independent drag include a drag contribution due to the upsweep of the aft fuselage. The formula to compute this contribution expects the upsweep of the centerline in radians, but (figure 5.17) it was given the upsweep of the aircraft bottom line in degrees.

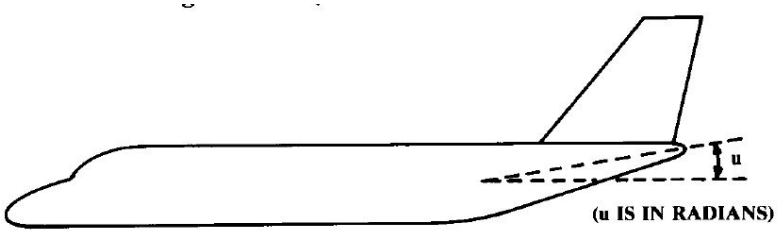

Figure 5.17: Fuselage upsweep

Finally, the lift dependent drag which comes from the Tornado calculations was altered by Vaessen. His main aim was to improve the wake prediction of the aerodynamical tool. For the drag prediction important to this research this modification came useful since the original Prandtl-Glauert (equation 5.6) correction which was used to predict lift and drag was only

valid up to Mach 0.7.

$$\begin{aligned} \beta &= \sqrt{1 - M_\infty^2} \\ C_L &= \frac{2\pi\alpha}{\beta + \frac{2}{A}} \end{aligned} \tag{5.6}$$

To verify the new aerodynamic efficiency analyses module, a new verification run was carried out, forcing the existing geometry and weights on the reference aircraft. The reduction of the Mach numbers in combination with the correction of the fuselage drag resulted in more accurate L/D predictions. The results can be found in appendix C.

5.9 Validation design routine

To validate the design routine a run was made for the maximum payload range case as well as for the design range case. The results can be seen in appendix C. The results are not uniformly improved. The main reason found for this is the inaccuracy of the top level requirements of the database. A mistake in payload and range will automatically show up in the results. However, some clear conclusions can be drawn.

- The lightest aircraft with an over prediction of their OEW all end up with a $MTOW$ that is higher than the actual values included in the database.
- The accuracy for the maximum payload reference values is higher than for the design range values.
- The aircraft with a weight under prediction, the tail mounted engine aircraft and the heavier aircraft, with the exception of the B747-400 all end up with an under prediction of their $MTOW$ with respect to the reference
- All the small Boeing aircraft feature an under prediction of weight.
- The rest of the aircraft has relative low deviations from the standard.

Chapter 6

Conceptual design of the Recreate cruiser and comparative study of direct, staged & IFR flight

This chapter discuss the conceptual design of the Recreate cruiser as performed by means of the Initiator tool described in the previous chapters. Firstly, the requirements for the design are described as specified within the Recreate project. The generated design is extensively reported in terms of geometry, performance data and compared with a list of reference aircraft to illustrate the main differences due to the specific IFR requirements.

The second part of this chapter provides a comparative study of direct, staged and IFR flight. To this purpose dedicated aircraft for all the three operation modes have to be designed using the Initiator. The obtained results have been compared with those reported by Hahn [4] and Greener by Design [16]. The main purpose of this comparison is the estimation of the fuel used by aircraft flying IFR, staged and direct flight missions and evaluate the potential fuel saving of IFR. Although no tanker aircraft designs (and relative fuel consumption) have been performed in this work fuel budgets for tanker operations have been estimated. Literature values for tanker fuel consumption are used to evaluated potential fuel efficiency benefits of IFR compared to staged and direct operations.

6.1 Requirements on the conceptual design of the cruiser

The payload of the Recreate cruiser was defined to be 250 passengers. A survey by Berdowski [41] on the average mass of passengers concluded a new standard mass per passenger had to be used. Since the people of today are heavier on average than a couple of decades ago the report advised to increase the standard from 100kg per passengers to 106kg per passengers, including luggage. Hence, the passenger mass defined in the Recreate requirements is 106kg and the design payload 26500kg. The top level requirements for the cruiser are listed in table 6.1.

Table 6.1: The top level requirements of the cruiser

Design payload	26500	kg
Design Range	2500	nm
Cruise speed	0.82	Mach
Cruise altitude	10500	m
Take-off distance (BFL)	2000	m
Landing distance (BFL)	2600	m
Take-off altitude	0	m
Landing altitude	0	m
Accommodation payload		
Passengers	250	
Single class		
Twin aisle		
LD-3 container capability		

Operating point	D point	
$ff_{Take-off}$	0.995	
ff_{Climb}	0.98	
$ff_{Descent}$	0.99	
$ff_{Landing}$	0.992	
Propulsion system		
Engine type	Turbo fan	-
SFC_{cr}	0.525	$1/hr$
SFC_{lr}	0.473	$1/hr$

The current fuel prediction method uses weight fractions for the fuel used during non cruise phases of the flight. The fractions are retrieved from literature [29]. The point of operation is required for the generation of the payload range diagram.

The mission is build up differently for IFR operations as it would be for staged and non-stop operations. Figure 6.1 depicts the mission build up for a 7500nm mission flown directly (top) or in three parts, for both an IFR (bottom) and staged flight (middle) operation.

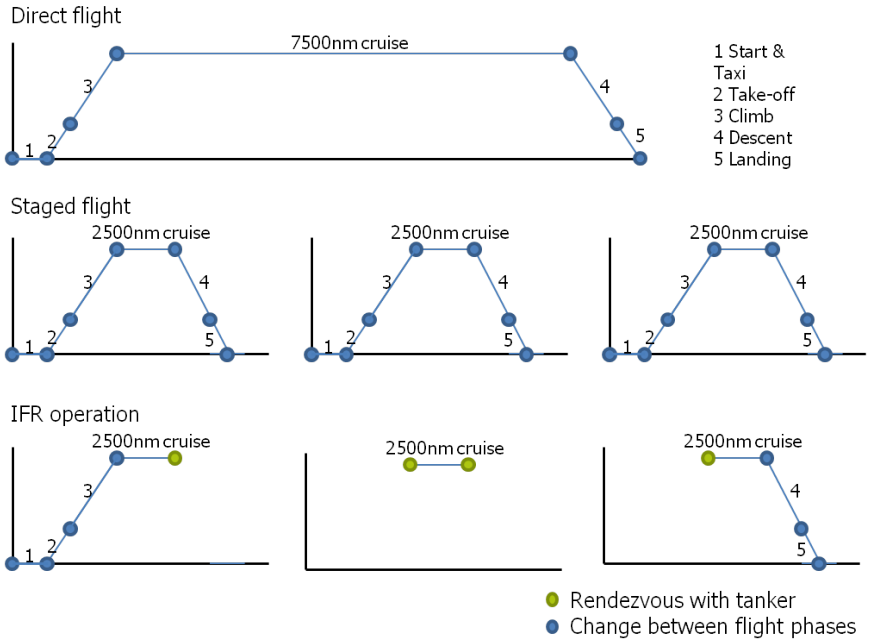

Figure 6.1: Mission build up for a 7500nm mission in direct, staged flight and IFR operation

When a 7500nm mission is divided in three part for staged flight operation, all three parts are

equally fuel intensive, since no difference in mission build up can be seen (see figure 6.1). For the IFR operation the first part, which includes the take-off is more fuel intensive than the other two. However, taking into account the required deviation manoeuvre (see figure 6.2) it can be argued that an aircraft flown in IFR has to be designed to the same fuel fractions as normal aircraft, because the mission profile including the deviation manoeuvre is equal for both mission types. Furthermore, the deviation manoeuvre start for both mission types at the end of the cruise phase, when either the refueling fails (IFR operation) or the intended airport is unavailable (normal operation).

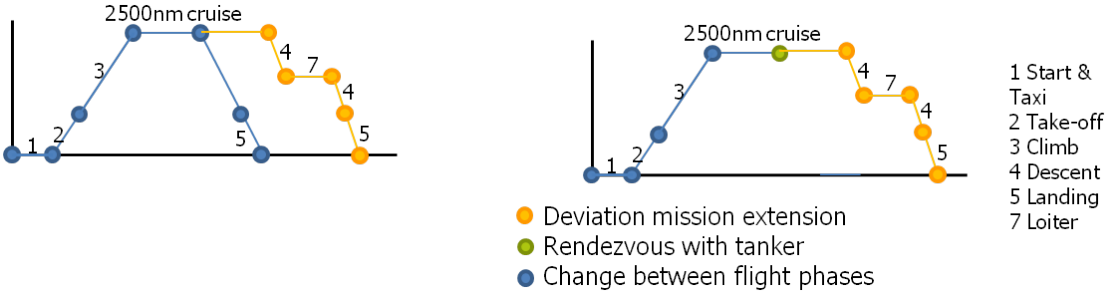

Figure 6.2: Mission deviation for a IFR and staged flight operations

The reserve fuel can be computed by the fuel required for a deviation manoeuvre. This manoeuvre was defined in the Recreate requirements to be as follows: 10% longer mission range + 30min loiter time. This added up to 3.0% of $MTOW$. However, reference aircraft [3] were found to carry 4.5%. Therefore, 4.5% of $MTOW$ was selected as reserve fuel weight.

Furthermore, the landing field length is defined by the top level requirements to be 2600m balanced field length. The balanced field length times 0.6 gives the landing field length. $2600 \cdot 0.6 = 1560m$ is the landing field length used for the design. The take-off distance of 1500 was found to be very strict. It resulted in a T/W of 0.4. (The minimum thrust loading constraint by take-off performance is active, figure 6.3 dashed pink line). The T/W of 0.4 is higher than that all reference aircraft. A relaxation of the take-off distance to 2000m yielded 20 % lower T/W ratio ($T/W = 0.32$). Figure 6.3 depicts the thrust and wing loading for both the 1500m and 2000m take-off length. Furthermore, a 8ton decrease in $MTOW$ and 1.5ton decrease in WFB was found, when the take-off constraint was relaxed. Therefore, the take-off distance requirement is increased to 2000nm. Moreover, the difference in landing and take-off distance was very large 1500m versus 2600m. This would be unpractical since to take-off the aircraft should also be able to arrive, hence land on a given runway.

The details of the payload were retrieved from a small literature study. This study can be found in Appendix E. The number of seats abreast was chosen to be 8, since this produced the most convenient slenderness ratio for the fuselage. The container type was a requirement set by the Recreate group (see table 6.1). The number of aisles is automatically determined by the fuselage design tool and is based on the number of seats abreast. The twin aisle cabin layout is therefore a direct result of the 8 seats abreast requirement (6 or less seats abreast, single aisle and 7 till 10 seats abreast, twin aisle). The payload details as provided to the fuselage design tool are listed below in table 6.2.

Chapter 3 described the trade-off for the tanker-cruiser close formation. The winning configuration (configuration D) featured no extra constrains on the configuration of the cruiser

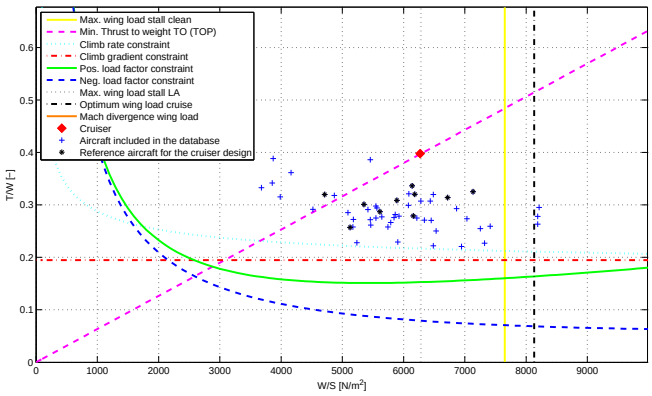

(a) Conceptual design with 1500m take-off distance

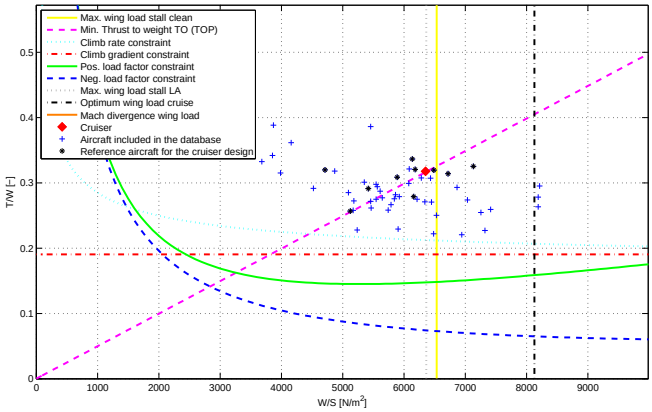

(b) Conceptual design with 2000m take-off distance

Figure 6.3: Thrust and wing loading diagrams

Table 6.2: Payload details of the cruiser

Input name	value
Seats abreast	8
Number of passengers	250
Fraction economy class	0.73
Fraction business class	0.20
Fraction first	0.07
Cargo type	container
Container type	LD-3
Double containers	true

nor on the performance of the cruiser. Therefore, configuration settings common to modern aircraft can be used. The configuration features a low wing, a conventional tail and two wing mounted engines. The configuration settings are listed in table 6.3. If the tanker-cruiser close formation changes (for example due to technical challenges regarding the forward swept

boom) there will be consequences to the cruisers design. Configuration C, where the cruiser flies in front and below the tanker will most likely require a H-tail, in order to provide a save connection point for the cruiser receptacle, since the refueling boom will approach the cruiser in this configuration from behind and above. Configuration A, the configuration which is currently used by the military requires the cruiser to be able to perform a climb of 2degrees at cruise conditions, since the cruiser trails the tanker in this configurations and thus experiences downwash from the tanker as described in chapter 3.

Table 6.3: Configuration setting of the cruiser for the Initiator

Configuration	
Aircraft type	Conventional
# Engines$_{group1}$	2
# Engines$_{group2}$	0
Connection$_{group1}$	Main wing
Connection$_{group2}$	Main wing
Tail type	Standard
Wing location	Low

6.2 Reference aircraft for the cruiser design

The design of the cruiser is based on a number of reference aircraft, as mentioned in section 4.1.1. The selected aircraft can have an influence on the end product of the Initiator, because many parameters, such as quarter chord sweep, are derived directly from curve fits built using these reference aircraft.

The reference aircraft for the design are automatically selected by the Initiator out of the 54 aircraft in the database. However, the user can specify the minimum initial service date of the reference aircraft. An minimum initial service date of 1982 was selected for this design. The selection of the Initial service date is a compromise between the selection of up-to-date aircraft and aircraft with similar top level requirements. Setting the initial service date to far in the past will result in the inclusion of aircraft with high main wing sweep angles, due to the absence of supercritical airfoil technology at that time. Setting the initial service data to far to the present will result in the inclusion only the most modern aircraft, which may have very different top level requirements. The list of aircraft selected as reference aircraft for the cruiser design can be seen in table 6.4a. The final search margin on the two main top level requirements payload and range was found to be 55%.

Table 6.4: Aircraft selected as reference for the cruiser design

- Airbus A310-300
- Airbus A320-200
- Airbus A321-200
- Boeing B737-600
- Boeing B737-800
- Boeing B757-200
- Boeing B757-300
- Boeing B767-200
- Boeing B767-300
- McDonnell Douglas MD-90-30

Furthermore, the operation point used for the top level requirements comparison can be varied between maximum payload and design points. It was found that due to the unique top level requirements of the cruiser it was better to select reference aircraft based on their top level maximum payload requirements than on their design point requirements. Figure 6.4 depicts the payload and range requirements for both the case where reference aircraft are selected based on maximum payload point and the case where they are selected on design point. Apart from the larger difference in top level requirements also the aircraft selected were different. When the reference aircraft were selected based on design point requirements the British Aerospace RJ115 was selected among the 10 reference aircraft, since all wide body aircraft featured to large range requirements.

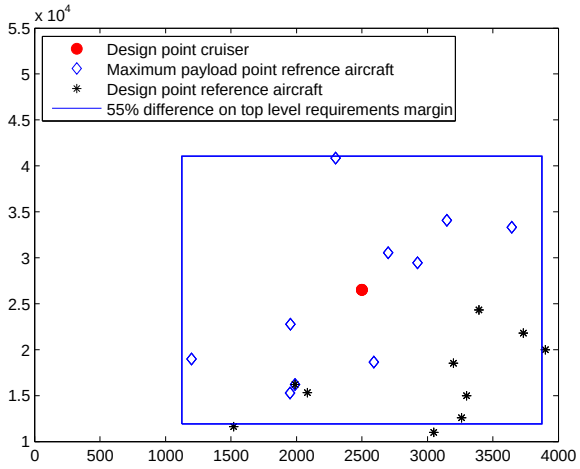

Figure 6.4: Difference in top level requirements of the selected reference aircraft

Figure 6.5a shows the maximum payload values of the reference aircraft compared to the design payload of the cruiser. Figure 6.5b shows the maximum payload range of reference aircraft compared to the design range of the cruiser. It should be noted that the selected reference aircraft either have similar payload, similar range, or a mix of payload and range, but equivalent range and payload requirements are never found, due to the unique mission of the cruiser.

(a) Payload requirements of reference aircraft

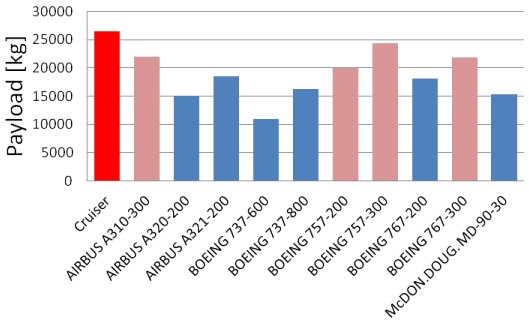

(b) Range requirements of reference aircraft

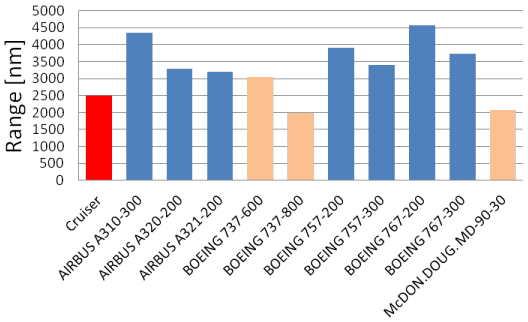

Figure 6.5: Requirements reference aircraft

6.3 Cruiser design presentation

Figure 6.6 presents the front and side view of the cruiser as generated by the Initiator. Figure 6.7 shows the top and isometric view. The small size of the wing compared to the size of the fuselage can immediately be noticed in both figures. This results from the relative large payload requirements compared to the range requirements. (A twin aisle aircraft operating the mission of a short range aircraft.)

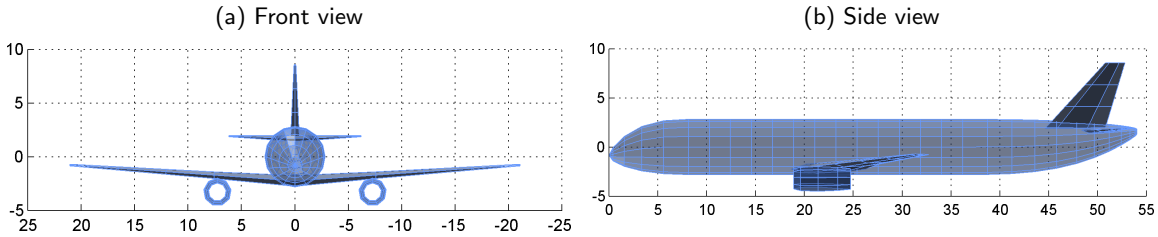

Figure 6.6: Front and side view of the cruiser

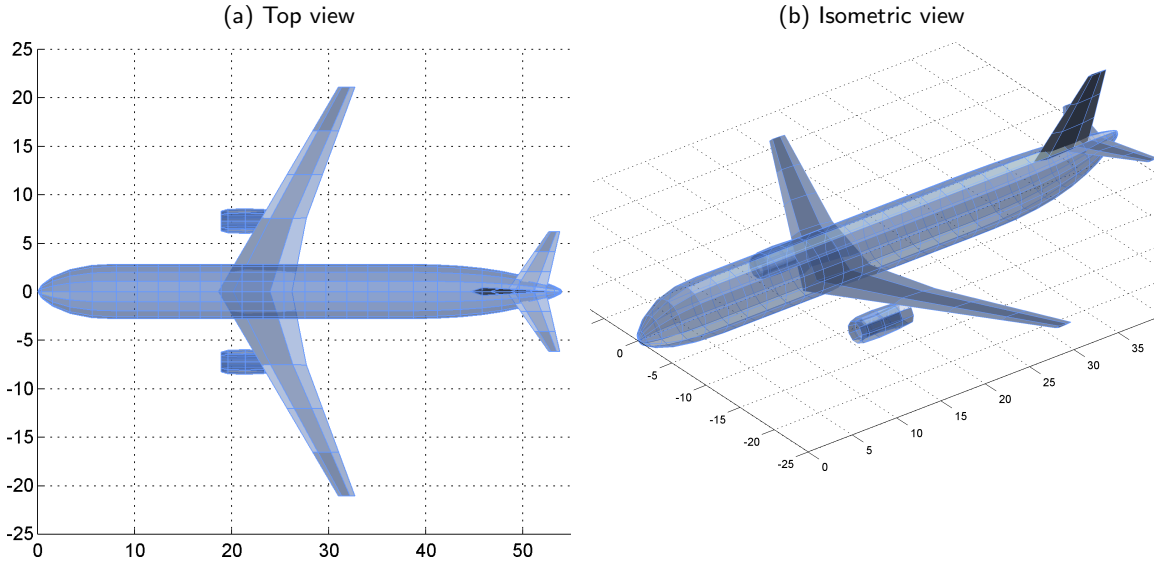

Figure 6.7: Top and isometric view of the cruiser

Figure 6.8 shows the interior layout of the fuselage for the twin aisle one class configuration defined in the Recreate top level of the cruiser design.

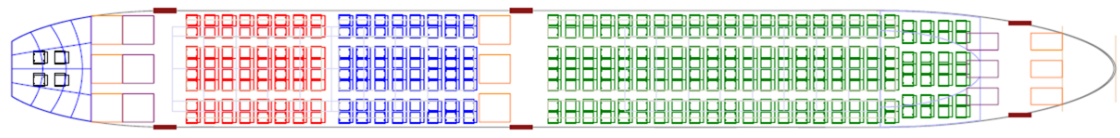

Figure 6.8: 250 seats in single class layout

The fuselage dimensions obtained from the fuselage design tool together with geometry data

of the wing, vertical and horizontal tail are listed in table 6.5. More information can be found in appendix D, which shows the automatically generated design report of the cruiser.

Table 6.5: Geometry data of the conceptual cruiser design

Main wing			
S	=	178.2	m^2
b	=	42.2	m
A	=	10.00	$-$
λ	=	0.226	$-$
Λ_{25}	=	27.3	$^\circ$
Γ	=	4.0	$^\circ$
MAC	=	4.86	m

Horizontal tail			
S_{HT}	=	32.09	m^2
b_{HT}	=	12.39	m
A_{HT}	=	4.79	$-$
λ_{HT}	=	0.282	$-$
Λ_{HT25}	=	30.3	$^\circ$
S_{HT}/S	=	0.180	$-$

Fuselage			
L_{fus}	=	54.0	m
H_{fus}	=	5.63	m
W_{fus}	=	5.63	m

Vertical tail			
S_{VT}	=	27.16	m^2
h_{VT}	=	6.67	m
A_{VT}	=	1.64	$-$
λ_{VT}	=	0.326	$-$
Λ_{VT25}	=	37.5	$^\circ$
S_{VT}/S	=	0.152	$-$

Performance parameters are documented in table 6.6. The table lists among other parameters the masses used in the generation of the payload range diagram of the cruiser. Figure 6.9 shows this payload range diagram. The maximum payload and design points of the 10 reference aircraft are shown in the same figure. The relative short range and high payload mass of the cruiser compared to the reference aircraft can be noticed. (The OEW of the cruiser is added to the maximum and design payloads of the reference aircraft. Hence, the zero fuel weight of the reference aircraft can not be deducted from this figure, only the payload mass and the range).

Table 6.6: Performance dat of the cruiser design

$MTOW$	=	115396	kg
OEW	=	62774	kg
WP_A	=	31176	kg
WP_D	=	26500	kg
WFB_A	=	16253	kg
WFB_D	=	20928	kg
$MZFW$	=	93951	kg
MLW	=	95778	kg

L/D_{cr}	=	17.9	$-$
SFC_{cr}	=	0.525	$1/hr$
V_{cr}	=	243.2	m/s
X_{cr}	=	16116	nm
PRE	=	3174	nm
PRE/X	=	0.197	$-$
R/X	=	0.155	$-$

6.4 Comparison of the cruiser design with reference aircraft

Figure 6.10 shows the thrust loading versus wing loading plot of the cruiser design. The cruiser design is constrained on wing loading by the constraint on maximum wing loading during landing (The dotted grey line). The minimum thrust loading is constrained by the minimum thrust loading required for the take-off performance (The dashed pink line). The

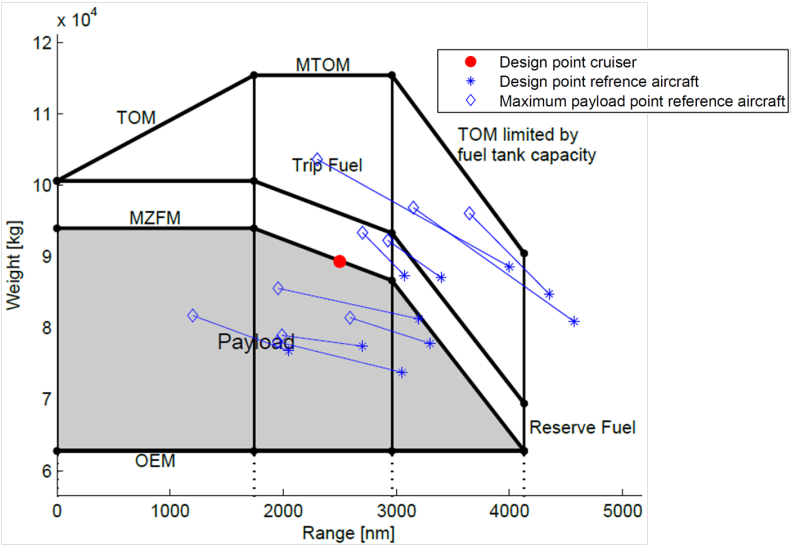

Figure 6.9: Payload range diagram of the cruiser

aircraft included in the database are depicted by blue cross markers. The blue cross markers do not include the 10 aircraft selected as reference aircraft for the cruiser design, these are depicted by a black star. The wing loading of the cruiser is quite close to the average of both the database aircraft and the selected reference aircraft. The thrust loading of the cruiser design is comparable to that of the selected reference aircraft and relatively high compared to the rest of the database aircraft.

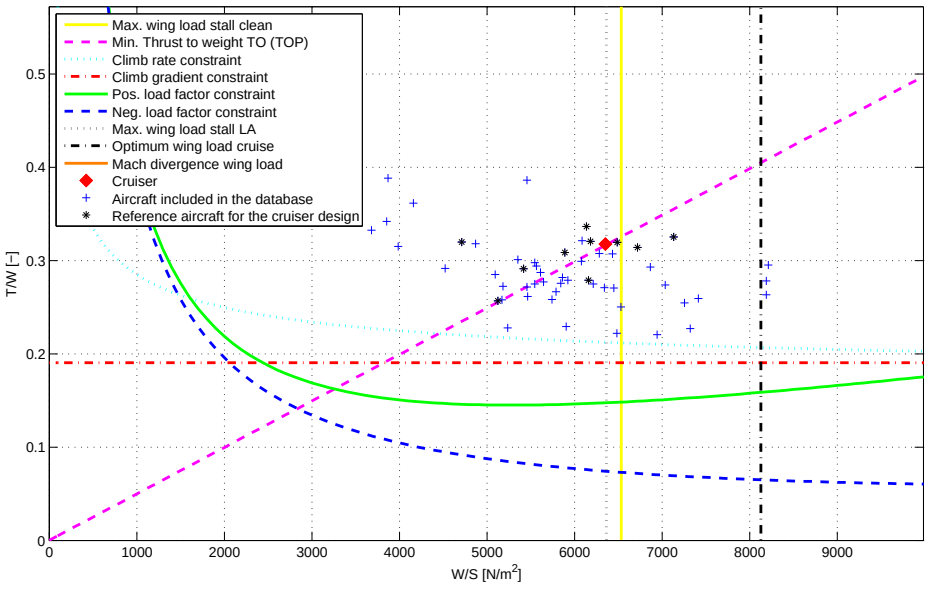

Figure 6.10: Thrust and wing loading

Table 6.7 lists all information required for the thrust loading versus wing loading plot. The wing

and thrust loading are also included in the table. Since the selected refueling configuration featured the cruiser flying in front of the tanker, the 2degrees of climb requirement during cruise is not implemented. If the refueling configuration would change (for example because of technical challanges with the forward swept boom) the 2 degrees of climb constraint should be implemented.

Table 6.7: Wing and thrust loading values

Thrust loading	0.32	
Wing loading	6347	N/m^2
Maximum C_L in clean config.	1.4	
Maximum C_L in take-off config.	2.7	
Maximum C_L in landing config.	3.0	
Aspect ratio	10	
Oswald factor	0.9	

Figure 6.11 shows a PRE versus range plot of the cruiser and aircraft from literature (derived from weight fraction, see figure 2.6). The cruiser can be found in the left top of the plot. With good L/D and SFC values and a favorable mission length it is to be expected that the design point of the cruiser is higher than most. The maximum payload PRE is however low compared to the aircraft of literature. This has two mean reasons: First of all the maximum payload is limited to decrease the maximum zero fuel weight and thereby the landing weight. Normal aircraft with similar fuselage sizes would have higher maximum payload weights, this was however found unpractical since it would result in a very low maximum payload range. Figure 6.12 shows the trend of design payload divided by maximum payload with respect to design range. Furthermore there is a decrease in achievable PRE with very short range as shown in chapter two by the example of the flight from Eindhoven to Pisa and Faro.

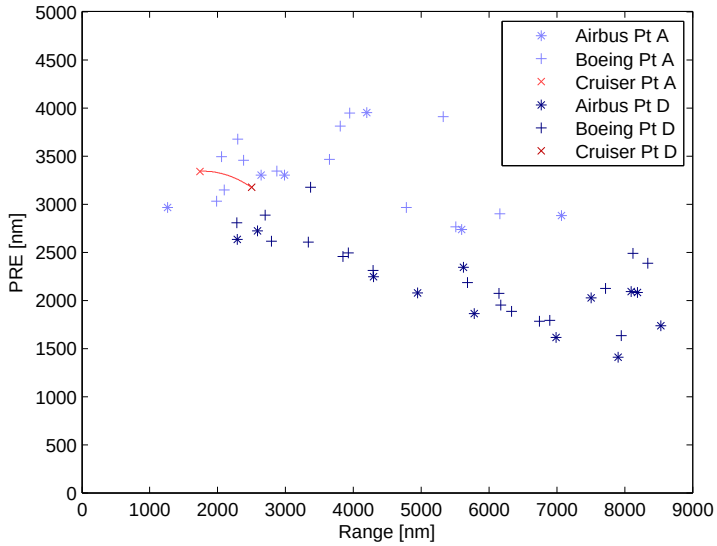

Figure 6.11: PRE and Range relationships based on weight fractions

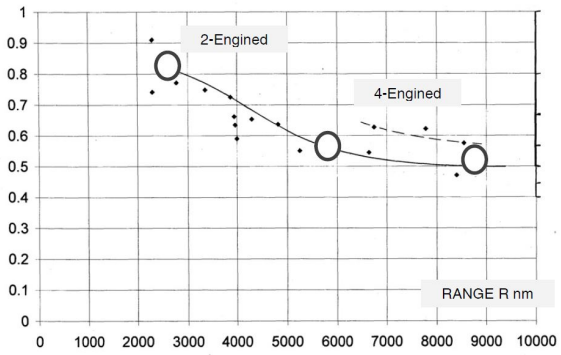

Figure 6.12: Design payload divided by maximum payload versus design range, Nangia [3]

Figure 6.13 depicts the dimensionless PRE/X value of the design point of the cruiser. In contrast to the PRE versus range plot the cruiser is now located below the aircraft from literature. It is argued that the low PRE/X value is the result of the relative large fuselage (compared to the wing and tail surface) of the cruiser, hence the relative high OEW. Other parameters such as L/D and SFC have little influence because they influence PRE as well as X

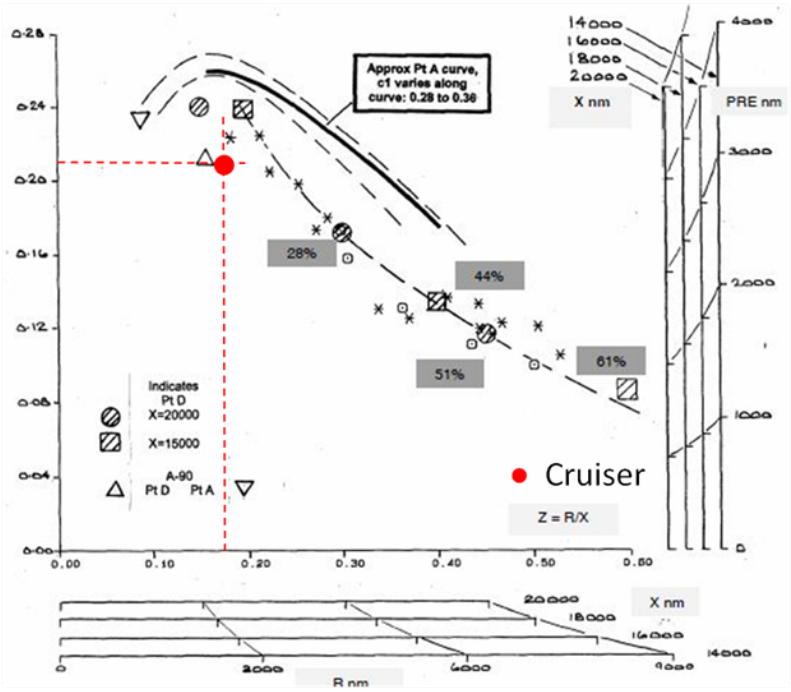

Figure 6.13: Normalized PRE versus normalized range for the design point of the cruiser

6.5 Comparison of staged to direct flight

The first fuel efficiency comparison is made between staged and non-stop flight. As mentioned in section 6.1 the fuel fractions used for the IFR operation are equal to those of normal

operation. Hence, the cruiser can also be used to perform staged flight missions of 2500nm. Hereby, the cruiser can be compared to aircraft operating direct flights on a 5000nm and 7500nm mission. The results of this comparison can be validated with the staged flight studies in literature of Greener by Design [16] and Hahn [4]. The difference in mission profile can be seen in figure 6.14.

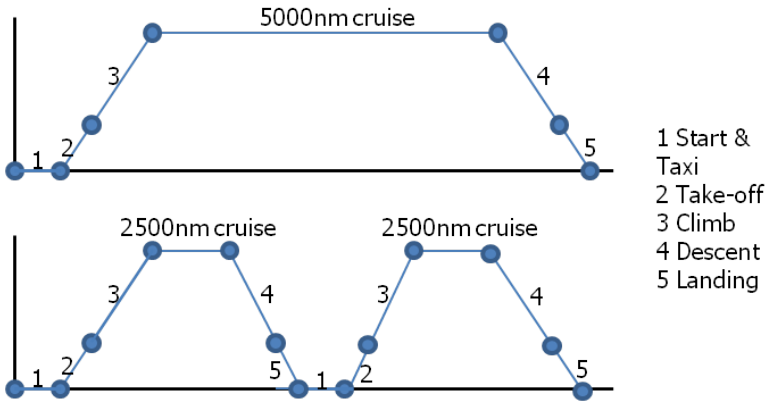

Figure 6.14: Difference in mission profile between staged (bottom) and direct (top) flight

It has to be acknowledged that the mission length of 2500nm for staged flight can be reduced, since the climb and the descent also accomplish quite some range. Nevertheless, this thesis uses weight fractions for both the climb and the descent and does not include any range coverage during these flight phases. Not including range coverage by these phases results in slightly higher fuel masses of the designed aircraft. For the operation type comparisons consequences are a a higher estimated fuel consumption for the staged flight, with respect to IFR and direct flight, since staged flight features two (5000nm mission) or three (7500nm mission) landing phases instead of one as for IFR and direct flight.

Two conceptual design are generated for direct flights of respectively, 5000nm and 7500nm missions. Table 6.8 lists the weights of the different versions as well as the PRE values. Figures 6.15 and 6.16 depict the top views of the three aircraft for a visual comparison. More aircraft details can be found in appendix D.

Table 6.8: Non-stop cruiser variations

Aircraft	MTOW		OEW		WFB		PRE	
	abs [kg]	diff [%]	abs [kg]	diff [%]	abs [kg]	diff [%]	abs [nm]	diff [%]
Cruiser	115396	-	62774	-	20873	-	3174	-
5000nm non-stop	163983	40.9	83452	31.9	46652	123	2844	-10.4
7500nm non-stop	236892	107	110784	80.8	88948	326	2237	-29.5

In table 6.8 the difference in PRE can be noticed between the non-stop aircraft and the cruiser. For a 5000nm mission the WFB is multiplied by 2 for the cruiser, it is compared to the fuel consumption of the 5000nm non-stop aircraft. The results of the fuel consumption are plotted in figure 6.17. The blue bar depicts the fuel consumption by the cruiser and serves as a reference. The extra fuel used by the non-stop aircraft is given in red. Flying a 5000nm mission in two stages gives a fuel saving of 11.5%.

(a) Cruiser

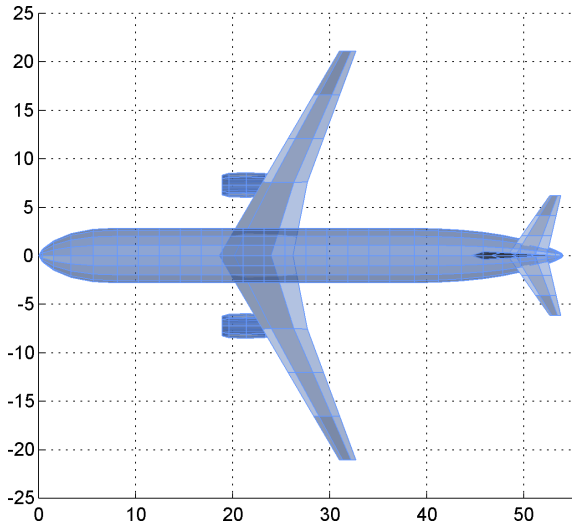

Figure 6.15: Top view of the cruiser

(a) 5000nm non-stop aircraft

(b) 7500nm non-stop aircraft

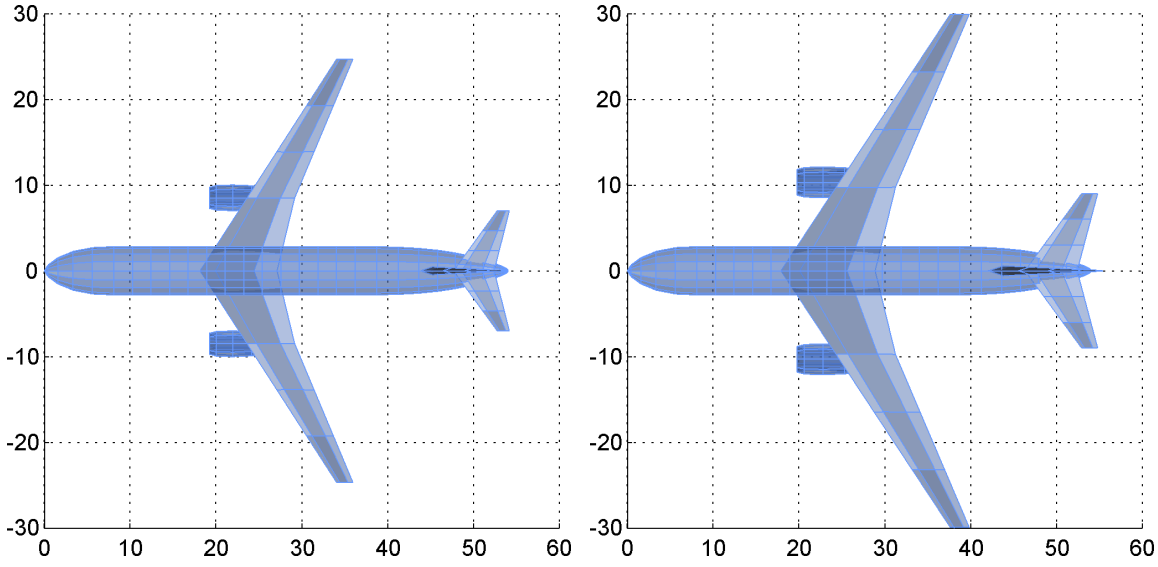

Figure 6.16: 5000nm non-stop and 7500nm non-stop variant of the cruiser

The WFB is multiplied by 3 for a cruiser performing on a 7500nm mission. Flying a 7500nm mission in three stages gives a fuel saving of 41.7%. These results can be put in context by looking at the results of the literature study of chapter 2. Both Greener by Design and Hahn, made a similar study. They state:

The Greener by Design report [16]. *A 40% increase in fuel burn was found, when the large range aircraft flew a 8099nm mission, compared to the short range aircraft flying three 2700nm missions.*

The report by Hahn [4]. *Using three stages for a total of 15,000 km would likely yield a 17%*

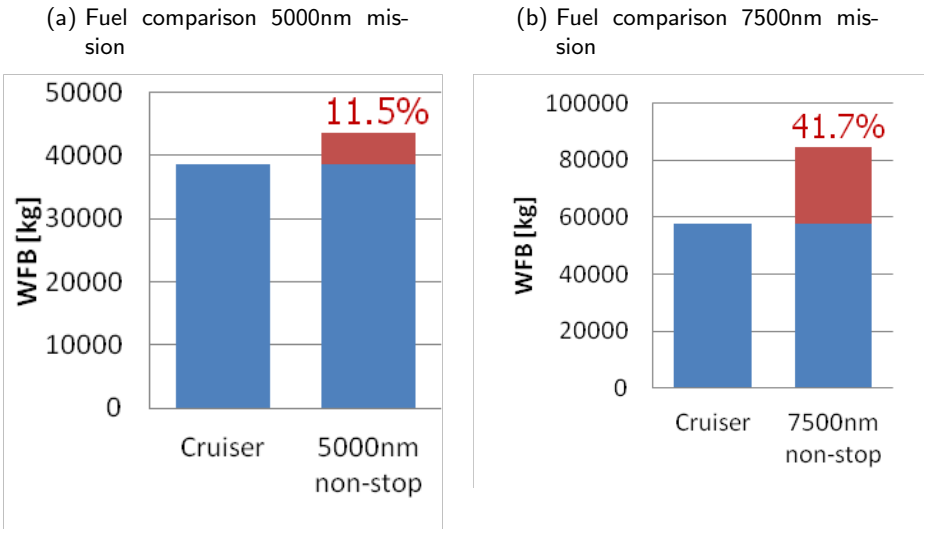

Figure 6.17: Fuel comparison between staged and non-stop flight

improvement from operation alone, a further 12% improvement from redesign for the 5,000 km stage length, resulting in a total possible improvement of 29%.

It has to be noticed that both studies divide a 8099nm mission instead of a 7500nm mission in three stages. However, the fuel increase of 41.7% relates close to the report of Greener by Design.

6.6 Comparison of staged flight to in-flight refueling

This section compares the fuel consumption of staged flight to IFR. The difference in mission type is that for the IFR concept the tanker takes the responsible of landing and taking-off. Figure 6.18 depicts the different operation modes, for a 5000nm mission and figure 6.19 for the 7500nm mission.

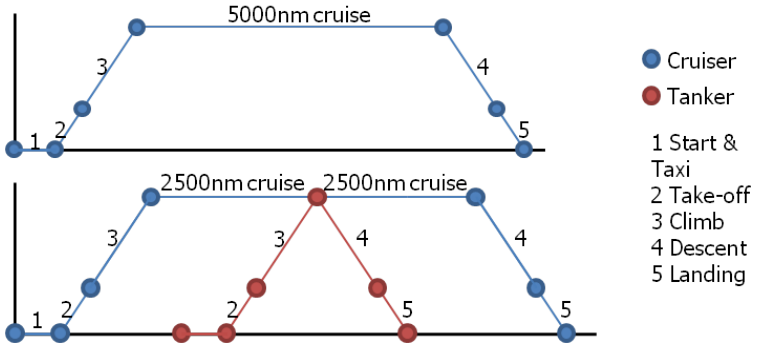

Figure 6.18: Mission descriptions of non-stop, staged and IFR operations for a 5000nm mission

As mentioned already in the introduction no tanker designs are produced during this thesis. Hence, the fuel saving between staged flight and IFR operation will not be quantified. This

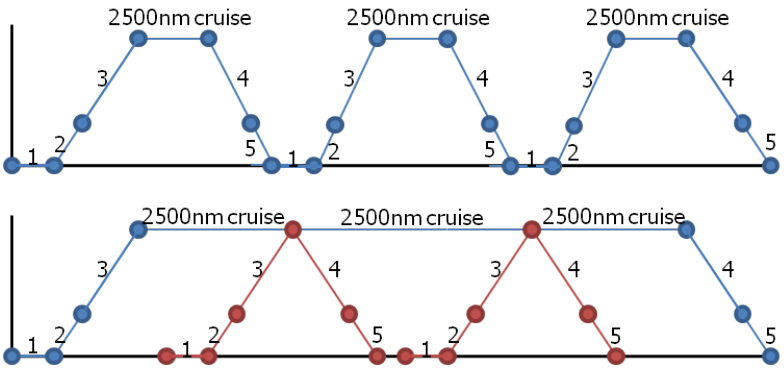

Figure 6.19: Mission descriptions of non-stop, staged and IFR operations for a 7500nm mission

section will produce a fuel 'budget' for the tanker operation. The difference in fuel consumption between the cruiser in staged and IFR operation is computed. If a tanker aircraft can deliver the required fuel within this fuel budget, IFR is more fuel efficient than staged flight and if the tanker consumes more fuel staged flight is more fuel efficient. Figure 6.19 shows that the cruiser, when flying a 7500nm mission saves two landing take-off cycles and for a 5000nm mission it saves one cycle. The fuel consumption during take-off and landing is subtracted from the fuel consumption of the cruiser. Subsequently, the fuel consumption of the cruisers is listed in tables 6.9 and 6.10. Dividing the difference in consumed fuel by the number of cycles gives the fuel available for the tanker to perform the refueling manoeuvre. The subscripts 1, 2 and 3 denoted the different parts of the mission.

Table 6.9: 5000nm mission

Operation type	$WFB_1[kg]$	$WFB_2[kg]$	$WFB_T[kg]$
Staged operation	20928	20928	41856
IFR operation	18955	18182	37137
Tanker budget			4719
Tanker budget per refueling			4719

Table 6.10: 7500nm mission

Operation type	$WFB_1[kg]$	$WFB_2[kg]$	$WFB_3[kg]$	$WFB_T[kg]$
Staged operation	20928	20928	20928	62784
IFR operation	18955	16259	18182	53396
Tanker budget				9388
Tanker budget per refueling				4694

6.7 Comparison of direct flight to IFR operation

In this section, direct flight is compared to IFR operation. The difference in mission profile can be seen in figure 6.20.

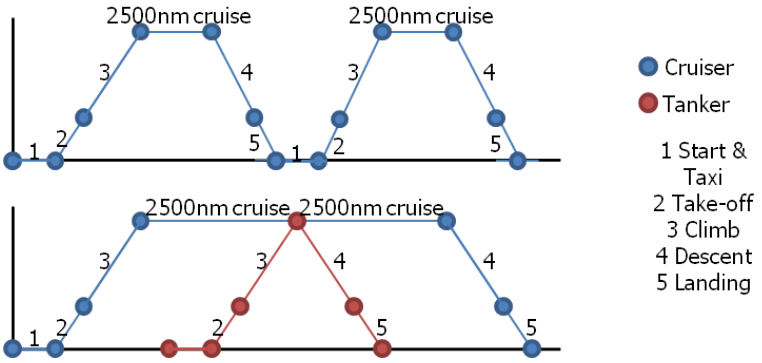

Figure 6.20: Comparing IFR and direct flight, 5000nm mission

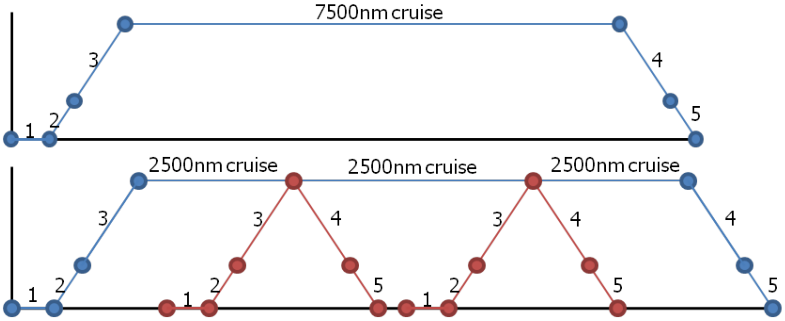

Figure 6.21: Comparing IFR and direct flight, 7500nm mission

Table 6.11: 5000nm mission

Operation type	$MTOW[kg]$	$WFB_1[kg]$	$WFB_2[kg]$	$WFB_T[kg]$
Non-stop operation	163983	46652	-	46652
IFR operation	115396	18955	18182	37137
Tanker budget				9515
Tanker budget per refueling				9515

Comparing the fuel budget to the first estimations of tanker fuel consumption by Mo Li [42] an assessment can be made on the viability of the IFR operation. Mo Li designed a number of tankers. The table includes two different configuration, conventional and flying wing, two different tanker to cruiser ranges, 250nm and 500nm and 3 different number of aircrafts refueled per tanker mission. These results yield 12 different tankers ($2 \cdot 2 \cdot 3 = 12$). The fuel consumption of the tankers is computed for a fuel delivery mass of 16259kg. This 16259 complies with the fuel burned by the cruiser in the cruise phase. The results are shown in table 6.13. Based on these fuel consumptions, IFR would outperform direct flight with all 12 tanker designs. Furthermore, IFR would outperform staged flight with 9 of the 12 concepts.

Table 6.12: 7500nm mission

Operation type	$MTOW[kg]$	$WFB_1[kg]$	$WFB_2[kg]$	$WFB_3[kg]$	$WFB_T[kg]$
Non-stop operation	236892	88948	-	-	88948
IFR operation	115396	18955	16259	18182	53396
Tanker budget					35552
Tanker budget per refueling					17776

Table 6.13: Fuel consumption tankers

Refueling Radius [nm]	250	250	250	500	500	500
Refueling cruiser num.	1	3	5	1	3	5
Fuel consumed by Conventional Tanker [kg]	2165	3498	5443	2997	4257	6431
Fuel consumed by Flying-wing Tanker [kg]	1790	2741	4074	2449	3448	4806

6.8 Comparison of the cruiser to existing aircraft

As stated by Hahn, the fuel savings of staged flight can be divided into a part due to operations alone and the other part due to the redesign of the aircraft. This section compares two existing aircraft to the cruiser, to verify the claim that new aircraft are required for the new concept. The first aircraft has comparable payload requirements, the Boeing B767-300. The second aircraft has a comparable range requirements, the Boeing B737-800. Both concept are designed by the Initiator. This will give a fairer comparison than the literature values, since the deviations of the Initiator are passed through all the concepts. Hence, the starting point of both designs are the top level requirements and not the actual geometry of respectively the B767-300 and the B737-800. The B737-800 is designed based on its design point requirements. Since the design point requirements of the B737-800 match the 2500nm range requirement of the cruiser. The B767-300 is designed to the top level requirements of its maximum payload point, because these come closer than its design point requirements to both the cruiser requirements and its point of operation (2500nm range and 250 passengers no cargo). Both sets of top level requirements are listed in table 6.22.

The Boeing B737-800 has already the same range as the cruiser. This makes comparison between both aircraft easy. However, the fuselage has to be refitted in order to provide the same level of passenger comfort as the cruiser. Long range flights feature namely more flight attendants, galley and toilet per passenger as well as a higher seat pitch. These extra requirements on the cabin layout will lower the amount of passengers that can be accommodated in the aircraft. Hence, the payload weight for a passengers only (including luggage but no cargo) flight will be lower than in normal 2500nm direct flights. The fuselage design tool was used to compute the amount of passengers that could be accommodated in the B737-800 if similar passenger comfort levels were used as for the cruiser. The amount of passengers that could be accommodated was found to be 142 in single class, 47 less than the maximum density configuration which is used by airliners for budget short range operations (see figure 6.24).

The other reference aircraft, the B767-300 has similar payload capabilities so the same number of passenger (n=250) was accommodated in B767-300, for the fuel efficiency comparison. The

Figure 6.22: Top level requirements of existing aircraft used for comparison

(a) Top level requirements of the B737-800

Requirements		
$Payload$	18597	kg
$Range$	2500	nm
$Mach_{cr}$	0.81	-
Alt_{cr}	41000	ft
TO_{dist}	2000	m
LA_{dist}	1600	m
TO_{Alt}	0	ft
LA_{Alt}	0	ft

(b) Top level requirements of the B767-300

Requirements		
$Payload$	39140	kg
$Range$	3221	nm
$Mach_{cr}$	0.81	-
Alt_{cr}	39000	ft
TO_{dist}	2545	m
LA_{dist}	1646	m
TO_{Alt}	0	ft
LA_{Alt}	0	ft

(a) Boeing B737-800

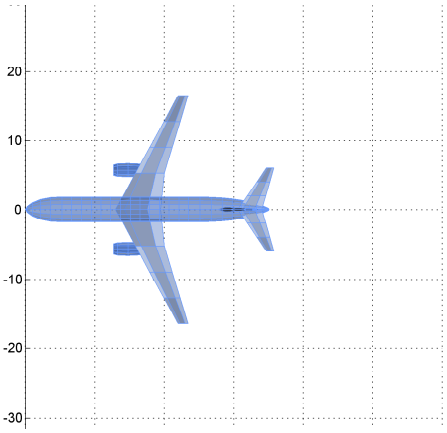

(b) Boeing 767-300

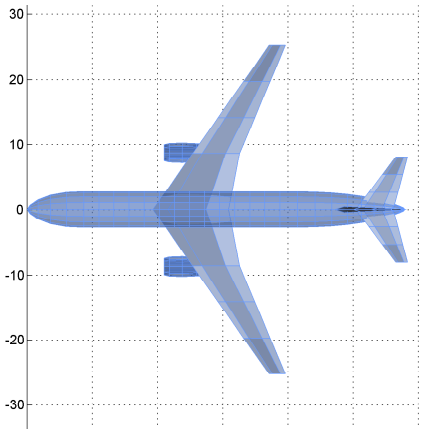

Figure 6.23: Existing concepts compared to the cruiser

B767-300 has a slightly smaller fuselage resulting in a little less passenger comfort, furthermore the PRE value of the Boeing B737-800 was found to be 9.6% lower as that of the cruiser. Also the B737-800 had a lower PRE value (7.3% lower). The results of the comparison can be found in table 6.14.

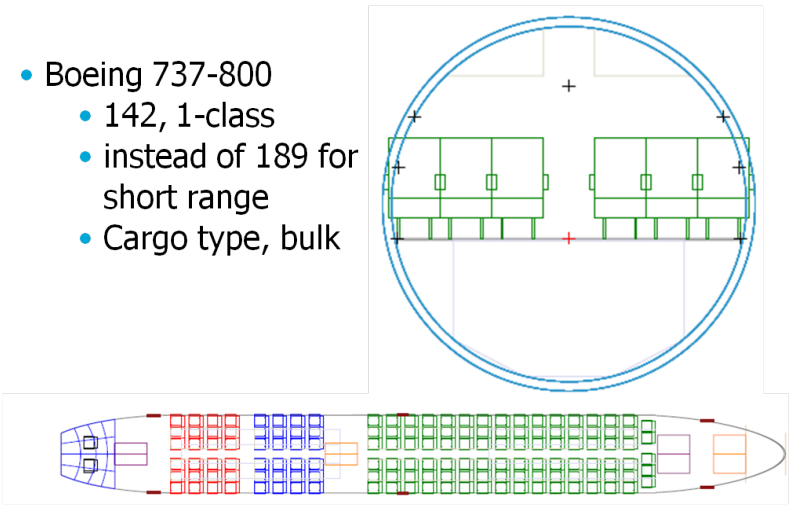

Figure 6.24: Interior layout of a B737-800 refitted for similar passenger comfort as the cruiser.

Table 6.14: Comparison cruiser to a B767-300 and a B737-800 carrying passengers only at a 2500nm mission.

Aircraft	WP[kg]	Diff [%]	WFB[kg]	Diff [%]	PRE[kg]	Diff [%]
Cruiser	26500	-	20873	-	3174	-
Boeing 737-800	15052	-43.2	12788	-38.7	2942	-7.3
Boeing 767-300	26500	0	23089	10.6	2869	-9.6

Chapter 7

Conclusions & recommendations

Based on the research and developments presented in the preceding chapters, different conclusions are drawn. Additionally, several recommendations can be given for further developments of these tools and further research on these topics. The conclusions and recommendations are divided into two parts. A part concerning the main research goal: *Develop the conceptual design of a passenger aircraft, the cruiser, for IFR operation and compare its fuel consumption to non-stop and staged flight operation.* and a part concerning the subgoal: *Improve the Initiator in order to make it capable of producing the conceptual designs required to achieve the main research goal.*

7.1 Conclusions concerning the IFR concept

- A conceptual cruiser design is produced.
- Two non-stop variants are designed, with mission ranges of 5000nm and 7500nm.
- For these ranges non-stop operations had a fuel consumption increase of 11.5% and 41.7%, for respectively 5000nm and 7500nm mission range.
- Comparing fuel burn of the cruiser in IFR operation to staged and non-stop operations yielded a tanker fuel "budget" for operations. Based on tanker concept from literature, 9 out of 12 tanker concepts are more fuel efficient than staged flight. For non-stop operations 12 out of 12 tanker concepts yield a more fuel efficient solution.
- Designs based on the top level requirements of existing aircraft, with similar payload requirements or range requirements, were found to be less fuel efficient than the cruiser, for the same level of passenger comfort.
- IFR allows for shorter mission durations than staged flight, due to the absence of extra take-offs and landings. This gives higher passenger comfort as well as shorter turnaround times for the airliners. Furthermore, the absence of extra take-offs and landings reduces fatigue on the fuselage, wear on the tyres and does not involve the cost of extra take-off and landing fees.
- Operating aircraft on maximum payload range increases their fuel efficiency with respect to operating the aircraft at design point range. A cruiser operating with maximum payload at 2500nm would outperform existing aircraft in terms of fuel efficiency.

7.2 Recommendations concerning the IFR concept

- Investigate the use of oval fuselages, to maintain cabin size for passengers and decrease unused cargo area.
- Investigate unconventional configurations for the cruiser design.
- Investigate weight penalties for the cruiser related to IFR operation, such as the extra weight related to the pipes and receptacle needed for the fuel transfer in mid-air.
- The climb and descent phases are not considered to cover any of the mission range distance. This should be investigated since with the current assumption staged operations are in a clear disadvantage, since the extra take-off and landings of this mode cost fuel and do not contribute to any mission range coverage (In contrast to reality).

7.3 Conclusions concerning the Initiator

- The Initiator is able to incorporate a fuselage design tool in the design process.
- The Initiator can design existing aircraft within a reasonable margin of accuracy, from only the top level requirements.
- Individual analysis modules can be verified separately, by fixing geometries settings and performance settings.
- The results of a design can be exported in multiple formats (CPACS, MMG input, Latex, etc..)

7.4 Recommendations concerning the Initiator

- Restructuring the Initiator in a more modular setup, to make data flows more transparent.
- Decrease the designs database dependency, by replacing parameter determination using the mean of the reference aircraft by empirical relations in the design modules.
- Increase knowledge on the design by increasing the capabilities of the current modules, so that the non-cruise phases can be analyzed based on L/D graphs and engine maps instead of fuel fractions.
- Examine alternative design routines to include optimizing routines.

References

[1] Rocca, G. L., *Wing Design Part II*, Delft University of Technology, 2011.

[2] Li, M., "Benefit of Staging Airliner Operations," Delft University of Technology.

[3] Nangia, R., "Effiency parameters for modern commercial aircraft," *The Aeronautical Journal*, 2006.

[4] Hahn, A. S., "Staging Airliner Service," *AIAA Aviation Technoly*, Vol. 7th, 2007.

[5] Anon., "Official Site of the U.S. Air Force," `http://www.af.mil`, October 2012.

[6] Cobham, "Air-to-Air Refuelling Takes Off," `http://www.cobham75.com/cobham-the-company-1934-1985/air-to-air-refuelling-takes-off.aspx`, October 2009.

[7] Birdsall, S., *Superfortress, the Boeing B-29 - Aircraft Specials series*, Squadron/Signal Publications, 1980.

[8] Winchester, J., editor, *Aircraft of WWII*, 2004.

[9] Scott, J., "V-Formation Flight of Birds," `http://www.aerospaceweb.org/question/nature/q0237.`, 2005.

[10] Talay, T. A., *Introduction to the aerodynamics of flight*, President, Hallgren Associates, Inc, 2006.

[11] Blake, W. and Multhopp, D., "Design, performance and modeling considerations for close formation flight," *AIAA Aviation Technoly*, Vol. AIAA-98-4343, 1998.

[12] Brouwers, Y., *Development of KBE application to support the conceptual design of passengers aircraft fuselages*, Master's thesis, Delft University of Technology, June 2011.

[13] Langen, T., *Development of a conceptual design tool for conventional and boxwing aircraft*, Master's thesis, Delft University of Technology, 2011.

[14] Boeing, "Typical 3-Class Seating," http://www.boeing.com/commercial/767family/pf/pf_seating_charts.html, October 2012.

[15] Anon., "Boeing B-47 Stratojet," http://en.wikipedia.org/wiki/Boeing_B-47_Stratojet, February 2012.

[16] Air Travel - Greener by Design, *The Technology Challenge*.

[17] Melkert, J. A., *Preliminary sizing of Aircraft*, TU Delft, 2009.

[18] Kenway, G., "Reducing Aviation's Environmental Impact Through Large Aircraft For Short Ranges," *AIAA Aviation Technology*, Vol. 48th, 2010, pp. 11.

[19] Anon., "Aerial refueling," http://en.wikipedia.org/wiki/Aerial_refueling#cite_ref-0, October 2012.

[20] Bomberguy, "In-flight refueling of the Empire Flying Boat," http://www.youtube.com/watch?v=NOlgtozYPh8, October 2007.

[21] Anon., "Devolopment of aviation technology," http://www.century-of-flight.net/Aviation%20history/evolution%20of%20technology/Aerial%20Refueling.htm, October 2012.

[22] Pennington, R. J., "Tankers," *Air&Space*, October 1997, pp. 26–37.

[23] Callander, B. D., "Lucky Lady II," http://www.airforce-magazine.com/MagazineArchive/Pages/1999/March%201999/0399lucky.aspx, March 1999.

[24] Cobb, M. R., *Aerial Refueling: The Need for a Multipoint, Dual-System Capability*, Air University Press, 1987.

[25] Airbus, "A330MRTT About," http://www.a330mrtt.com/Aircraft/A330MRTT, 2012.

[26] Cobham, "Aerial Refuelling Systems," http://www.cobham.com/about-cobham/mission-systems/about-us/mission-equipment/air-to-air-refuelling/products-and-services/hose-and-drogue-systems/fuselage-refuelling-units/a330mrtt-refuelling-systems-datasheet.aspx, May 2012.

[27] Li, M., "Trade-off and selection of cruiser-feeder approach configurations for in-flight refueling," .

[28] Melin, T., *Users guide and reference manual for Tornado*, Royal Institute of Technology (KTH), Department of aeronautics, December 2000.

[29] Raymer, D., *Aircraft Design: A Conceptual approach*, AIAA, 2006.

[30] Roskam, J., *Airplane design*, Roskam aviation and engineering corporation, 1985.

[31] Kok, H., *Quantitative Assessment of a Distributed Propulsion System*, Master's thesis, Delft University of Technology, 2008.

[32] Élodie Roux, *Influence de l'allongement voilure d'un avion basse vitesse sur ses performances conceptuelles*, SupAéro, 2006.

[33] Seider, D., "Remote Component Environment (RCE)," `http://www.dlr.de/sc/desktopdefault.aspx/tabid-5625/9170_read-17513/`, July 2013.

[34] Bolsunovsky, A., "Flying wing: Problems and Decisions," *Innovative configurations and adanced concepts for future civil aircraft*, 2005.

[35] Lee, J. J., *Historical and Future Trends in Aircraft Performance, Cost, and Emissions*, Master's thesis, Massachusetts Institute of Technology, 2000.

[36] Linke, F., Langhaus, S., and Gollnick, V., "Global Fuel Analysis of Intermediate Stop Operations on Long-Haul Routes," *AIAA Aviation Technology*, Vol. 11th, 2011, pp. 12.

[37] Babikian, R., "The Historical Fuel Efficiency Characteristics of Regional Aircraft from Technological, Operational, and Cost Perspectives," *Massachusetts Institute of Technology*, 2012.

[38] Jackson, P., *Jane's All the world's Aircraft 2004-2005*, Jane's Information Group Limited, 2004.

[39] Torenbeek, E., *Synthesis of Subsonic Airplane Design*, Delft University of Technology, 1976.

[40] Vaessen, F., *Improved aerodynamic analysis to predict wing interaction of high-subsonic three-surface aircraft*, Master's thesis, Delft University of Technology, 2013.

[41] Berdowski, Z., "Survey on standard weights of passengers and baggage," Tech. rep., European Aviation Safety Agency, May 2009.

[42] Li, M., "Tanker design for in-flight refueling opeations," 2013.

[43] TripAdvisor, "Seat arrangements," `http://www.seatguru.com/airlines/KLM/KLM_Airbus_A330-200.php`, Augustus 2012.

[44] Forum, C. A., "Define Long Haul," `http://www.airliners.net/aviation-forums/general_aviation/read.main/2260348/`, 2012.

Appendix A

The previous performance and geometry database of reference aircraft

This appendix shows the database used by the Initiator as available at the beginning of this thesis. It contains information on the performance of reference aircraft as well as information on the geometry of the different aircraft parts.

Table A.1 Performance and geometry data of reference aircraft, used by the Initiator as available at the begining of this thesis

	Performance Parameters																									
	Main Requirements				Aerodynamics				Weights					TO & Landing			Speeds		Engines							
	[kg]	[ft]	[-]	[NM]	[-]	[-]	[-]	[-]	[kg]	[kg]	[kg]	[kg]	[kg]	[m]	[m]	[ft]	[kts]	[kts]	[kN]	[-]	[kN]	[kg]	[m]	[m]	[1/hr]	[1/hr]
Aircraft	Maximum payload	Cruise altitude	Cruise Mach no.	Maximum payload range	L/D cruise	CL-max take-off	CL-max landing	CDO clean	Max. take-off mass	Operational Empty mass	Max. landing mass	Max. zero-fuel mass	Max. Payload fuel mass	Take-off distance	Landing distance	Max. take-off & landing alt.	Rotation speed (V2)	Approach speed (Vapp)	Total static thrust/power	No. of engines	Static thrust/ power per engine	Engine mass	Engine length	Engine diameter	SFC cruise	SFC loiter
AIRBUS A300-600R	41100	31000	0.82	3283	12.58	2.44	2.98	0.0260	170500	88900	140000	130000	40500	2280	1489	0	153.00	136.00	514.00	2	257.00	5824	6.70	2.70	0.340	0.306
AIRBUS A310-300	33300	35000	0.84	3645	13.06	2.45	3.02	0.0292	150000	79666	123000	113000	37000	2290	1490	0	156.00	138.00	462.00	2	231.00	4888	6.30	2.70	0.340	0.306
AIRBUS A320-200	19190	28000	0.82	1955	10.54	2.56	3.00	0.0285	73500	41310	64500	60500	13000	2180	1440	0	143.00	134.00	222.40	2	111.20	2118	4.44	2.37	0.296	0.266
AIRBUS A321-200	22780	28000	0.82	1955	11.73	3.10	3.23	0.0293	89000	48000	73500	71500	17500	2000	1580	0	143.00	138.00	284.00	2	142.00	2684	4.44	2.37	0.396	0.357
AIRBUS A330-200	36400	33000	0.84	4210	14.43	2.21	2.74	0.0211	230000	120200	177150	165142	64858	2470	1750	0	158.00	135.00	620.00	2	310.00	6134	7.00	3.10	0.405	0.365
AIRBUS A330-300	48400	33000	0.86	3888	14.75	2.51	2.73	0.0213	217000	118189	179000	169000	48000	2320	1600	0	144.00	136.00	600.00	2	300.00	6071	7.00	3.10	0.313	0.281
AIRBUS A340-200	49400	33000	0.86	6393	15.84	2.60	2.84	0.0212	257000	120228	181000	172000	85000	2790	1856	0	154.00	134.00	556.00	4	139.00	2621	4.95	2.37	0.380	0.342
AIRBUS A340-300	48150	33000	0.86	6371	15.82	2.61	2.89	0.0214	271000	129850	190000	178000	93000	3000	1964	0	160.00	136.00	604.00	4	151.00	2853	4.95	2.37	0.403	0.363
AIRBUS A340-500	51635	33000	0.86	7050	17.17	2.61	2.86	0.0198	365000	170390	236000	222000	143000	3100	2090	0	160.00	139.00	943.20	4	235.80	4425	6.10	3.05	0.482	0.434
AIRBUS A340-600	63000	33000	0.86	5700	17.44	2.61	2.87	0.0200	365000	177010	254000	240000	125000	3100	2240	0	160.00	144.00	996.40	4	249.10	4700	6.10	3.05	0.495	0.445
AIRBUS A380-800	85000	35000	0.88	6200	15.73	2.61	2.60	0.0192	540000	271000	386000	356000	184000	3700	2500	0	160.00	143.00	1176.00	4	294.00	5568	7.30	4.00	0.413	0.372
BOEING 707-320C	38100	25000	0.87	3150	14.10	1.90	2.22	0.0163	151315	66224	112037	104330	46985	3054	1905	0	170.00	135.00	338.16	4	84.54	1852	6.00	1.60	0.651	0.586
BOEING 717-200	12220	25000	0.87	1200	8.06	2.15	3.01	0.0295	51710	31675	46266	43545	8165	2500	1445	0	165.00	130.00	195.80	2	97.90	1715	6.10	1.75	0.319	0.287
BOEING 727-200Adv	18597	25000	0.88	2140	9.72	1.90	2.51	0.0226	95028	46164	72575	63318	31710	3033	1494	0	166.00	137.00	213.60	3	71.20	1456	7.00	1.50	0.749	0.674
BOEING 737-200	15445	25000	0.81	1549	9.48	2.32	3.06	0.0314	52390	27646	46720	43091	9299	1829	1350	0	147.00	131.00	142.40	2	71.20	1484	7.00	1.50	0.339	0.305
BOEING 737-300	16030	26000	0.82	1578	9.98	2.47	3.28	0.0321	56470	31869	51710	47630	8840	1939	1396	0	148.00	133.00	178.00	2	89.00	1897	4.70	2.00	0.278	0.250
BOEING 737-600	9800	41000	0.88	3050	12.61	2.49	3.32	0.0265	65090	36440	54650	51480	13610	1832	1268	0	142.00	120.00	164.00	2	82.00	1421	4.70	2.06	0.306	0.275
BOEING 737-700	11610	41000	0.88	3050	13.29	2.49	3.32	0.0267	69400	37585	58060	54650	14750	1900	1356	0	142.00	125.00	178.00	2	89.00	1565	4.70	2.06	0.331	0.298
BOEING 737-800	14690	41000	0.88	2700	14.32	2.49	3.32	0.0273	78220	41480	65310	61680	16540	2000	1600	0	142.00	130.00	214.00	2	107.00	1904	4.70	2.06	0.400	0.360
BOEING 747-100	69625	35000	0.88	4427	14.19	2.03	2.58	0.0227	340195	169190	255830	238815	101380	3050	1890	0	169.00	141.00	835.20	4	208.80	4786	5.61	2.80	0.426	0.384
BOEING 747-200	62820	35000	0.88	5930	14.58	2.06	2.58	0.0227	377840	175995	255830	238815	139025	3190	1890	0	177.00	141.00	944.00	4	236.00	5371	5.61	2.80	0.449	0.404
BOEING 747-400	61186	35000	0.88	6857	15.50	1.92	2.38	0.0223	396830	181484	285760	242670	154160	3310	2130	0	185.00	153.00	1009.60	4	252.40	5218	5.64	2.90	0.448	0.403
BOEING 757-200	25690	31000	0.87	3812	12.81	2.42	2.81	0.0234	115900	58040	95450	84550	31350	2226	1564	0	150.00	137.00	382.60	2	191.30	3998	5.20	2.60	0.390	0.351
BOEING 757-300	29470	31000	0.86	2925	12.82	2.17	2.78	0.0240	122470	65980	101600	95250	27220	2550	1700	0	163.00	142.00	384.00	2	192.00	3598	5.20	2.60	0.368	0.331
BOEING 767-200	34065	39000	0.86	3150	14.24	2.08	2.39	0.0224	136078	80921	122470	112491	23587	1770	1463	0	142.00	136.00	427.00	2	213.50	4511	6.22	2.68	0.240	0.216
BOEING 767-200ER	35652	39000	0.86	5050	15.27	2.03	2.38	0.0224	175540	83788	129293	117934	57606	2670	1524	0	163.00	140.00	515.20	2	257.60	5546	6.22	2.68	0.448	0.403
BOEING 767-300	39140	39000	0.86	3221	15.30	1.86	2.47	0.0228	156489	87135	136078	126099	30390	2545	1646	0	161.00	141.00	447.00	2	223.50	4744	6.22	2.68	0.308	0.277
BOEING 767-300ER	45541	39000	0.86	3500	16.51	1.87	2.49	0.0228	181437	89902	145149	130634	50803	2926	1740	0	173.00	145.00	547.20	2	273.60	5926	6.22	2.68	0.547	0.492
BOEING 777-200	54635	39000	0.88	3250	15.65	1.90	2.53	0.0215	242670	135875	201850	190510	52160	2360	1585	0	170.00	138.00	700.00	2	350.00	7147	7.30	3.20	0.378	0.340
BOEING 777-300	68570	39000	0.88	3800	16.66	1.90	2.55	0.0221	299370	155960	237685	224530	74840	2650	1860	0	170.00	145.00	860.00	2	430.00	8792	7.30	3.20	0.438	0.394
DOUG. DC 9-10	9570	25000	0.83	1200	7.54	2.20	2.99	0.0298	35245	20550	33565	30120	5125	1615	1411	0	127.00	115.00	109.00	2	54.50	1121	5.30	1.56	0.243	0.219
DOUG. DC 9-30	14000	26000	0.84	1546	8.96	2.45	3.12	0.0289	49000	25400	45000	39500	9500	1777	1317	0	137.00	126.00	124.00	2	62.00	1275	5.30	1.56	0.386	0.347
DOUG. DC 9-40	15510	27000	0.84	1423	9.69	2.13	2.97	0.0293	51710	27800	46265	42184	9526	2091	1457	0	151.00	131.00	137.80	2	68.90	1423	5.30	1.56	0.413	0.372
DOUG. DC 9-50	15265	27000	0.84	1361	9.81	1.99	3.15	0.0297	54420	29300	49885	44670	9750	2362	1439	0	160.00	132.00	137.80	2	68.90	1360	5.30	1.56	0.416	0.375
McDON.DOUG. MD-81	17953	27000	0.84	1385	10.24	2.25	2.99	0.0272	63500	35570	58000	53500	10000	2195	1481	0	148.00	133.00	171.20	2	85.60	1672	6.10	2.00	0.334	0.301
McDON.DOUG. MD-82	18802	27000	0.84	1860	10.70	2.25	2.99	0.0272	67812	35630	58970	55340	12472	2274	1500	0	153.00	134.00	185.40	2	92.70	1825	6.10	2.00	0.347	0.312
McDON.DOUG. MD-83	18721	27000	0.84	2369	10.98	2.41	2.98	0.0272	72580	36620	63280	55340	17240	2551	1585	0	153.00	139.00	193.00	2	96.50	1908	6.10	2.00	0.428	0.385
McDON.DOUG. MD-87	17619	27000	0.84	1863	10.35	2.48	2.99	0.0268	63500	33253	58000	53524	9976	1865	1451	0	141.00	133.00	185.40	2	92.70	1825	6.10	1.95	0.250	0.225
McDON.DOUG. MD-90-30	17350	27000	0.80	2085	10.89	2.48	2.99	0.0277	70760	39415	64410	58965	11795	2135	1564	0	142.00	136.00	222.42	2	111.21	2025	5.75	1.55	0.251	0.226
DOUG. DC10-10	48330	31000	0.85	2900	12.11	1.84	2.34	0.0227	190854	111344	164854	151956	38898	2625	1720	0	157.00	140.00	534.00	3	178.00	3964	6.50	2.70	0.301	0.271
DOUG. DC10-30	48330	31000	0.90	4000	13.35	1.85	2.35	0.0226	263636	121364	182798	166922	96714	2996	1820	0	184.00	147.00	708.00	3	236.00	5337	6.50	2.70	0.634	0.571
McDON.DOUG. MD-11	55566	31000	0.88	5994	13.72	2.33	2.86	0.0238	283720	134081	207744	195043	88677	2926	1966	0	177.00	148.00	822.00	3	274.00	5638	6.50	2.70	0.332	0.299
LOCKHD L1011-100	33355	33000	0.88	4006	11.79	2.27	2.60	0.0253	211374	111795	166922	145150	66224	3292	1768	0	159.00	143.00	561.00	3	187.00	4131	6.30	2.75	0.426	0.384
ILYUSHIN Il-62M	23000	33000	0.84	4160	16.13	2.45	2.31	0.0194	165000	71600	105000	94600	70400	3300	2500	0	145.00	129.00	431.60	4	107.90	2242	6.15	2.35	0.849	0.764
TUPOLEV Tu-154M	18000	31000	0.88	2019	11.84	2.27	2.77	0.0200	100000	55300	80000	74000	26000	2100	2060	0	138.00	121.00	312.00	3	104.00	2181	7.10	2.20	0.642	0.578
Bae RJ70	9072	29000	0.73	1105	9.44	3.25	3.42	0.0321	40823	23360	37875	32432	8391	1440	1170	0	119.00	121.00	109.08	4	27.27	469	2.60	1.40	0.539	0.485
Bae RJ85	11749	29000	0.73	1148	10.06	3.09	3.43	0.0324	42184	24086	38555	35834	6350	1646	1192	0	124.00	122.00	124.56	4	31.14	543	2.60	1.40	0.314	0.282
Bae RJ100	12429	29000	0.73	1166	10.19	3.09	3.51	0.0328	44225	24993	40143	37421	6804	1829	1265	0	127.00	123.00	124.56	4	31.14	543	2.60	1.40	0.327	0.294
Bae RJ115	11265	29000	0.73	1470	10.06	3.22	3.51	0.0328	46040	26160	40143	37421	8619	1829	1265	0	127.00	123.00	124.56	4	31.14	543	2.60	1.40	0.368	0.331
CADAIR Reg.Jet 100	5488	37000	0.80	980	11.79	1.70	2.00	0.0297	21523	13653	20275	19141	2382	1605	1440	0	130.00	138.00	82.00	2	41.00	689	3.80	1.50	0.218	0.196
CADAIR Reg.Jet 100ER	6295	37000	0.80	1600	12.72	1.70	2.10	0.0297	23133	13663	21319	19958	3175	1605	1440	0	130.00	138.00	82.00	2	41.00	689	3.80	1.50	0.249	0.224
EMBRAER EMB-145	5515	37000	0.72	850	12.96	1.90	2.35	0.0283	19200	11585	18700	17100	2100	1500	1290	0	130.00	126.00	62.64	2	31.32	496	4.00	1.50	0.238	0.214
FOKKER F70	9302	26000	0.77	1085	8.84	2.16	2.63	0.0259	36740	22673	34020	31975	4765	1296	1210	0	126.00	119.00	123.20	2	61.60	1106	5.10	1.70	0.225	0.203
FOKKER F100	11108	26000	0.76	1290	10.41	2.17	2.59	0.0265	43090	24593	38780	35830	7260	1856	1321	0	136.00	128.00	123.20	2	61.60	1106	5.10	1.70	0.379	0.341

Table A.1 Performance and geometry data of reference aircraft, used by the Initiator as available at the begining of this thesis

	Miscellaneous					Aircraft Part Parameters																		
						Fuselage			Main wing										Vertical tail					
	[-]	[-]	[kg]	[-]	[l]																			
Aircraft	Date of initial service	Two class seating pax	kg/pax (two class seating)	No. of wheels (main)	Total tank volume	Length FL [m]	Height FL [m]	Width FL [m]	Wing area [m^2]	Wing span [m]	Wing aspect ratio [-]	Wing taper ratio [-]	Root chord length [m]	Wing 1/4 Chord sweep [º]	Root LE X pos [% FL]	Root LE Z pos [% FL]	Kinch location [%span]	Kinch location [%chord]	Area VT [m^2]	Height VT [m]	Aspect Ratio VT [-]	Taper Ratio VT [-]	1/4 Chord Sweep VT [º]	Volume Coefficient VT
AIRBUS A300-600R	1974	266	155	8	68150	53.30	5.64	5.64	260.00	44.84	7.73	0.26	11.01	28.00	30.59	10.00	40.00	40.00	45.20	8.60	1.64	0.365	40.00	0.097
AIRBUS A310-300	1983	218	153	8	61100	45.13	5.64	5.64	219.00	43.89	8.80	0.24	9.98	28.00	30.06	10.00	40.00	40.00	45.20	8.10	1.45	0.395	40.00	0.095
AIRBUS A320-200	1988	150	128	4	23860	37.57	4.14	3.95	122.40	33.91	9.39	0.21	7.74	25.00	32.11	10.00	40.27	40.27	21.50	6.26	1.82	0.303	34.00	0.065
AIRBUS A321-200	1993	186	122	4	23700	44.51	4.14	3.95	122.40	33.91	9.39	0.21	7.40	25.00	36.71	10.00	40.00	40.00	21.50	6.26	1.82	0.303	34.00	0.079
AIRBUS A330-200	1998	293	124	8	139090	57.77	5.64	5.64	363.10	58.00	9.26	0.20	12.65	29.70	30.12	10.00	27.27	27.27	47.65	9.44	1.87	0.350	45.00	0.057
AIRBUS A330-300	1994	335	144	8	98250	62.47	5.64	5.64	363.10	58.00	9.26	0.20	12.65	29.70	32.07	10.00	27.27	27.27	45.20	8.45	1.58	0.350	45.00	0.059
AIRBUS A340-200	1993	303	163	10	140000	58.21	5.64	5.64	363.10	58.00	9.26	0.20	12.65	29.70	30.80	10.00	27.27	27.27	45.20	8.45	1.58	0.350	45.00	0.055
AIRBUS A340-300	1994	335	144	10	141500	62.47	5.64	5.64	363.10	58.00	9.26	0.20	12.65	29.70	32.07	10.00	27.27	27.27	45.20	8.45	1.58	0.350	45.00	0.059
AIRBUS A340-500	2002	350	148	12	195620	65.60	5.64	5.64	437.30	61.20	8.56	0.19	13.91	31.10	31.38	10.00	25.45	25.45	47.65	9.44	1.87	0.350	45.00	0.049
AIRBUS A340-600	2002	440	143	12	195620	69.57	5.64	5.64	437.30	61.20	8.56	0.19	13.91	31.10	34.39	10.00	25.45	25.45	47.65	9.44	1.87	0.350	45.00	0.049
AIRBUS A380-800	2004	700	121	22	317000	67.46	8.50	7.02	817.00	79.80	7.79	0.20	19.22	30.00	24.73	10.00	30.00	30.00	134.20	13.66	1.39	0.424	43.00	0.060
BOEING 707-320C	1962	147	259	8	90299	44.35	3.76	3.76	283.40	44.42	6.96	0.25	11.51	35.00	30.05	10.00	18.18	18.18	30.47	7.20	1.70	0.410	30.00	0.051
BOEING 717-200	1999	106	115	4	13892	33.00	3.61	3.61	92.97	28.40	8.68	0.24	5.47	24.50	44.60	10.00	30.00	30.00	19.50	4.35	0.97	0.780	45.00	0.095
BOEING 727-200Adv	1970	136	137	4	30622	41.51	3.76	3.76	157.90	32.92	6.86	0.27	8.98	32.00	39.65	10.00	38.18	38.18	33.07	4.60	0.64	0.780	53.00	0.090
BOEING 737-200	1967	115	134	4	19532	29.54	3.73	3.73	91.04	28.35	8.83	0.22	6.96	25.00	32.28	10.00	34.55	48.00	19.70	5.85	1.74	0.288	35.00	0.092
BOEING 737-300	1967	128	125	4	20105	32.30	3.73	3.73	91.04	28.90	9.17	0.22	7.09	25.00	32.54	10.00	34.55	48.00	23.13	6.00	1.56	0.310	35.00	0.120
BOEING 737-600	1998	108	91	4	26024	29.88	3.73	3.73	124.60	34.30	9.44	0.22	7.48	25.00	31.31	10.00	32.73	45.00	23.13	6.00	1.56	0.310	35.00	0.073
BOEING 737-700	1997	128	91	4	26024	32.18	3.73	3.73	124.60	34.30	9.44	0.22	7.48	25.00	32.95	10.00	32.73	45.00	23.13	6.00	1.56	0.310	35.00	0.080
BOEING 737-800	1998	160	92	4	26024	38.08	3.73	3.73	124.60	34.30	9.44	0.22	7.48	25.00	34.39	10.00	32.73	45.00	23.13	6.00	1.56	0.310	35.00	0.096
BOEING 747-100	1969	442	158	16	183380	68.63	8.10	6.50	511.00	59.64	6.96	0.24	17.08	37.50	25.28	10.00	40.00	40.00	77.10	10.16	1.34	0.330	45.00	0.076
BOEING 747-200	1972	442	142	16	198385	68.63	8.10	6.50	511.00	59.64	6.96	0.24	16.81	37.50	25.28	10.00	36.36	36.36	77.10	10.16	1.34	0.330	45.00	0.076
BOEING 747-400	1988	496	123	16	204350	68.63	8.10	6.50	525.00	62.30	7.39	0.20	16.60	37.50	24.53	10.00	40.15	40.15	77.10	10.16	1.34	0.330	45.00	0.071
BOEING 757-200	1982	186	138	8	42597	46.96	4.10	4.00	185.25	38.05	7.82	0.22	9.34	25.00	36.83	10.00	40.00	40.00	34.37	7.33	1.56	0.351	39.00	0.092
BOEING 757-300	1999	239	123	8	43490	53.96	4.10	4.00	185.25	38.05	7.82	0.22	9.34	25.00	39.10	10.00	40.00	40.00	34.37	7.33	1.56	0.351	39.00	0.092
BOEING 767-200	1982	216	158	8	63216	47.24	5.03	5.03	283.30	47.57	7.99	0.22	11.89	31.50	29.29	10.00	32.73	32.73	46.14	9.01	1.76	0.306	39.00	0.068
BOEING 767-200ER	1982	216	165	8	91380	47.24	5.03	5.03	283.30	47.57	7.99	0.22	11.89	31.50	29.29	10.00	32.73	32.73	46.14	9.01	1.76	0.306	39.00	0.068
BOEING 767-300	1982	261	150	8	63216	53.67	5.03	5.03	283.30	47.57	7.99	0.22	11.89	31.50	32.23	10.00	32.73	32.73	46.14	9.01	1.76	0.306	39.00	0.079
BOEING 767-300ER	1982	261	174	8	91380	53.67	5.03	5.03	283.30	47.57	7.99	0.22	11.89	31.50	32.23	10.00	32.73	32.73	46.14	9.01	1.76	0.306	39.00	0.079
BOEING 777-200	1995	375	146	12	117348	62.78	6.20	6.20	427.80	60.90	8.67	0.15	14.95	31.60	31.75	10.00	30.91	30.91	53.23	9.24	1.60	0.290	46.00	0.054
BOEING 777-300	1998	479	143	12	171170	72.88	6.20	6.20	427.80	60.90	8.67	0.15	14.95	31.60	34.18	10.00	30.91	30.91	53.23	9.24	1.60	0.290	46.00	0.065
DOUG. DC 9-10	1965	68	141	4	14000	27.91	3.60	3.60	86.77	27.25	8.56	0.23	5.33	24.00	38.17	10.00	30.00	30.00	14.96	3.90	1.02	0.750	42.00	0.074
DOUG. DC 9-30	1967	97	144	4	13925	32.28	3.60	3.60	92.97	28.47	8.72	0.24	5.42	24.00	43.30	10.00	30.00	30.00	14.96	4.90	1.02	0.750	42.00	0.074
DOUG. DC 9-40	1968	105	148	4	13925	34.70	3.60	3.60	92.97	28.47	8.72	0.24	5.42	24.00	42.51	10.00	30.00	30.00	14.96	5.90	1.02	0.750	42.00	0.082
DOUG. DC 9-50	1975	122	125	4	16120	37.14	3.60	3.60	92.97	28.47	8.72	0.24	5.42	24.00	43.90	10.00	30.00	30.00	14.96	6.90	1.02	0.750	42.00	0.089
McDON.DOUG. MD-81	1980	155	116	4	22106	41.30	3.61	3.61	112.30	32.87	9.62	0.19	7.17	24.50	47.03	10.00	30.91	30.91	15.60	4.10	1.08	0.707	42.00	0.066
McDON.DOUG. MD-82	1980	155	121	4	22106	41.30	3.61	3.61	112.30	32.87	9.62	0.19	7.17	24.50	47.03	10.00	30.91	30.91	15.60	4.10	1.08	0.707	42.00	0.066
McDON.DOUG. MD-83	1980	155	121	4	26495	41.30	3.61	3.61	112.30	32.87	9.62	0.19	7.17	24.50	47.03	10.00	30.91	30.91	15.60	4.10	1.08	0.707	42.00	0.066
McDON.DOUG. MD-87	1980	114	155	4	22106	36.30	3.61	3.61	112.30	32.87	9.62	0.19	7.17	24.50	45.28	10.00	30.91	30.91	18.50	4.20	0.95	0.750	42.50	0.068
McDON.DOUG. MD-90-30	1995	153	113	4	22107	43.00	3.61	3.61	112.30	32.87	9.62	0.19	7.17	24.50	48.64	10.00	30.91	30.91	21.40	4.70	1.03	0.770	43.00	0.090
DOUG. DC10-10	1971	277	174	8	138165	51.97	6.02	6.02	367.70	50.40	6.91	0.25	14.66	35.00	40.55	10.00	39.09	39.09	56.21	11.16	2.22	0.475	40.00	0.063
DOUG. DC10-30	1973	277	174	10	138165	51.97	6.02	6.02	367.70	50.40	6.91	0.25	14.66	35.00	37.03	10.00	39.09	39.09	56.21	11.16	2.22	0.475	40.00	0.063
McDON.DOUG. MD-11	1990	323	172	10	152108	58.65	6.02	6.02	338.90	51.77	7.91	0.20	13.88	35.00	37.72	10.00	36.36	36.36	56.20	11.16	2.22	0.369	40.00	0.067
LOCKHD L1011-100	1973	304	110	8	100000	54.20	6.06	6.06	321.50	47.35	6.97	0.21	14.42	35.00	35.74	10.00	40.00	40.00	51.10	9.90	1.92	0.290	35.00	0.069
ILYUSHIN Il-62M	1974	140	164	8	105300	49.00	4.30	4.30	279.55	43.20	6.68	0.26	12.17	32.50	40.07	10.00	29.09	29.09	35.60	6.05	1.03	0.540	40.00	0.049
TUPOLEV Tu-154M	1972	154	117	12	41300	43.50	3.80	3.80	201.45	37.55	7.00	0.19	10.39	35.00	38.54	10.00	32.14	32.14	31.70	5.60	0.99	0.650	45.00	0.060
Bae RJ70	1982	70	130	4	11728	24.00	3.56	3.56	77.30	26.21	8.89	0.37	4.35	15.00	35.44	95.00	30.00	30.00	15.51	4.85	1.52	0.670	36.00	0.098
Bae RJ85	1982	85	138	4	11728	26.50	3.56	3.56	77.30	26.21	8.89	0.37	4.35	15.00	36.03	95.00	30.00	30.00	15.51	4.85	1.52	0.670	36.00	0.110
Bae RJ100	1982	100	124	4	11728	28.90	3.56	3.56	77.30	26.21	8.89	0.37	4.35	15.00	39.64	95.00	30.00	30.00	15.51	4.85	1.52	0.670	36.00	0.117
Bae RJ115	1982	115	98	4	12901	28.90	3.56	3.56	77.30	26.21	8.89	0.37	4.35	15.00	39.64	95.00	30.00	30.00	15.51	4.85	1.52	0.670	36.00	0.117
CADAIR Reg.Jet 100	1992	52	106	4	5300	24.38	2.69	2.69	54.54	20.52	7.72	0.22	5.04	24.75	34.43	10.00	34.55	34.55	9.18	2.60	0.74	0.730	41.00	0.088
CADAIR Reg.Jet 100ER	1992	52	121	4	8080	24.38	2.69	2.69	54.54	20.52	7.72	0.22	5.04	24.75	34.43	10.00	34.55	34.55	9.18	2.60	0.74	0.730	41.00	0.088
EMBRAER EMB-145	1997	50	110	4	5146	27.93	2.28	2.28	51.18	20.04	7.85	0.22	4.92	22.73	45.01	10.00	37.27	37.27	7.20	3.10	1.33	0.600	32.00	0.081
FOKKER F70	1988	70	133	4	9640	27.88	3.30	3.30	93.50	28.08	8.43	0.24	5.39	17.45	31.13	10.00	30.00	30.00	12.30	3.30	0.89	0.740	41.00	0.053
FOKKER F100	1988	107	104	4	13365	32.50	3.30	3.30	93.50	28.08	8.43	0.24	5.39	17.45	40.84	10.00	30.00	30.00	12.30	3.30	0.89	0.740	41.00	0.064

Table A.1 Performance and geometry data of reference aircraft, used by the Initiator as available at the begining of this thesis

	Horizontal tail							Nacelles									
								Nacelle 1					Nacelle 2				
Aircraft	Area HT [m^2]	Span HT [m]	Aspect Ratio HT [-]	Taper Ratio HT [-]	1/4 Chord Sweep HT [º]	Volume Coefficient HT	T-Tail	NC1 Connect to	NC1 Symm	NC1 X	NC1 Y	NC1 Z	NC2 Connect to	NC2 Symm	NC2 X	NC2 Y	NC2 Z
AIRBUS A300-600R	69.45	16.26	3.81	0.420	34.00	1.06	false	wing	true	70.00	36.00	-70.00					
AIRBUS A310-300	64.00	16.26	4.13	0.417	34.00	1.12	false	wing	true	70.00	35.00	-70.00					
AIRBUS A320-200	31.00	12.45	5.00	0.256	29.00	0.80	false	wing	true	70.00	34.00	-70.00					
AIRBUS A321-200	31.00	12.45	5.00	0.256	29.00	0.96	false	wing	true	70.00	34.00	-70.00					
AIRBUS A330-200	72.90	19.06	4.98	0.360	30.00	0.96	false	wing	true	70.00	31.00	-70.00					
AIRBUS A330-300	72.90	19.06	4.98	0.360	30.00	0.79	false	wing	true	70.00	31.00	-70.00					
AIRBUS A340-200	72.90	19.06	4.98	0.360	30.00	0.73	false	wing	true	70.00	31.00	-70.00	wing	true	70.00	67.00	-70.00
AIRBUS A340-300	72.90	19.06	4.98	0.360	30.00	0.79	false	wing	true	70.00	31.00	-70.00	wing	true	70.00	67.00	-70.00
AIRBUS A340-500	93.00	21.50	4.97	0.360	30.00	0.73	false	wing	true	70.00	30.00	-70.00	wing	true	70.00	63.00	-70.00
AIRBUS A340-600	93.00	21.50	4.97	0.360	30.00	0.73	false	wing	true	70.00	30.00	-70.00	wing	true	70.00	63.00	-70.00
AIRBUS A380-800	222.57	31.29	4.40	0.383	30.00	0.71	false	wing	true	70.00	35.00	-70.00	wing	true	70.00	68.00	-70.00
BOEING 707-320C	58.06	13.95	3.35	0.400	36.00	0.57	false	wing	true	70.00	44.00	-70.00	wing	true	70.00	71.00	-70.00
BOEING 717-200	24.20	10.80	4.82	0.380	30.00	0.96	true	fuselage	true	70.00	0.00	0.00					
BOEING 727-200Adv	34.93	10.90	3.40	0.380	36.00	0.81	true	fuselage	true	74.00	0.00	0.00	tail	false	20.00	30.00	0.00
BOEING 737-200	31.31	12.70	5.15	0.260	30.00	1.34	false	wing	true	70.00	35.00	-70.00					
BOEING 737-300	31.31	12.70	5.15	0.260	30.00	1.36	false	wing	true	70.00	34.00	-70.00					
BOEING 737-600	32.40	13.40	5.54	0.186	30.00	0.85	false	wing	true	70.00	28.00	-70.00					
BOEING 737-700	32.40	13.40	5.54	0.186	30.00	0.92	false	wing	true	70.00	28.00	-70.00					
BOEING 737-800	32.40	13.40	5.54	0.186	30.00	1.10	false	wing	true	70.00	28.00	-70.00					
BOEING 747-100	136.60	22.08	3.57	0.265	32.00	0.89	false	wing	true	70.00	40.00	-70.00	wing	true	70.00	70.00	-70.00
BOEING 747-200	136.60	22.08	3.57	0.265	32.00	0.89	false	wing	true	70.00	40.00	-70.00	wing	true	70.00	70.00	0.00
BOEING 747-400	136.60	22.08	3.57	0.265	32.00	0.87	false	wing	true	70.00	38.00	-70.00	wing	true	70.00	67.00	-70.00
BOEING 757-200	50.35	15.21	4.59	0.326	27.50	0.96	false	wing	true	70.00	34.00	-70.00					
BOEING 757-300	50.35	15.21	4.59	0.326	27.50	0.96	false	wing	true	70.00	34.00	-70.00					
BOEING 767-200	77.69	18.62	4.46	0.200	32.00	0.80	false	wing	true	70.00	32.00	-70.00					
BOEING 767-200ER	77.69	18.62	4.46	0.200	32.00	0.80	false	wing	true	70.00	32.00	-70.00					
BOEING 767-300	77.69	18.62	4.46	0.200	32.00	0.93	false	wing	true	70.00	32.00	-70.00					
BOEING 767-300ER	77.69	18.62	4.46	0.200	32.00	0.93	false	wing	true	70.00	32.00	-70.00					
BOEING 777-200	101.26	21.35	4.50	0.300	35.00	0.75	false	wing	true	70.00	33.00	-70.00					
BOEING 777-300	101.26	21.35	4.50	0.300	35.00	0.89	false	wing	true	70.00	33.00	-70.00					
DOUG. DC 9-10	25.60	11.23	4.93	0.318	30.00	1.15	true	fuselage	true	66.00	0.00	0.00					
DOUG. DC 9-30	25.60	11.23	4.93	0.318	30.00	1.17	true	fuselage	true	71.00	0.00	0.00					
DOUG. DC 9-40	25.60	11.23	4.93	0.318	30.00	1.27	true	fuselage	true	72.00	0.00	0.00					
DOUG. DC 9-50	25.60	11.23	4.93	0.318	30.00	1.36	true	fuselage	true	72.00	0.00	0.00					
McDON.DOUG. MD-81	29.17	12.24	5.14	0.330	30.00	1.15	true	fuselage	true	75.00	0.00	0.00					
McDON.DOUG. MD-82	29.17	12.24	5.14	0.330	30.00	1.15	true	fuselage	true	75.00	0.00	0.00					
McDON.DOUG. MD-83	29.17	12.24	5.14	0.330	30.00	1.15	true	fuselage	true	75.00	0.00	0.00					
McDON.DOUG. MD-87	29.17	12.24	5.14	0.400	30.00	1.04	true	fuselage	true	71.00	0.00	0.00					
McDON.DOUG. MD-90-30	33.00	12.24	4.54	0.360	30.00	1.34	true	fuselage	true	77.00	0.00	0.00					
DOUG. DC10-10	124.30	21.69	3.78	0.344	35.00	0.78	false	wing	true	86.00	34.00	-70.00	tail	false	20.00	30.00	0.00
DOUG. DC10-30	124.30	21.69	3.78	0.344	35.00	0.78	false	wing	true	80.00	34.00	-70.00	tail	false	20.00	30.00	0.00
McDON.DOUG. MD-11	85.50	18.03	3.80	0.383	35.00	0.69	false	wing	true	83.00	31.00	-70.00	tail	false	20.00	30.00	0.00
LOCKHD L1011-100	119.10	21.90	4.03	0.310	35.00	0.83	false	wing	true	73.00	44.00	-70.00	tail	false	20.00	30.00	0.00
ILYUSHIN Il-62M	50.50	12.23	2.96	0.360	35.00	0.54	true	fuselage	true	80.00	0.00	-10.00	fuselage	true	80.00	0.00	95.00
TUPOLEV Tu-154M	42.20	13.40	4.25	0.480	40.00	0.61	true	fuselage	true	74.00	0.00	0.00	tail	false	20.00	30.00	0.00
Bae RJ70	15.61	11.09	7.88	0.410	20.00	0.69	true	wing	true	70.00	32.00	-70.00	wing	true	70.00	50.00	-70.00
Bae RJ85	15.61	11.09	7.88	0.410	20.00	0.79	true	wing	true	70.00	32.00	-70.00	wing	true	70.00	50.00	-70.00
Bae RJ100	15.61	11.09	7.88	0.410	20.00	0.86	true	wing	true	70.00	32.00	-70.00	wing	true	70.00	50.00	-70.00
Bae RJ115	15.61	11.09	7.88	0.410	20.00	0.86	true	wing	true	70.00	32.00	-70.00	wing	true	70.00	50.00	-70.00
CADAIR Reg.Jet 100	9.44	6.35	4.27	0.550	30.00	0.71	true	fuselage	true	65.00	0.00	0.00					
CADAIR Reg.Jet 100ER	9.44	6.35	4.27	0.550	30.00	0.71	true	fuselage	true	65.00	0.00	0.00					
EMBRAER EMB-145	11.20	7.60	5.16	0.560	17.00	0.90	true	fuselage	true	73.00	0.00	0.00					
FOKKER F70	21.72	10.04	4.64	0.390	26.00	0.88	true	fuselage	true	64.00	0.00	0.00					
FOKKER F100	21.72	10.04	4.64	0.390	26.00	0.98	true	fuselage	true	68.00	0.00	0.00					

Appendix B

The present performance and geometry database of reference aircraft

This appendix shows the database used by the Initiator as available during the writing of this thesis. It contains information on the performance of reference aircraft as well as information on the geometry of the different aircraft parts.

Table B.1 Performance and geometry data of reference aircraft, used by the present Initiator

	Performance Parameters																				
	Main Requirements						Aerodynamics				Weights					TO & Landing			Speeds		Engines	
	[kg]	[ft]	[-]	[NM]	[kg]	[NM]	[-]	[-]	[-]	[-]	[kg]	[kg]	[kg]	[kg]	[kg]	[m]	[m]	[ft]	[kts]	[kts]	[kN]	[-]
Aircraft	Maximum payload	Cruise altitude	Cruise Mach no.	Maximum payload range	Design payload	Design range	L/D cruise	CL-max take-off	CL-max landing	CD0 clean	Max. take-off mass	Operational Empty mass	Max. landing mass	Max. zero-fuel mass	Max. Payload fuel mass	Take-off distance	Landing distance	Max. take-off & landing alt.	Rotation speed (V2)	Approach speed (Vapp)	Total static thrust/power	No. of engines
AIRBUS A300-600R	41100	31000	0.78	3283	26600	4050	16.00	2.44	2.98	0.0260	170500	88900	140000	130000	40500	2280	1489	6000	153.00	136.00	514.00	2
AIRBUS A310-300	33300	35000	0.79	3645	22000	4350	16.29	2.45	3.02	0.0292	150000	79666	123000	113000	37000	2290	1490	6000	156.00	138.00	462.00	2
AIRBUS A320-200	18633	37000	0.78	2592	15000	3300	15.79	2.56	3.00	0.0298	73500	42100	64500	61000	12500	1960	1490	6000	143.00	134.00	222.40	2
AIRBUS A321-200	22780	28000	0.76	1955	18500	3200	16.80	3.10	3.23	0.0293	89000	48000	73500	71500	17500	2000	1580	6000	143.00	138.00	284.00	2
AIRBUS A330-200	47500	33000	0.81	4210	25300	7500	20.13	2.21	2.74	0.0211	230000	120200	177150	165142	64858	2470	1750	6000	158.00	135.00	620.00	2
AIRBUS A330-300	48400	33000	0.80	3888	29500	6400	20.13	2.51	2.73	0.0213	217000	118189	179000	169000	48000	2320	1600	6000	144.00	136.00	600.00	2
AIRBUS A340-200	49400	33000	0.82	6393	26100	6700	20.00	2.60	2.84	0.0212	257000	120228	181000	172000	85000	2790	1856	6000	154.00	134.00	556.00	4
AIRBUS A340-300	48150	33000	0.82	6371	29500	7400	20.00	2.61	2.89	0.0214	271000	129850	190000	178000	93000	3000	1964	6000	160.00	136.00	604.00	4
AIRBUS A340-500	51635	33000	0.77	7050	31300	9000	20.00	2.61	2.86	0.0198	365000	170390	236000	222000	143000	3100	2090	6000	160.00	139.00	943.20	4
AIRBUS A340-600	63000	33000	0.77	5700	38000	7900	20.00	2.61	2.87	0.0200	365000	177010	254000	240000	125000	3100	2240	6000	160.00	144.00	996.40	4
AIRBUS A380-800	90975	35000	0.78	6214	52500	8500	20.00	2.61	2.60	0.0192	540000	271000	386000	356000	184000	3700	2104	6000	160.00	143.00	1176.00	4
BOEING 707-320C	38100	25000	0.79	3150	14100	5352	15.57	1.90	2.22	0.0163	151315	66224	112037	104330	46985	3054	1905	6000	170.00	135.00	338.16	4
BOEING 717-200	12220	25000	0.73	1200	10600	1745	15.57	2.15	3.01	0.0295	51710	31675	46266	43545	8165	2500	1445	6000	165.00	130.00	195.80	2
BOEING 727-200Adv	18597	25000	0.78	2140	14800	2500	13.69	1.90	2.51	0.0226	95028	46164	72575	63318	31710	3033	1494	6000	166.00	137.00	213.60	3
BOEING 737-200	15445	25000	0.70	1549	11500	1900	13.69	2.32	3.06	0.0314	52390	27646	46720	43091	9299	1829	1350	6000	147.00	131.00	142.40	2
BOEING 737-300	16030	26000	0.72	1578	12800	2850	14.00	2.47	3.28	0.0321	56470	31869	51710	47630	8840	1939	1396	6000	148.00	133.00	178.00	2
BOEING 737-600	15270	41000	0.80	1950	11000	3050	16.00	2.49	3.32	0.0265	65090	36440	54650	51480	13610	2000	1268	6000	142.00	120.00	164.00	2
BOEING 737-700	11610	41000	0.81	3050	12600	3260	16.00	2.49	3.32	0.0267	69400	37585	58060	54650	14750	1900	1356	6000	142.00	125.00	178.00	2
BOEING 737-800	14690	41000	0.81	2700	16200	1990	16.00	2.49	3.32	0.0273	78220	41480	65310	61680	16540	2000	1600	6000	142.00	130.00	214.00	2
BOEING 747-100	69625	35000	0.84	4427	40700	5000	16.42	2.03	2.58	0.0227	340195	169190	255830	238815	101380	3050	1890	6000	169.00	141.00	835.20	4
BOEING 747-200	62820	35000	0.84	5930	40100	5200	16.42	2.06	2.58	0.0227	377840	175995	255830	238815	139025	3190	1890	6000	177.00	141.00	944.00	4
BOEING 747-400	61186	35000	0.85	6857	42000	7000	17.00	1.92	2.38	0.0223	396830	181484	285760	242670	154160	3310	2130	6000	185.00	153.00	1009.60	4
BOEING 757-200	25690	31000	0.78	3812	20000	3900	16.83	2.42	2.81	0.0234	115900	58040	95450	84550	31350	2226	1564	6000	150.00	137.00	382.60	2
BOEING 757-300	29470	31000	0.79	2925	24300	3395	16.83	2.17	2.78	0.0240	122470	65980	101600	95250	27220	2550	1700	6000	163.00	142.00	384.00	2
BOEING 767-200	34065	39000	0.81	3150	18100	4568	16.54	2.08	2.39	0.0224	136078	80921	122470	112491	23587	1770	1463	6000	142.00	136.00	427.00	2
BOEING 767-200ER	35652	39000	0.81	5050	18100	5125	16.54	2.03	2.38	0.0224	175540	83788	129293	117934	57606	2670	1524	6000	163.00	140.00	515.20	2
BOEING 767-300	39140	39000	0.81	3221	21800	3734	16.00	1.86	2.47	0.0228	156489	87135	136078	126099	30390	2545	1646	6000	161.00	141.00	447.00	2
BOEING 767-300ER	45541	39000	0.81	3500	21800	5230	16.00	1.87	2.49	0.0228	181437	89902	145149	130634	50803	2926	1740	6000	173.00	145.00	547.20	2
BOEING 777-200	54635	39000	0.84	3250	30500	4585	18.05	1.90	2.53	0.0215	242670	135875	201850	190510	52160	2360	1585	6000	170.00	138.00	700.00	2
BOEING 777-300	68570	39000	0.79	3800	36800	6571	18.05	1.90	2.55	0.0221	299370	155960	237685	224530	74840	2650	1860	6000	170.00	145.00	860.00	2
DOUG. DC 9-10	9570	30000	0.82	1200	8000	1099	13.61	2.20	2.99	0.0298	35245	20550	33565	30120	5125	1615	1615	6000	127.00	132.00	109.00	2
DOUG. DC 9-30	14000	30000	0.82	1546	8000	1421	13.61	2.45	3.12	0.0289	49000	25400	45000	39500	9500	1777	1317	6000	137.00	126.00	124.00	2
DOUG. DC 9-40	15510	30000	0.82	1423	8000	1464	13.61	2.13	2.97	0.0293	51710	27800	46265	42184	9526	2091	1457	6000	151.00	131.00	137.80	2
DOUG. DC 9-50	15265	30000	0.82	1361	8000	1421	13.61	1.99	3.15	0.0297	54420	29300	49885	44670	9750	2362	1439	6000	160.00	132.00	137.80	2
McDON.DOUG. MD-81	17953	27000	0.74	1385	15500	1565	16.00	2.25	2.99	0.0272	63500	35570	58000	53500	10000	2195	1481	6000	148.00	133.00	171.20	2
McDON.DOUG. MD-82	18802	27000	0.74	1860	15200	2052	16.00	2.25	2.99	0.0272	67812	35630	58970	55340	12472	2274	1500	6000	153.00	134.00	185.40	2
McDON.DOUG. MD-83	18721	27000	0.74	2369	15500	2504	16.00	2.41	2.98	0.0272	72580	36620	63280	55340	17240	2551	1585	6000	153.00	139.00	193.00	2
McDON.DOUG. MD-87	17601	33000	0.75	1400	13000	2374	16.00	2.48	2.99	0.0268	63503	33203	58000	53524	9979	1865	1451	6000	141.00	133.00	185.40	2
McDON.DOUG. MD-90-30	17350	27000	0.73	2085	15300	2085	16.00	2.48	2.99	0.0277	70760	39415	64410	58965	11795	2135	1564	6000	142.00	136.00	222.42	2
DOUG. DC10-10	48330	31000	0.83	2900	27700	3302	15.03	1.84	2.34	0.0227	190854	111344	164854	151956	38898	2625	1720	6000	157.00	140.00	534.00	3
DOUG. DC10-30	47180	31000	0.83	4200	27700	5405	15.03	1.85	2.35	0.0226	263636	121364	182798	166922	96714	2996	1820	6000	184.00	147.00	708.00	3
McDON.DOUG. MD-11	55566	31000	0.81	5994	28500	6630	15.75	2.33	2.86	0.0238	283720	134081	207744	195043	88677	2926	1966	6000	177.00	148.00	822.00	3
LOCKHD L1011-100	33355	33000	0.83	4006	30400	3455	14.11	2.27	2.60	0.0253	211374	111795	166922	145150	66224	3292	1768	6000	159.00	143.00	561.00	3
ILYUSHIN II-62M	23000	33000	0.76	4160	17400	5400	14.11	2.45	2.31	0.0194	165000	71600	105000	94600	70400	3300	2500	6000	145.00	155.00	431.60	4
TUPOLEV Tu-154M	18000	31000	0.78	2019	13000	2752	14.11	2.27	2.77	0.0200	100000	55300	80000	74000	26000	2100	2060	6000	138.00	138.00	312.00	3
Bae RJ70	9072	29000	0.60	1105	7000	1610	13.36	3.25	3.42	0.0321	40823	23360	37875	32432	8391	1440	1170	6000	119.00	121.00	109.08	4
Bae RJ85	11749	29000	0.60	1148	8500	1520	13.36	3.09	3.43	0.0324	42184	24086	38555	35834	6350	1646	1192	6000	124.00	122.00	124.56	4
Bae RJ100	12429	29000	0.63	1166	10000	1380	13.36	3.09	3.51	0.0328	44225	24993	40143	37421	6804	1829	1265	6000	127.00	123.00	124.56	4
Bae RJ115	11265	29000	0.63	1470	11600	1520	13.36	3.22	3.51	0.0328	46040	26160	40143	37421	8619	1829	1265	6000	127.00	123.00	124.56	4
CADAIR Reg.Jet 100	5488	37000	0.74	980	5200	980	13.36	1.70	2.00	0.0297	21523	13653	20275	19141	2382	1605	1440	6000	130.00	138.00	82.00	2
CADAIR Reg.Jet 100ER	6295	37000	0.74	1600	5200	1620	13.36	1.70	2.10	0.0297	23133	13663	21319	19958	3175	1605	1440	6000	130.00	138.00	82.00	2
EMBRAER EMB-145	5515	37000	0.64	850	5000	1270	16.79	1.90	2.35	0.0283	19200	11585	18700	17100	2100	1500	1290	6000	130.00	126.00	62.64	2
FOKKER F70	9302	26000	0.67	1085	7900	1295	16.79	2.16	2.63	0.0259	36740	22673	34020	31975	4765	1296	1210	6000	126.00	119.00	123.20	2
FOKKER F100	11108	26000	0.69	1290	10700	1290	16.79	2.17	2.59	0.0265	43090	24593	38780	35830	7260	1856	1321	6000	136.00	128.00	123.20	2

Table B.1 Performance and geometry data of reference aircraft, used by the present Initiator

							Miscellaneous				
	[kN]	[kg]	[m]	[m]	[1/hr]	[1/hr]	[-]	[-]	[kg]	[-]	[l]
Aircraft	Static thrust/ power per engine	Engine mass	Engine length	Engine diameter	SFC cruise	SFC loiter	Date of initial service	Two class seating pax	kg/pax (two class seating)	No. of wheels (main)	Total tank volume
AIRBUS A300-600R	257.00	5824	6.70	2.70	0.578	0.520	1974	266	155	8	68150
AIRBUS A310-300	231.00	4888	6.30	2.70	0.623	0.561	1983	218	153	8	61100
AIRBUS A320-200	111.20	2118	4.44	2.37	0.596	0.536	1988	150	124	4	23860
AIRBUS A321-200	142.00	2684	4.44	2.37	0.574	0.517	1993	186	122	4	23700
AIRBUS A330-200	310.00	6134	7.00	3.10	0.562	0.506	1998	293	162	8	139090
AIRBUS A330-300	300.00	6071	7.00	3.10	0.562	0.506	1994	335	144	8	98250
AIRBUS A340-200	139.00	2621	4.95	2.37	0.545	0.491	1993	303	163	10	140000
AIRBUS A340-300	151.00	2853	4.95	2.37	0.545	0.491	1994	335	144	10	141500
AIRBUS A340-500	235.80	4425	6.10	3.05	0.545	0.491	2002	350	148	12	195620
AIRBUS A340-600	249.10	4700	6.10	3.05	0.545	0.491	2002	440	143	12	195620
AIRBUS A380-800	294.00	5568	7.30	4.00	0.500	0.450	2004	700	130	22	317000
BOEING 707-320C	84.54	1852	6.00	1.60	0.870	0.783	1962	147	259	8	90299
BOEING 717-200	97.90	1715	6.10	1.75	0.620	0.558	1999	106	115	4	13892
BOEING 727-200Adv	71.20	1456	7.00	1.50	0.690	0.621	1970	136	137	4	30622
BOEING 737-200	71.20	1484	7.00	1.50	0.737	0.663	1967	115	134	4	19532
BOEING 737-300	89.00	1897	4.70	2.00	0.667	0.600	1967	128	125	4	20105
BOEING 737-600	82.00	1421	4.70	2.06	0.600	0.540	1998	108	141	4	26024
BOEING 737-700	89.00	1565	4.70	2.06	0.600	0.540	1997	128	91	4	26024
BOEING 737-800	107.00	1904	4.70	2.06	0.600	0.540	1998	160	92	4	26024
BOEING 747-100	208.80	4786	5.61	2.80	0.598	0.538	1969	442	158	16	183380
BOEING 747-200	236.00	5371	5.61	2.80	0.570	0.513	1972	442	142	16	198385
BOEING 747-400	252.40	5218	5.64	2.90	0.570	0.513	1988	496	123	16	204350
BOEING 757-200	191.30	3998	5.20	2.60	0.598	0.538	1982	186	138	8	42597
BOEING 757-300	192.00	3598	5.20	2.60	0.598	0.538	1999	239	123	8	43490
BOEING 767-200	213.50	4511	6.22	2.68	0.576	0.518	1982	216	158	8	63216
BOEING 767-200ER	257.60	5546	6.22	2.68	0.576	0.518	1982	216	165	8	91380
BOEING 767-300	223.50	4744	6.22	2.68	0.570	0.513	1982	261	150	8	63216
BOEING 767-300ER	273.60	5926	6.22	2.68	0.570	0.513	1982	261	174	8	91380
BOEING 777-200	350.00	7147	7.30	3.20	0.545	0.491	1995	375	146	12	117348
BOEING 777-300	430.00	8792	7.30	3.20	0.545	0.491	1998	479	143	12	171170
DOUG. DC 9-10	54.50	1121	5.30	1.56	0.740	0.666	1965	68	141	4	14000
DOUG. DC 9-30	62.00	1275	5.30	1.56	0.740	0.666	1967	97	144	4	13925
DOUG. DC 9-40	68.90	1423	5.30	1.56	0.740	0.666	1968	105	148	4	13925
DOUG. DC 9-50	68.90	1360	5.30	1.56	0.740	0.666	1975	122	125	4	16120
McDON.DOUG. MD-81	85.60	1672	6.10	2.00	0.737	0.663	1980	155	116	4	22106
McDON.DOUG. MD-82	92.70	1825	6.10	2.00	0.737	0.663	1980	155	121	4	22106
McDON.DOUG. MD-83	96.50	1908	6.10	2.00	0.737	0.663	1980	155	121	4	26495
McDON.DOUG. MD-87	92.70	1825	6.10	1.95	0.737	0.663	1980	114	154	4	22106
McDON.DOUG. MD-90-30	111.21	2025	5.75	1.55	0.574	0.517	1995	153	113	4	22107
DOUG. DC10-10	178.00	3964	6.50	2.70	0.640	0.576	1971	277	174	8	138165
DOUG. DC10-30	236.00	5337	6.50	2.70	0.640	0.576	1973	277	170	10	138165
McDON.DOUG. MD-11	274.00	5638	6.50	2.70	0.570	0.513	1990	323	172	10	152108
LOCKHD L1011-100	187.00	4131	6.30	2.75	0.570	0.513	1973	304	110	8	100000
ILYUSHIN Il-62M	107.90	2242	6.15	2.35	0.700	0.630	1974	140	164	8	105300
TUPOLEV Tu-154M	104.00	2181	7.10	2.20	0.700	0.630	1972	154	117	12	41300
Bae RJ70	27.27	469	2.60	1.40	0.720	0.648	1982	70	130	4	11728
Bae RJ85	31.14	543	2.60	1.40	0.720	0.648	1982	85	138	4	11728
Bae RJ100	31.14	543	2.60	1.40	0.720	0.648	1982	100	124	4	11728
Bae RJ115	31.14	543	2.60	1.40	0.720	0.648	1982	115	98	4	12901
CADAIR Reg.Jet 100	41.00	689	3.80	1.50	0.670	0.603	1992	52	106	4	5300
CADAIR Reg.Jet 100ER	41.00	689	3.80	1.50	0.670	0.603	1992	52	121	4	8080
EMBRAER EMB-145	31.32	496	4.00	1.50	0.650	0.585	1997	50	110	4	5146
FOKKER F70	61.60	1106	5.10	1.70	0.690	0.621	1988	70	133	4	9640
FOKKER F100	61.60	1106	5.10	1.70	0.690	0.621	1988	107	104	4	13365

Appendix C

Verification & Validation results

This appendix shows the verification and validation results for the Initiator. Tables C.1 and C.2 present verifications for the analytical capabilities of some of the Initiator modules. For these verifications all information needed for the module is taken from literature. Table C.1 tests the OEW module. The geometry used as well as the $MTOW$ are taken from literature. Table C.2 is dedicated to aerodynamic efficiency calculations. It compares the L/D values of the Initiator to reference values.

Tables C.3, C.4 and C.5 present validation results of concepts designed with the top level requirements of existing aircraft. Hence, these concepts do not have the same geometry as their existing counterparts, but are the product of a design run by the Initiator. The tables list the differences in percentage between the values from literature and those produced by the Initiator. Table C.3 gives the results when all aircraft are designed with the analysis modules as available at the beginning of this thesis. Table C.4 gives the results of the design run with the use of the present version of the Initiator. Table C.5 lists the results, when the top level requirements are changed from the maximum payload range case to the designed payload range case. The difference in requirements can be found in appendix B, which list the present database of the Initiator. All analyses modules are kept equal between table C.4 and C.5. The content of each table is listed once more below, this time bullets wise.

- Table C.1: Verification of the OEW analysis module
- Table C.2: Verification of the L/D analysis module
- Table C.3: Validation with the original analysis modules
- Table C.4: Validation with the final analysis modules
- Table C.5: Validation with the final analysis modules & Design point requirements

Table C.1: Operational empty weight analyses verification

Aircraft	Original OEW [kg]	Analysis OEW [kg]	Difference [%]
AIRBUS A300-600R	88900	84369	-5.10
AIRBUS A310-300	79666	73691	-7.50
AIRBUS A320-200	42100	38928	-7.53
AIRBUS A321-200	48000	45504	-5.20
AIRBUS A330-200	120200	111539	-7.21
AIRBUS A330-300	118189	110371	-6.61
AIRBUS A340-200	120228	114006	-5.17
AIRBUS A340-300	129850	119237	-8.17
AIRBUS A340-500	170390	152361	-10.58
AIRBUS A340-600	177010	157379	-11.09
AIRBUS A380-800	271000	242785	-10.41
BOEING 707-320C	66224	69350	4.72
BOEING 717-200	31675	29442	-7.05
BOEING 727-200Adv	46164	42675	-7.56
BOEING 737-200	27646	28238	2.14
BOEING 737-300	31869	30833	-3.25
BOEING 737-600	36440	33197	-8.90
BOEING 737-700	37585	34562	-8.04
BOEING 737-800	41480	38991	-6.00
BOEING 747-100	169190	162726	-3.82
BOEING 747-200	175995	170964	-2.86
BOEING 747-400	181484	179532	-1.08
BOEING 757-200	58040	57761	-0.48
BOEING 757-300	65980	61425	-6.90
BOEING 767-200	80921	74484	-7.95
BOEING 767-200ER	83788	83976	0.22
BOEING 767-300	87135	81772	-6.15
BOEING 767-300ER	89902	89714	-0.21
BOEING 777-200	135875	126878	-6.62
BOEING 777-300	155960	148105	-5.04
DOUG. DC 9-10	20550	22128	7.68
DOUG. DC 9-30	25400	27154	6.90
DOUG. DC 9-40	27800	28622	2.96
DOUG. DC 9-50	29300	29718	1.43
McDON.DOUG. MD-81	35570	35063	-1.43
McDON.DOUG. MD-82	35630	36233	1.69
McDON.DOUG. MD-83	36620	37354	2.00
McDON.DOUG. MD-87	33203	34326	3.38
McDON.DOUG. MD-90-30	39415	38264	-2.92
DOUG. DC10-10	111344	97028	-12.86
DOUG. DC10-30	121364	112680	-7.16
McDON.DOUG. MD-11	134081	120139	-10.40
LOCKHD L1011-100	111795	96661	-13.54
ILYUSHIN Il-62M	71600	72272	0.94
TUPOLEV Tu-154M	55300	49312	-10.83
Bae RJ70	23360	21511	-7.91
Bae RJ85	24086	23044	-4.33
Bae RJ100	24993	23999	-3.98
Bae RJ115	26160	24207	-7.46
CADAIR Reg.Jet 100	13653	14705	7.70
CADAIR Reg.Jet 100ER	13663	15269	11.75
EMBRAER EMB-145	11585	13811	19.22
FOKKER F70	22673	22196	-2.11
FOKKER F100	24593	24677	0.34
Average difference			-3.30

Table C.2: Aerodynamic efficiency analyses verification

Aircraft	Original L/D [-]	Analysis L/D [-]	Difference [%]
AIRBUS A300-600R	14.5	18.1	25.1
AIRBUS A310-300	16.3	18.7	14.8
AIRBUS A320-200	15.8	19.2	21.4
AIRBUS A321-200	16.8	17.2	2.3
AIRBUS A330-200	20.1	20.9	3.7
AIRBUS A330-300	20.1	20.6	2.1
AIRBUS A340-200	20.0	20.9	4.3
AIRBUS A340-300	20.0	20.8	4.2
AIRBUS A340-500	20.0	21.1	5.7
AIRBUS A340-600	20.0	20.7	3.3
AIRBUS A380-800	20.0	21.2	6.1
BOEING 707-320C	15.6	16.2	3.9
BOEING 717-200	15.6	13.1	-15.7
BOEING 727-200Adv	13.7	14.2	3.8
BOEING 737-200	13.7	15.3	11.5
BOEING 737-300	14.0	15.7	11.9
BOEING 737-600	16.0	18.8	17.5
BOEING 737-700	16.0	18.6	16.5
BOEING 737-800	16.0	19.0	18.7
BOEING 747-100	16.4	18.7	13.7
BOEING 747-200	16.4	19.1	16.4
BOEING 747-400	17.0	19.3	13.3
BOEING 757-200	16.8	17.5	3.9
BOEING 757-300	16.8	17.4	3.4
BOEING 767-200	16.5	19.4	17.2
BOEING 767-200ER	16.5	19.7	19.0
BOEING 767-300	15.2	19.4	28.2
BOEING 767-300ER	15.2	19.5	28.7
BOEING 777-200	18.1	20.0	11.1
BOEING 777-300	18.1	18.9	4.7
DOUG. DC 9-10	13.6	11.9	-12.5
DOUG. DC 9-30	13.6	13.6	0.0
DOUG. DC 9-40	13.6	14.3	4.9
DOUG. DC 9-50	13.6	14.3	5.2
McDON.DOUG. MD-81	16.0	14.9	-6.6
McDON.DOUG. MD-82	16.0	15.2	-4.9
McDON.DOUG. MD-83	16.0	15.5	-3.4
McDON.DOUG. MD-87	16.0	15.9	-0.7
McDON.DOUG. MD-90-30	16.0	14.9	-6.9
DOUG. DC10-10	14.1	14.7	4.7
DOUG. DC10-30	15.0	16.5	9.9
McDON.DOUG. MD-11	15.8	18.5	17.5
LOCKHD L1011-100	14.1	16.4	15.9
ILYUSHIN Il-62M	14.1	16.9	20.0
TUPOLEV Tu-154M	14.1	16.0	13.6
Bae RJ70	13.4	13.7	2.3
Bae RJ85	13.4	13.6	1.9
Bae RJ100	13.4	13.1	-1.9
Bae RJ115	13.4	13.1	-2.1
CADAIR Reg.Jet 100	13.4	15.0	12.2
CADAIR Reg.Jet 100ER	13.4	15.3	14.8
EMBRAER EMB-145	16.8	13.2	-21.7
FOKKER F70	16.8	15.2	-9.2
FOKKER F100	16.8	15.0	-10.7
Average difference			6.90

Table C.3: Verification design ability, with the original analysis modules

Aircraft	mTOW	W/S	T/W	L/D	SFC	OEW	WFB	SHT/S	SVT/S
AIRBUS_A300_600R	-4.9	31.1	12.5	-2.6	-18.4	-4.8	-10.0	41.1	39.5
AIRBUS_A310_300	-7.0	33.1	11.7	-1.9	-21.2	-6.5	-14.6	42.2	45.7
AIRBUS_A320_200	-1.9	24.0	12.9	2.3	-29.0	1.3	-14.7	30.2	27.3
AIRBUS_A321_200	4.4	35.3	9.1	6.9	8.9	3.3	9.4	30.2	28.5
AIRBUS_A330_200	10.1	23.1	-1.6	8.9	-12.3	11.7	1.0	10.3	9.6
AIRBUS_A330_300	-14.3	19.1	-6.3	8.3	-32.3	-12.8	-38.4	24.6	20.4
AIRBUS_A340_200	-20.1	21.1	-14.5	9.0	-10.2	-23.4	-30.5	25.8	21.4
AIRBUS_A340_300	-10.2	25.7	-3.1	9.8	-4.1	-9.9	-15.9	25.9	21.6
Bae_RJ100	5.1	31.9	20.3	12.6	-4.6	9.0	-0.3	2.6	26.0
Bae_RJ115	10.1	35.0	17.3	12.1	7.0	14.2	10.8	5.0	26.4
Bae_RJ70	15.8	36.5	3.9	18.4	42.5	15.6	33.7	25.0	33.6
Bae_RJ85	3.0	31.5	18.4	11.9	-9.8	6.4	-4.5	8.0	29.4
BOEING_707_320C	-20.3	8.1	6.6	29.8	32.5	-38.0	-11.8	19.3	-3.0
BOEING_717_200	8.0	29.1	42.8	15.3	-7.3	14.2	-0.1	31.4	35.7
BOEING_737_200	-15.9	27.0	-1.6	8.7	0.2	-24.4	-17.2	53.9	46.8
BOEING_737_300	-11.9	31.1	12.0	9.4	-27.0	-12.2	-29.1	51.3	52.3
BOEING_737_600	12.3	24.2	-23.0	10.7	-17.3	7.4	0.5	34.2	34.1
BOEING_737_700	16.5	26.0	-14.8	14.3	4.7	10.2	14.6	31.5	26.6
BOEING_737_800	9.8	30.6	-8.0	15.1	9.6	1.2	10.2	27.1	30.4
BOEING_757_200	-31.7	24.3	10.8	8.6	-9.9	-41.6	-42.8	33.9	33.2
BOEING_757_300	-2.4	29.1	25.1	14.1	-12.7	2.7	-16.6	35.3	36.4
BOEING_767_200	-22.1	11.3	-5.6	6.3	-46.4	-18.8	-52.5	37.9	29.8
BOEING_767_300	-9.1	15.4	7.2	8.8	-30.6	-5.5	-30.6	41.2	33.7
BOEING_767_300ER	-14.1	24.7	20.3	14.6	21.1	-21.1	-3.8	37.0	29.5
BOEING_777_300	-7.7	25.3	5.4	12.3	1.3	-9.3	-11.5	35.0	21.5
DOUG_DC_9_30	-21.8	25.0	-14.0	6.8	13.3	-37.8	-12.1	43.2	29.6
DOUG_DC_9_40	-17.4	22.3	-1.9	8.2	14.6	-25.4	-8.3	37.6	22.8
DOUG_DC_9_50	-7.6	27.5	2.9	11.0	13.9	-14.0	-1.5	38.1	22.9
FOKKER_F100	3.5	15.7	17.0	25.4	9.7	6.6	-3.1	17.4	-12.1
FOKKER_F70	-0.4	16.7	10.3	21.3	-37.7	4.9	-26.5	38.2	4.0
McDONDOUG_MD_81	-4.3	22.0	3.2	9.0	-7.3	-5.1	-9.1	34.3	10.6
McDONDOUG_MD_82	-9.7	24.3	4.1	9.1	-7.8	-15.4	-15.9	30.9	8.4
McDONDOUG_MD_83	-9.7	28.7	8.8	10.3	11.2	-17.3	-4.2	27.5	9.9
McDONDOUG_MD_87	-15.0	20.8	-5.2	6.8	-42.7	-24.8	-39.3	35.1	26.8
McDONDOUG_MD_90_30	2.4	28.5	19.1	7.7	-49.4	5.7	-23.2	41.5	35.3
AIRBUS_A340_500	1.8	31.0	19.9	10.6	11.2	-1.7	6.5	32.7	15.9
AIRBUS_A340_600	7.3	34.2	18.4	16.5	15.7	7.5	10.7	29.5	11.2
BOEING_727_200Adv	12.4	23.3	-9.1	8.3	50.1	-1.1	43.4	17.3	38.1
BOEING_747_100	0.9	19.1	5.7	-0.6	0.2	-1.5	5.7	44.2	36.1
BOEING_747_200	-0.2	24.6	18.0	-6.3	5.9	-9.6	11.6	43.3	34.8
DOUG_DC10_10	-4.7	7.9	5.9	-3.9	-34.7	5.2	-17.9	49.9	26.9
ILYUSHIN_Il_62M	21.3	20.9	8.1	24.2	48.9	7.6	42.3	1.9	2.8
LOCKHD_L1011_100	2.3	26.5	9.1	-3.2	-6.6	1.7	4.5	49.9	23.3
McDONDOUG_MD_11	-26.9	30.4	21.1	-3.7	-27.3	-35.2	-38.9	42.1	42.9
TUPOLEV_Tu_154M	21.9	7.1	3.7	12.4	41.5	18.7	41.9	17.2	20.5
DOUG_DC_9_10	-15.5	16.2	10.4	17.4	-30.5	-16.3	-41.2	49.5	27.3
CADAIR_RegJet_100	-30.3	32.3	31.6	37.0	-42.0	-34.4	-77.0	22.7	32.9
CADAIR_RegJet_100ER	-35.0	22.3	23.1	36.6	-24.6	-39.5	-84.8	15.8	27.2
EMBRAER_EMB_145	-29.7	17.9	15.4	31.0	-30.1	-38.3	-60.2	28.0	5.4

Medium weight aircraft configurations

Heavy weight aircraft & tail mounted engine aircraft

Light weight aircraft

Table C.4: Verification design ability, with the final analysis modules

Aircraft	mTOW	W/S	T/W	L/D	SFC	OEW	WFB	SHT/S	SVT/S
AIRBUS_A300_600R	-5.3	-1.7	-9.2	30.3	0.0	-10.9	1.6	-22.5	-20.3
AIRBUS_A310_300	-2.7	-15.6	-20.2	19.3	0.0	-10.3	11.1	-29.1	-33.2
AIRBUS_A320_200	1.6	-3.1	-12.8	16.4	0.0	-7.8	38.2	-5.9	-6.2
AIRBUS_A321_200	-7.8	-7.6	-8.8	-1.8	0.0	-10.9	-5.7	0.6	3.7
AIRBUS_A330_200	-11.9	-1.4	-4.2	-3.6	0.0	-18.6	-11.5	-5.8	-5.4
AIRBUS_A330_300	-7.7	4.0	-1.5	-3.1	0.0	-17.3	12.7	-5.1	0.2
AIRBUS_A340_200	-1.2	-13.4	-16.6	0.0	0.0	-4.9	6.2	-13.0	-7.9
AIRBUS_A340_300	-9.9	-17.8	-24.7	-0.4	0.0	-16.0	-6.6	-12.4	-7.3
Bae_RJ100	2.4	-2.1	-32.3	22.2	0.0	-3.1	27.2	18.8	-10.5
Bae_RJ115	-4.0	-5.7	-30.4	23.5	0.0	-11.0	11.8	19.4	-7.2
Bae_RJ70	-12.5	-1.6	-16.5	19.5	0.0	-15.4	-18.0	4.8	-7.2
Bae_RJ85	4.0	8.6	-10.6	20.8	0.0	-1.0	30.4	24.9	-5.1
BOEING_707_320C	16.2	39.2	-14.8	6.6	0.0	16.7	28.7	23.0	55.1
BOEING_717_200	-15.4	13.0	-37.4	-9.0	0.0	-24.8	-5.6	4.2	-3.2
BOEING_737_200	14.2	3.4	-6.2	17.2	0.0	13.8	38.8	-31.9	-21.6
BOEING_737_300	7.0	-1.3	-15.6	13.2	0.0	0.7	39.5	-26.2	-28.0
BOEING_737_600	-10.8	1.4	-0.8	14.1	0.0	-13.7	-16.7	-20.0	-18.6
BOEING_737_700	-22.3	-8.1	-1.4	13.7	0.0	-24.2	-6.1	-12.8	-8.1
BOEING_737_800	-20.3	-16.7	-10.9	14.6	0.0	-20.6	-11.0	-11.9	-15.8
BOEING_757_200	-0.9	6.7	-16.6	6.8	0.0	-4.9	8.5	-11.9	-8.8
BOEING_757_300	-7.2	6.4	-16.4	4.3	0.0	-15.7	4.8	-8.1	-7.7
BOEING_767_200	6.0	11.2	-5.4	20.1	0.0	-6.5	46.3	-25.6	-15.7
BOEING_767_200ER	7.3	-21.9	-18.6	23.3	0.0	10.4	4.6	-42.3	-34.8
BOEING_767_300	0.3	-7.5	-16.0	32.3	0.0	-7.9	23.7	-39.5	-31.8
BOEING_767_300ER	4.4	-21.5	-20.3	34.5	0.0	7.3	-6.9	-40.5	-33.4
BOEING_777_200	-11.1	-5.5	-13.8	10.4	0.0	-17.9	-5.0	-30.4	-14.2
BOEING_777_300	0.0	-31.5	-14.7	18.1	0.0	-0.5	1.1	-41.1	-28.9
DOUG_DC_9_30	23.6	10.3	50.4	-0.4	0.0	31.2	39.3	-10.0	11.8
DOUG_DC_9_40	13.3	13.6	8.0	8.3	0.0	13.0	22.7	-5.1	17.7
DOUG_DC_9_50	3.2	6.9	0.4	8.0	0.0	2.1	12.5	-8.1	14.9
FOKKER_F100	-0.2	26.5	-9.1	-9.4	0.0	-4.3	15.5	10.0	49.4
FOKKER_F70	3.5	36.6	8.1	-7.5	0.0	-3.1	41.8	-7.6	43.6
McDONDOUG_MD_81	1.6	13.3	-8.6	-3.5	0.0	-5.5	29.4	-2.3	32.6
McDONDOUG_MD_82	8.0	7.0	-13.4	-3.2	0.0	3.4	41.1	3.3	36.9
McDONDOUG_MD_83	9.8	4.1	-12.8	-2.5	0.0	5.7	29.2	15.8	43.9
McDONDOUG_MD_87	1.7	11.5	-1.2	3.5	0.0	3.5	26.3	-2.7	11.3
McDONDOUG_MD_90_30	-7.7	5.7	-17.9	-2.7	0.0	-15.0	22.9	-9.7	-0.1
AIRBUS_A340_500	-15.4	-35.0	-36.0	5.4	0.0	-18.3	-17.5	-29.2	-11.6
AIRBUS_A340_600	-15.5	-33.8	-39.4	5.4	0.0	-19.1	-18.2	-29.4	-11.1
AIRBUS_A380_800	-13.0	-21.0	-22.9	8.9	0.0	-16.3	-17.3	-50.7	-47.9
BOEING_747_100	-11.4	-8.6	-28.4	23.0	0.0	-15.0	-13.4	-40.7	-32.1
BOEING_747_200	-13.5	-20.6	-33.8	22.9	0.0	-13.7	-19.4	-40.0	-31.0
BOEING_747_400	8.8	-21.5	-35.1	9.9	0.0	10.4	10.4	-28.2	-18.0
BOEING_727_200Adv	-24.6	7.2	-19.8	1.8	0.0	-25.3	-41.4	20.3	-9.9
DOUG_DC10_10	-7.4	36.5	-5.3	25.8	0.0	-24.6	14.1	-35.0	-5.1
DOUG_DC10_30	-23.8	-1.5	-16.3	19.9	0.0	-25.7	-34.3	-36.5	-7.9
McDONDOUG_MD_11	-5.6	-22.0	-32.2	24.0	0.0	-13.1	7.9	-31.0	-31.8
LOCKHD_L1011_100	-35.9	0.9	-28.0	22.5	0.0	-44.3	-40.0	-38.8	-5.5
ILYUSHIN_Il_62M	-31.3	0.0	-36.6	31.3	0.0	-29.1	-43.7	28.3	28.3
TUPOLEV_Tu_154M	-32.8	46.7	-11.3	11.8	0.0	-39.8	-38.8	34.8	30.1
DOUG_DC_9_10	16.2	-5.9	-14.3	-5.0	0.0	14.6	52.9	-47.3	-24.2
CADAIR_RegJet_100	16.1	26.4	-9.2	10.3	0.0	12.9	71.6	64.9	43.3
CADAIR_RegJet_100ER	40.9	29.3	19.0	20.0	0.0	40.5	123.2	56.9	35.8
EMBRAER_EMB_145	28.9	29.9	13.3	-6.8	0.0	32.7	83.9	26.8	66.7

	Medium weight aircraft configurations
	Heavy weight aircraft & tail mounted engine aircraft
	Light weight aircraft

Table C.5: Verification design ability, with the final analysis modules & Design point requirements

Aircraft	mTOW	W/S	T/W	L/D	SFC	OEW	WFB	SHT/S	SVT/S
AIRBUS_A300_600R	11.7	-1.7	-10.0	6.8	0.0	9.9	27.6	-33.4	-30.2
AIRBUS_A310_300	11.6	-18.7	-21.0	14.2	0.0	7.3	31.1	-46.1	-49.0
AIRBUS_A320_200	14.1	-4.9	-7.8	12.5	0.0	7.8	58.6	-21.6	-16.3
AIRBUS_A321_200	7.6	-7.6	-1.7	-8.9	0.0	10.2	15.1	12.5	12.8
AIRBUS_A330_200	5.7	-3.6	-5.9	-9.2	0.0	3.2	10.4	-22.5	-23.3
AIRBUS_A330_300	11.0	0.7	-1.8	-9.4	0.0	5.4	41.6	-23.0	-19.7
AIRBUS_A340_200	22.1	-15.0	-15.5	-3.8	0.0	24.7	34.6	-32.1	-30.9
AIRBUS_A340_300	10.9	-19.3	-23.6	-4.4	0.0	9.8	18.2	-31.1	-28.8
Bae_RJ100	14.1	-1.9	-32.3	-6.5	0.0	8.9	59.1	1.1	-23.3
Bae_RJ115	8.7	-5.6	-29.1	17.2	0.0	1.3	42.4	14.6	-16.3
Bae_RJ70	-2.9	8.1	12.5	11.8	0.0	-4.4	-2.1	11.8	-9.0
Bae_RJ85	21.3	9.3	-14.7	-0.1	0.0	13.8	89.3	9.5	-17.9
BOEING_707_320C	44.3	39.1	-17.7	-3.4	0.0	51.1	70.6	30.1	71.2
BOEING_717_200	-9.3	15.0	-26.4	-12.6	0.0	-16.3	-0.1	-8.5	-14.4
BOEING_737_200	25.3	3.4	-1.9	11.6	0.0	28.8	57.1	-40.3	-34.0
BOEING_737_300	16.8	-1.3	-14.5	8.0	0.0	13.1	57.1	-38.7	-42.6
BOEING_737_600	-2.6	0.7	2.0	10.2	0.0	-2.6	-7.1	-28.3	-29.8
BOEING_737_700	-16.9	-6.6	0.3	12.3	0.0	-17.0	1.0	-21.7	-20.3
BOEING_737_800	-3.9	-15.1	-6.5	12.6	0.0	-5.3	-1.8	-28.4	-26.2
BOEING_757_200	16.5	6.1	-12.0	1.8	0.0	17.2	31.6	-20.5	-21.7
BOEING_757_300	6.6	6.4	-13.8	-0.9	0.0	1.9	24.4	-18.8	-19.0
BOEING_767_200	22.6	8.6	1.0	16.2	0.0	13.7	72.7	-38.0	-25.4
BOEING_767_200ER	39.5	-13.5	-26.4	23.1	0.0	32.7	81.1	-53.1	-47.2
BOEING_767_300	18.6	-7.6	-15.0	16.9	0.0	14.8	52.9	-42.7	-33.3
BOEING_767_300ER	29.7	-19.3	-21.7	23.1	0.0	33.2	36.9	-52.7	-47.7
BOEING_777_200	12.0	-2.1	-18.7	6.1	0.0	0.9	55.0	-45.2	-31.5
BOEING_777_300	34.3	-22.9	-24.2	15.8	0.0	23.0	134.3	-52.9	-41.5
DOUG_DC_9_30	25.0	9.4	25.0	3.6	0.0	34.5	37.7	-23.0	-7.4
DOUG_DC_9_40	22.9	12.7	8.9	2.8	0.0	26.0	36.7	-21.2	-5.2
DOUG_DC_9_50	11.6	6.1	1.2	2.0	0.0	13.6	24.5	-24.4	-7.0
FOKKER_F100	6.9	26.3	-7.8	-13.5	0.0	4.8	26.2	0.9	31.8
FOKKER_F70	8.3	33.8	4.5	-11.4	0.0	2.8	50.2	-15.8	25.0
McDONDOUG_MD_81	13.0	13.4	-3.3	-7.9	0.0	9.6	47.9	-21.1	16.6
McDONDOUG_MD_82	23.1	7.1	-3.2	-7.8	0.0	23.1	66.8	-1.2	32.1
McDONDOUG_MD_83	22.0	4.2	-11.8	-6.5	0.0	21.2	47.5	-2.1	32.1
McDONDOUG_MD_87	12.8	11.6	6.2	0.8	0.0	20.0	42.3	-21.3	-2.0
McDONDOUG_MD_90_30	3.7	5.7	-9.7	-8.4	0.0	-0.7	43.4	-13.2	-3.2
AIRBUS_A340_500	2.9	-35.7	-36.0	4.0	0.0	5.2	1.1	-42.8	-27.8
AIRBUS_A340_600	4.1	-34.3	-39.4	2.0	0.0	6.3	3.0	-45.6	-33.0
AIRBUS_A380_800	6.9	-22.1	-23.3	8.4	0.0	10.4	1.8	-63.7	-62.2
BOEING_747_100	8.3	-11.9	-27.2	16.9	0.0	11.0	9.4	-57.7	-53.4
BOEING_747_200	4.3	-21.4	-34.0	21.1	0.0	10.7	-1.9	-55.2	-50.3
BOEING_747_400	15.6	-22.9	-35.1	18.1	0.0	24.1	11.8	-50.2	-44.8
BOEING_727_200Adv	-13.3	7.5	-14.2	-6.9	0.0	-10.8	-28.8	6.4	-18.3
DOUG_DC10_10	11.8	35.1	-3.0	6.5	0.0	-3.2	47.0	-37.2	-4.1
DOUG_DC10_30	-7.5	-3.5	-16.1	12.9	0.0	-4.0	-17.0	-47.1	-23.6
McDONDOUG_MD_11	17.3	-23.3	-30.3	18.5	0.0	15.4	38.1	-46.0	-47.3
LOCKHD_L1011_100	-25.8	-2.4	-26.9	17.7	0.0	-31.9	-28.6	-52.3	-26.3
ILYUSHIN_Il_62M	-21.0	-2.6	-36.8	26.9	0.0	-15.1	-33.9	7.2	3.6
TUPOLEV_Tu_154M	-23.5	52.7	2.2	1.7	0.0	-28.8	-26.3	35.2	31.4
DOUG_DC_9_10	25.8	-9.3	-16.3	-11.6	0.0	25.9	74.0	-51.4	-35.0
CADAIR_RegJet_100	33.9	48.3	-8.5	5.9	0.0	23.6	170.5	104.9	54.1
CADAIR_RegJet_100ER	37.7	30.2	-4.6	12.3	0.0	36.6	117.2	74.2	31.1
EMBRAER_EMB_145	33.3	31.3	9.8	-19.6	0.0	37.4	97.7	43.6	68.9

	Medium weight aircraft configurations
	Heavy weight aircraft & tail mounted engine aircraft
	Light weight aircraft

Appendix D

Cruiser design

- Cruiser
- 5000nm non-stop aircraft
- 7500nm non-stop aircraft

D.1 Cruiser

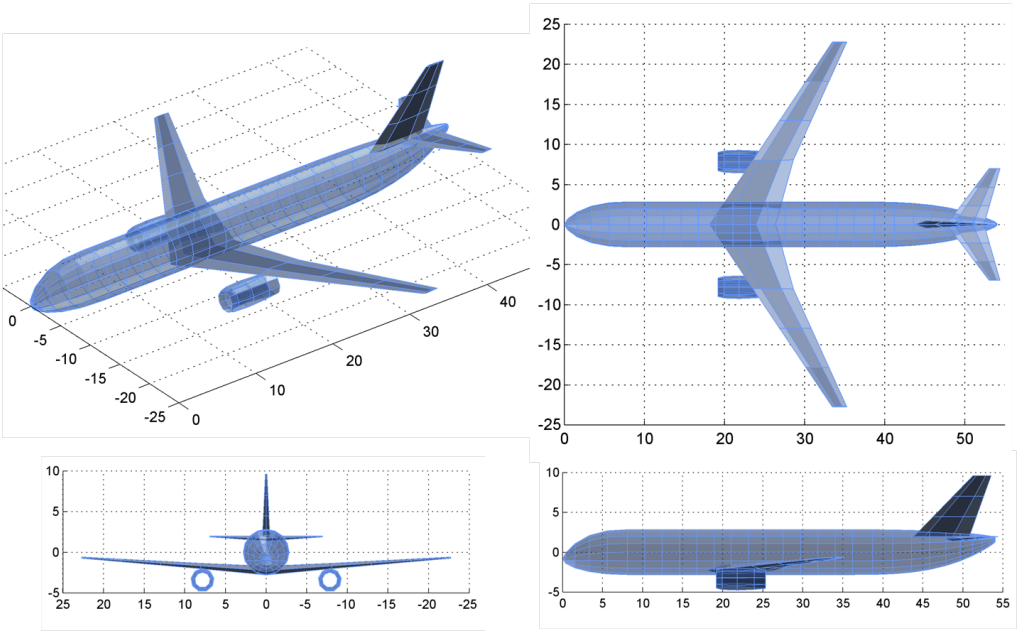

Figure D.1: Iso, side, top and front view

Dimensions:

Main wing			
S	=	178.2	m^2
b	=	42.2	m
A	=	10.00	–
λ	=	0.226	–
Λ_{25}	=	27.3	°
Γ	=	4.0	°
MAC	=	4.86	m

Horizontal tail			
S_{HT}	=	32.09	m^2
b_{HT}	=	12.39	m
A_{HT}	=	4.79	–
λ_{HT}	=	0.282	–
Λ_{HT25}	=	30.3	°
S_{HT}/S	=	0.180	–

Fuselage			
L_{fus}	=	54.0	m
H_{fus}	=	5.63	m
W_{fus}	=	5.63	m

Vertical tail			
S_{VT}	=	27.16	m^2
h_{VT}	=	6.67	m
A_{VT}	=	1.64	–
λ_{VT}	=	0.326	–
Λ_{VT25}	=	37.5	°
S_{VT}/S	=	0.152	–

Landing gear			
N_r	=	2+6	–

Masses:

$MTOW$	=	115396	kg	OEW	=	62774	kg	$OEW/MTOW$	=	55.2	%
$MZFW$	=	93951	kg	WP_{max}	=	31176	kg	$P/Lmax/MTOW$	=	32.7	%
MLW	=	95778	kg	$Fuelmax$	=	28771	kg	$Fuelmax/MTOW$	=	24.5	%
MRW	=	115846	kg	$Fuelmax$	=	35964	L	$MTOW/S$	=	647	kg/m^3

Propulsion:
L_{pod}=5.54m D_{pod}=2.40 Y_m= 35.0%

Version	Engine	Trust per Engine	Thurst/ MTOW	SFC cruise	SFC loiter	λ	D	L
Cruiser-XX1-100	Turbo Fan	179709	0.32	0.525	0.473	-	2.59	5.79

Performance

Alt TO LA	=	0	ft
TO dist	=	2000	m
LA dist	=	1560	m
M_{cr}	=	0.82	-
Alt_{cr}	=	35000	ft
V_{maxneg}	=	300	kts
n_{maxneg}	=	-1.0	-
V_{maxpos}	=	300	kts
n_{maxpos}	=	2.5	-

L/D_{cr}	=	17.9	-
L/D_{lr}	=	19.7	-
e_{clean}	=	0.9	-
CD_{0clean}	=	0.02014	-
$CL_{maxclean}$	=	1.40	-
$e_{take-off}$	=	0.86	-
$CD_{0take-off}$	=	0.03514	-
$CL_{maxtake-off}$	=	2.71	-
$e_{landing}$	=	0.85	-
$CD_{0landing}$	=	0.04014	-
$CL_{maxlanding}$	=	3.00	-

(a) CPACS representation

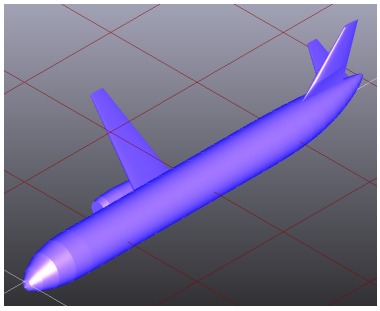

(b) .vrml representation

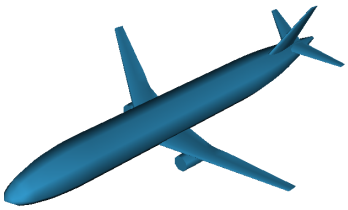

(c) .stp representation

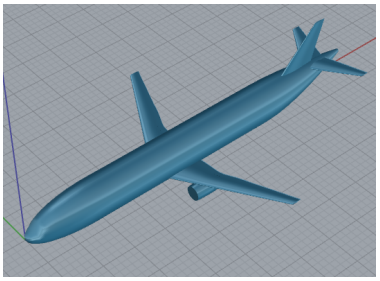

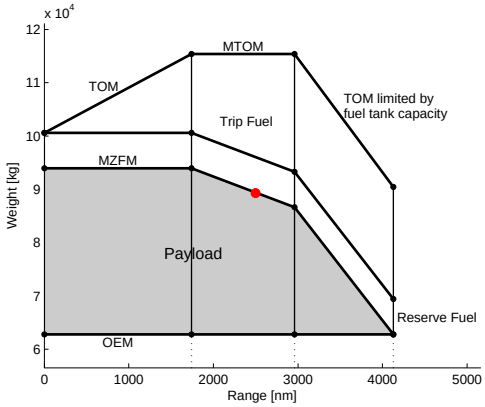

Interior design:

(a) 1 class seat configuration

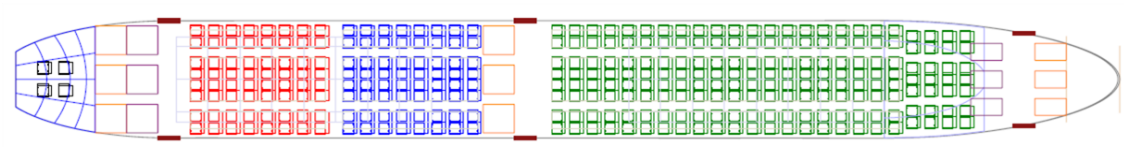

(b) 3 class seat configuration

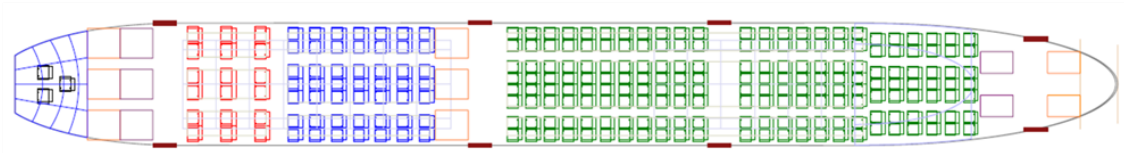

(a) Economy class (b) Business class (c) First class

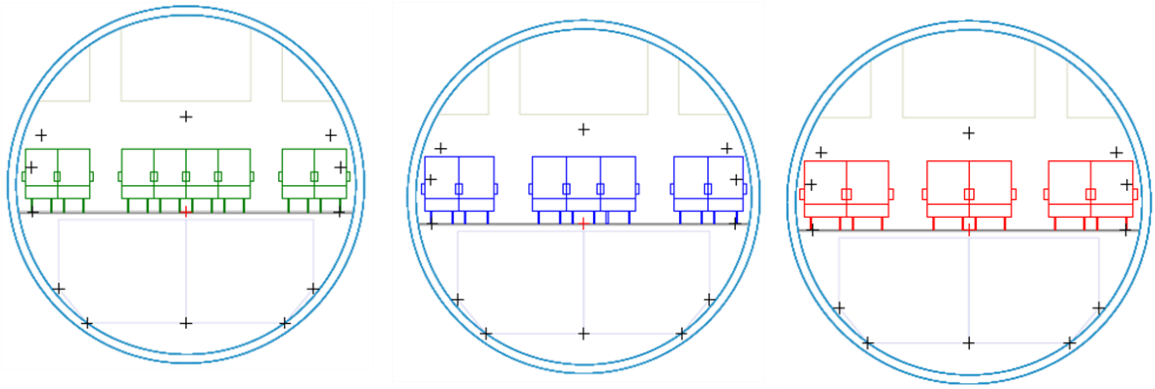

Figure D.2: Interior cross-sections

D.2 5000nm non-stop aircraft

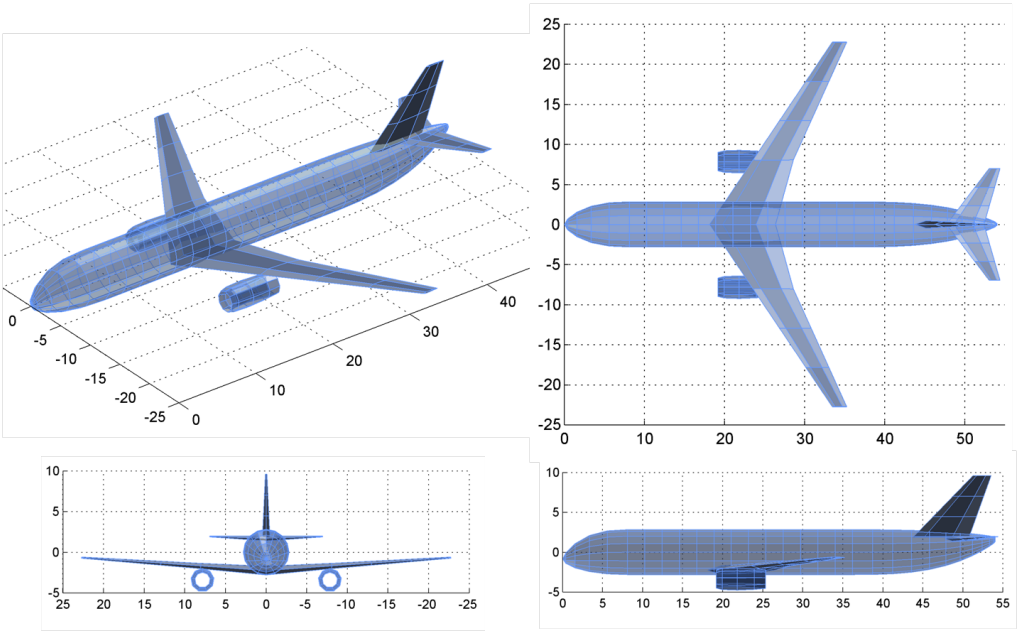

Figure D.3: Iso, side, top and front view

Dimensions:

Main wing			
S	=	253.1	m^2
b	=	50.3	m
A	=	10.00	–
λ	=	0.213	–
Λ_{25}	=	29.7	°
Γ	=	4.0	°
MAC	=	5.83	m

Horizontal tail			
S_{HT}	=	45.12	m^2
b_{HT}	=	14.36	m
A_{HT}	=	4.57	–
λ_{HT}	=	0.299	–
Λ_{HT25}	=	31.2	°
S_{HT}/S	=	0.178	–

Fuselage			
L_{fus}	=	54.0	m
H_{fus}	=	5.63	m
W_{fus}	=	5.63	m

Vertical tail			
S_{VT}	=	37.93	m^2
h_{VT}	=	8.02	m
A_{VT}	=	1.70	–
λ_{VT}	=	0.327	–
Λ_{VT25}	=	40.2	°
S_{VT}/S	=	0.150	–

Landing gear			
N_r	=	2+8	–

Masses:

$MTOW$	=	163983	kg	OEW	=	83452	kg	$OEW/MTOW$	=	50.9	%
$MZFW$	=	121309	kg	WP_{max}	=	37857	kg	$P/Lmax/MTOW$	=	23.1	%
MLW	=	136106	kg	$Fuelmax$	=	56681	kg	$Fuelmax/MTOW$	=	34.6	%
MRW	=	164433	kg	$Fuelmax$	=	70851	L	$MTOW/S$	=	648	kg/m^3

Propulsion:
L_{pod}=5.54m D_{pod}=2.40 Y_m= 35.0%

Version	Engine	Trust per Engine	Thurst/ MTOW	SFC cruise	SFC loiter	λ	D	L
Cruiser-XX1-100	Turbo Fan	259079	0.32	0.525	0.473	-	3.09	6.45

Performance

Alt TO LA	=	0	ft
TO dist	=	2000	m
LA dist	=	1560	m
M_{cr}	=	0.82	-
Alt_{cr}	=	35000	ft
V_{maxneg}	=	300	kts
n_{maxneg}	=	-1.0	-
V_{maxpos}	=	300	kts
n_{maxpos}	=	2.5	-

L/D_{cr}	=	18.8	-
L/D_{lr}	=	20.7	-
e_{clean}	=	0.9	-
CD_{0clean}	=	0.01701	-
$CL_{maxclean}$	=	1.40	-
$e_{take-off}$	=	0.86	-
$CD_{0take-off}$	=	0.03201	-
$CL_{maxtake-off}$	=	2.67	-
$e_{landing}$	=	0.85	-
$CD_{0landing}$	=	0.03701	-
$CL_{maxlanding}$	=	3.00	-

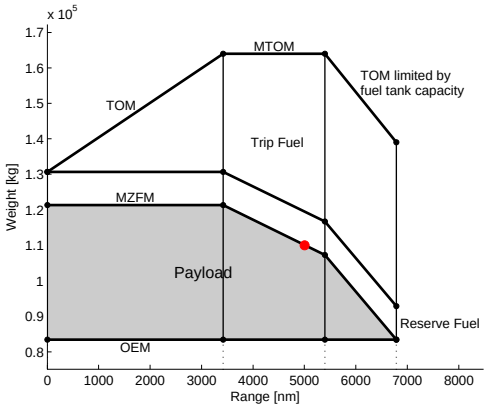

Interior design:

(a) 1 class seat configuration

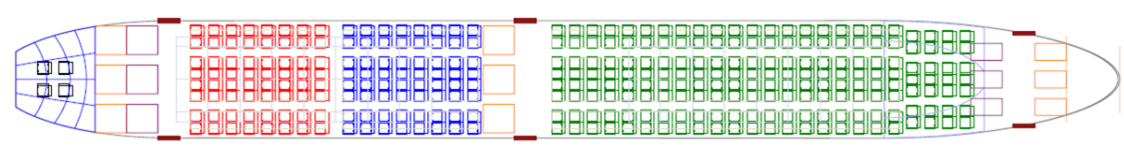

(b) 3 class seat configuration

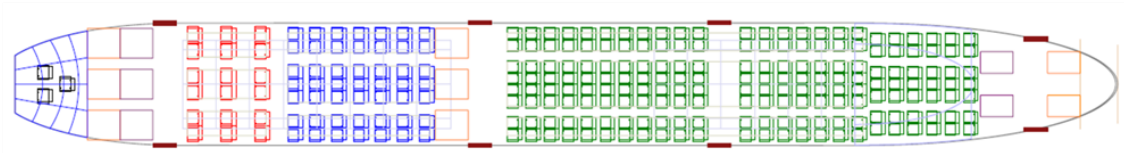

(a) Economy class (b) Business class (c) First class

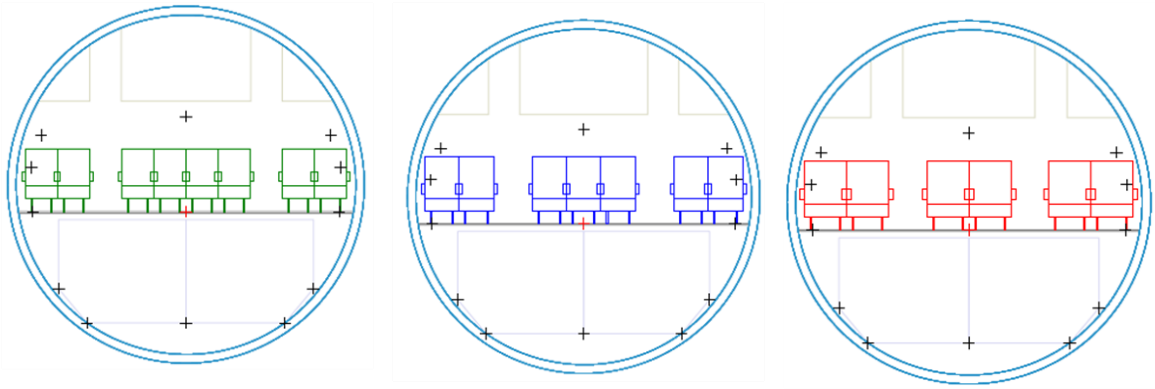

Figure D.4: Interior cross-sections

D.3 7500nm non-stop aircraft

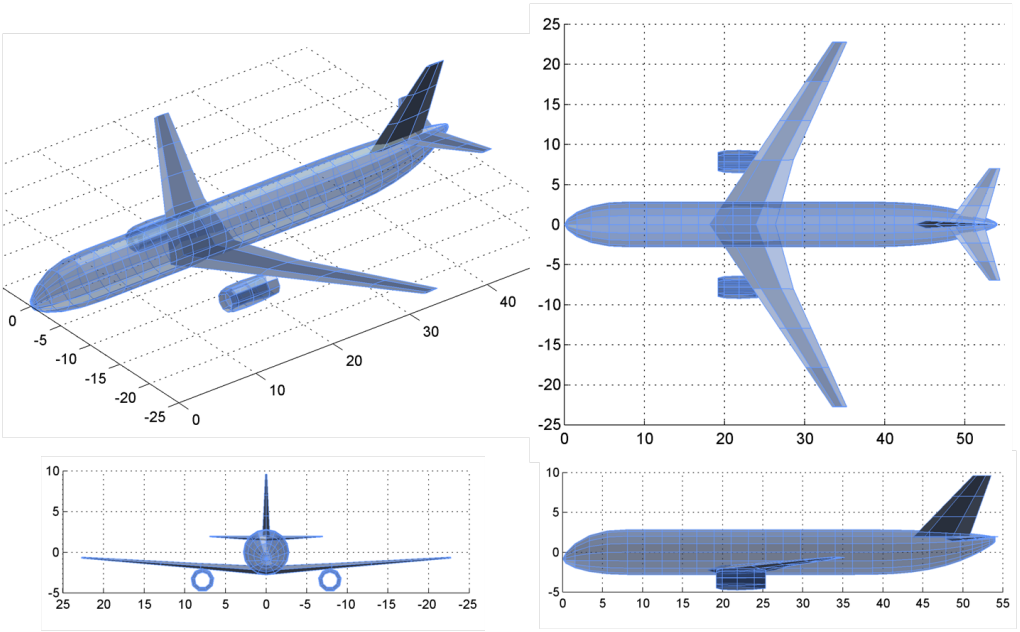

Figure D.5: Iso, side, top and front view

Dimensions:

Main wing			
S	=	365.6	m^2
b	=	57.4	m
A	=	9.00	–
λ	=	0.202	–
Λ_{25}	=	30.3	°
Γ	=	4.0	°
MAC	=	7.42	m

Horizontal tail			
S_{HT}	=	77.04	m^2
b_{HT}	=	18.69	m
A_{HT}	=	4.53	–
λ_{HT}	=	0.310	–
Λ_{HT25}	=	31.6	°
S_{HT}/S	=	0.211	–

Fuselage			
L_{fus}	=	54.0	m
H_{fus}	=	5.63	m
W_{fus}	=	5.63	m

Vertical tail			
S_{VT}	=	55.92	m^2
h_{VT}	=	9.76	m
A_{VT}	=	1.70	–
λ_{VT}	=	0.333	–
Λ_{VT25}	=	42.1	°
S_{VT}/S	=	0.153	–

Landing gear			
N_r	=	2+10	–

Masses:

$MTOW$	=	236891	kg	OEW	=	110783	$kgOEW/MTOW$	=	46.8	%
$MZFW$	=	148641	kg	WP_{max}	=	37857	$kgP/Lmax/MTOW$	=	16.0	%
MLW	=	196620	kg	$Fuelmax$	=	102258	$kgFuelmax/MTOW$	=	43.2	%
MRW	=	237341	kg	$Fuelmax$	=	127823	$L\ MTOW/S$	=	648	kg/m^3

Propulsion:
L_{pod}=5.54m D_{pod}=2.40 Y_m= 35.0%

Version	Engine	Trust per Engine	Thurst/ MTOW	SFC cruise	SFC loiter	λ	D	L
Cruiser-XX1-100	Turbo Fan	348221	0.30	0.525	0.473	-	3.65	7.20

Performance

Alt TO LA	=	0	ft
TO dist	=	2000	m
LA dist	=	1560	m
M_{cr}	=	0.82	-
Alt_{cr}	=	35000	ft
V_{maxneg}	=	300	kts
n_{maxneg}	=	-1.0	-
V_{maxpos}	=	300	kts
n_{maxpos}	=	2.5	-

L/D_{cr}	=	18	-
L/D_{lr}	=	19	-
e_{clean}	=	0.9	-
CD_{0clean}	=	0.01482	-
$CL_{maxclean}$	=	1.40	-
$e_{take-off}$	=	0.86	-
$CD_{0take-off}$	=	0.02982	-
$CL_{maxtake-off}$	=	2.87	-
$e_{landing}$	=	0.85	-
$CD_{0landing}$	=	0.03482	-
$CL_{maxlanding}$	=	3.00	-

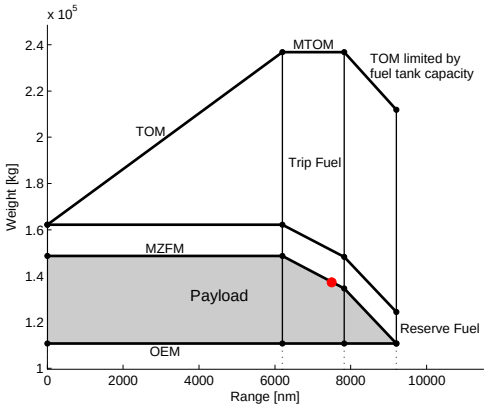

Interior design:

(a) 1 class seat configuration

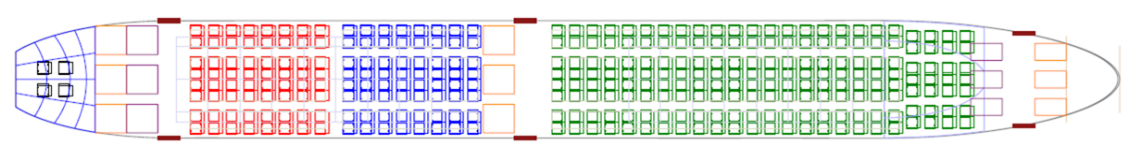

(b) 3 class seat configuration

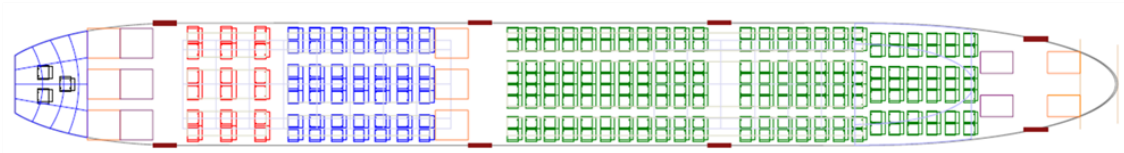

(a) Economy class (b) Business class (c) First class

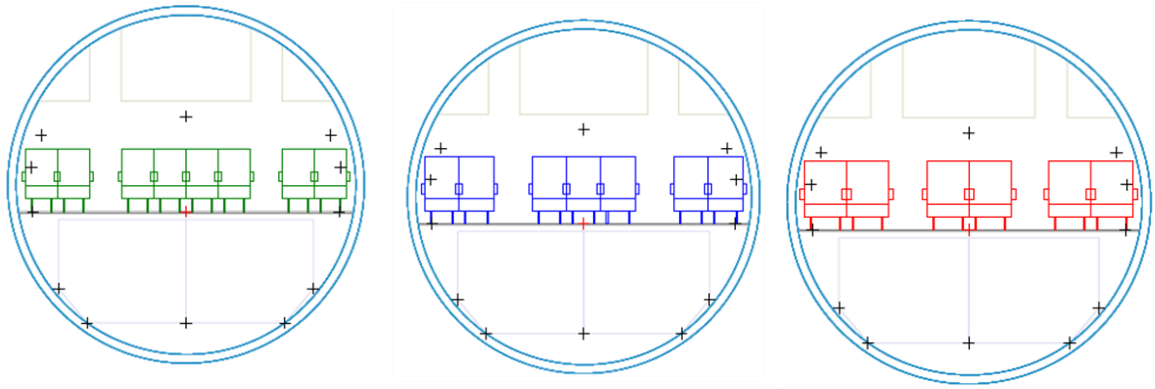

Figure D.6: Interior cross-sections 7500nm non-stop aircraft

Appendix E

Payload details

The KBE fuselage design tool requires the distribution between first, business and economy class. The next section is investigating how these percentage should be set for the cruiser.

A comparison was made between different airliners [43]. Not only the class division differed, but the entire class definition was found to be operator dependant. First class differed between a theater seat and a fold down bed. Economy seat widths varied as well. Some operators fitted 9 seats and others 10 seats abreast in the same wide body aircraft. Table E.1 gives an overview of some of the airliners and their seating arrangements for the B777-300ER. Even within one airliner fleet seating arrangements differ. Air France manages to fit a either 472 passengers in a 3 class configuration or 301 passengers in a 4 class configuration. Emirates fits either 42 or 49 business seats in the same aircraft with 385 economy seats.

Table E.1: B777-300ER Airliner Seating

Airliner	**Number of passengers**					**Percentage of total seat**			
	First	Busi	Eco+	Eco	Total	First	Busi	Eco+	Eco
Air France	0	14	36	422	472	0.00	2.97	7.63	89.41
	8	67	28	198	301	2.66	22.26	9.30	65.78
	0	42	24	315	381	0.00	11.02	6.30	82.68
TAM-Airlines	4	56	0	305	365	1.10	15.34	0.00	83.56
Singapore Airlines	18	49	0	265	332	5.42	14.76	0.00	79.82
	8	50	0	266	324	2.47	15.43	0.00	82.10
	8	42	0	288	338	2.37	12.43	0.00	85.21
Emirates	0	49	0	385	434	0.00	11.29	0.00	88.71
	18	42	0	320	380	4.74	11.05	0.00	84.21
	0	42	0	385	427	0.00	9.84	0.00	90.16
	12	42	0	304	358	3.35	11.73	0.00	84.92

An investigation on the seating layout by the operators did not yield conclusive numbers to work with. Boeing [14] does specify typical class arrangements. The value of some aircraft

with comparable size and range requirements (for cruiser range the total range of 5000nm is used, this is defined as long range [44]) are listed in table E.2. Using these values an aircraft will be made by a standard known to the airliners. They can fit the interior to their own specification, but at least they have a standard model to start from.

Table E.2: Typical seating wide body Boeing aircraft, from Boeing [14]

Aircraft Type	**Number of passengers**				**Percentage of total seat**		
	First	Business	Economic	Total	First	Business	Economic
777-200	24	54	227	305	7.87	17.70	74.43
777-200ER	16	58	227	301	5.32	19.27	75.42
777-300	30	84	254	368	8.15	22.83	69.02
777-300ER	22	70	273	365	6.03	19.18	74.79
747-400ER	23	80	313	416	5.53	19.23	75.24
767-200ER	15	40	126	181	8.29	22.10	69.61
767-300ER	18	46	154	218	8.26	21.10	70.64
767-400ER	20	50	175	245	8.16	20.41	71.43
Average					7.20	20.23	72.57

The value on average class division of all Boeing wide body, 2 aisle, aircraft was found to 7% first 20% business and 73% economy. The seat pitch was equal for both the B777-200 and the B767-400, being respectively 60inch, 38inch and 32inch.

Appendix F

Input files

```
function Input_file_FOKKER_F100

global project;

project.name =                              'FOKKER_F100';

project.Requirements.Payload=               11108;
project.Requirements.Range=                 1290;
project.Requirements.M_cr=                  0.69;
project.Requirements.Alt_cr=                26000;
project.Requirements.TOdist=                1856;
project.Requirements.LAdist=                1321;
project.Requirements.TO_Alt=                0;
project.Requirements.LA_Alt=                0;

project.Mission.Type=                       'FF_Res_Percentage';
project.Mission.Ffr_TO=                     0.995;
project.Mission.Ffr_climb=                  0.980;
project.Mission.Ffr_desc=                   0.990;
project.Mission.Ffr_LA=                     0.992;
project.Mission.Ffr_res=                    0.955;

project.AC_type=                            'Conventional';
project.EN_type=                            'Turbo_Fan';

project.Configuration.Number_EN_gr_1=       2;
project.Configuration.Number_EN_gr_2=       0;
project.Configuration.EN_gr_1_connect=      'Fuselage';
project.Configuration.EN_gr_2_connect=      'MainWing';
project.Configuration.Tail_Type=            'T-Tail';
project.Configuration.Wing_Location=        'Low';
project.Configuration.Airfoil_Type=         'Normal';

project.Fuselage.Type=                      'Simple';
project.Initial_Perf.Type=                  'Use_Reference_Performance_Data';
project.ToolSpecs.fixed.sfc=                1;
project.Fixed.sfc_cr=                       0.690;
project.Fixed.sfc_lr=                       0.621;
end
```

Figure F.1: Example of an Input file for the batch mode, which operates with matlab input files. The Input file is of an Fokker F100